ASSESSMENT AND MODELING OF WHITELEG SHRIMP PRODUCTION IN A LOW-SALINITY RECIRCULATING AQUACULTURE SYSTEM

by

Si Qi (Cindy) Yao

A thesis submitted in partial fulfillment of the requirements for
the degree of Master of Science

School of Environment and Sustainability
University of Michigan

August 2018

Thesis Committee:

Professor James Diana

Professor Lutgarde Raskin

Acknowledgments

There are many people to thank for their contributions and support that made this thesis research possible. I am deeply grateful to have been co-advised by Prof. Jim Diana and Prof. Lut Raskin, whose combined insights on aquaculture and water treatment guided my research in purposeful directions. Being part of two research groups was a great opportunity to share ideas across a diverse range of projects and learn from the experiences of fellow students with different perspectives.

Operation of the pilot aquaculture system was possible with the help of undergraduate research assistant Lindsay Rasmussen, who was instrumental in assisting with system maintenance, shrimp handling, and water analysis. Two Doris Duke Conservation Scholar fellows, Citralina Haruo and Jannice Newson, made valuable contributions to setting up the pilot system early on. The undergraduate senior design team consisting of Harrison Addy, Michael Graves, Katherine Rouen, and Jeremy Solomon used their mechanical engineering experience to design and construct the pilot system.

I am also thankful for the valuable support with lab operations offered by Sucila Fernandes, whose dedication to ensuring that proper conditions are maintained made her a great resource. Timely processing of shrimp deliveries was facilitated by the reliable communications from Jane Parish. Additional thanks to Tom Yavaraski and Nivea Vydiswaran for their help in the environmental engineering labs. Screen fabrication and installation by Bob Spence and Steve Donajkowski greatly improved pilot system operations.

Project funding and support in facilitating the design process was provided by REFRESCH at the University of Michigan Energy Institute. Lindsay Rasmussen also received the WISE RP summer research scholarship as part of her funding.

Table of Contents

	Page
Abstract	1
Introduction	2
Pilot Methods	7
Pilot Results	16
Pilot Discussion	34
Model Description	49
Simulation Results	61
Model Discussion	72
Conclusion	79
References	80

Abstract

Aquaculture is a rapidly growing food production industry currently producing around half of global seafood supply. Enhancing the sustainability of intensive aquaculture is important for food security and environmental protection, as ecological impacts can arise from discharge of nutrient-rich waste streams, land use changes, and escapement of cultured organisms. Recirculating aquaculture systems (RAS) employ an integrated biofilter to process culture water, which can thereby be reused instead of discharged. This enables RAS to use less water, discharge less waste, and operate in more diverse locations compared to conventional aquaculture systems. This study evaluated low-salinity RAS production of whiteleg shrimp (*Litopenaeus vannamei*), a high-value species with strong international markets, through operation of a pilot system and through system modeling. A 2000-L pilot system was operated for 366 days, and shrimp production and water quality metrics were monitored to assess capabilities and limitations of the system. The operational period spanned six batches of shrimp, with all batches reared to at least 10 g and two batches reaching 20 g at harvest. Survival, growth rate, and feed efficiency improved with adjustments in system management. Though the biofilter functioned reliably for around 11 months, it failed to provide sufficient treatment during the final month of operation, indicating that sludge removal is necessary for stable long-term operation. Data generated during RAS operation was used in conjunction with literature values to construct and calibrate a model that integrates operational methods, shrimp bioenergetics, and biofilter function to generate estimates of inputs and outputs needed for stable shrimp production in the RAS. Bioenergetics describe how energy consumed by the shrimp is partitioned into growth, respiration, and wastes; through bioenergetics, the model links shrimp production quantitatively to waste production, which in turn defines biofilter capacity required. Insights gained from pilot and modeling research are valuable for development of more sustainable aquaculture, as it requires interventions that act upon complex systems.

Introduction

Seafood production through aquaculture is undergoing rapid expansion

Global aquaculture production has been increasing for decades, reaching 76.6 million tons of production in 2015, which constituted 45% of combined production from fisheries and aquaculture (FAO 2017). Evidently, aquaculture is an increasingly important component of the global food production system, and its continued expansion has been identified as a key aspect of global food security as human population growth drives seafood demand (Godfray et al. 2010). In addition to its role in supporting human nutrition, seafood as a commodity is deeply integrated into international economic relationships. China is the largest producer and exporter of seafood, both in total production and from aquaculture, while major export markets are the EU, US, and Japan (FAO 2017). Of the numerous and varied species produced through aquaculture, whiteleg shrimp (*Litopenaeus vannamei*) constitutes the largest portion by value; in 2015, it made up 12% of aquaculture production by value at only 5.1% by quantity (FAO 2017). Demand for shrimp is projected by economic forecasts to increase in the future, making it important to understand the opportunities and challenges in sustainable shrimp production through aquaculture (Bush et al. 2010).

Intensification may accelerate negative environmental impacts from aquaculture

To meet increasing demand for seafood, farmers are incentivized to supply more shrimp by replacing traditional extensive pond systems with more intensive modes of production. Whereas extensive aquaculture relies on natural production, which can only support relatively low rearing densities, intensive systems use formulated feeds to rear at higher densities (Diana 2012). In addition to feed provision, regular aeration, water exchanges, and chemical supplements are also used to maintain water quality needed for good production at high rearing densities (Diana 2009). Less land is required for the same level of production in more intensive systems, but these higher yields come at the cost of greater inputs required and more wastes produced (Diana 2009). This central trade-off has important implications for the sustainability of aquaculture, because feed production, energy consumption, waste treatment, and land use all generate environmental impacts.

In formulated feeds used for shrimp production, fish meal and fish oil are key ingredients supplying desired protein content. The ratio of wild fish to farmed fish has been calculated as 2.81 for marine shrimp, indicating that almost three times as much fish is supplied to an aquaculture operation than shrimp ultimately harvested (Naylor et al. 2000). Another key input required for intensive aquaculture is electricity, which is needed for temperature control, water circulation, aeration, and filtration (Badiola et al. 2018). The production of both feed and electricity upstream from their use are associated with environmental impacts. Through a life cycle assessment (LCA) of shrimp farms, feed production and electricity production were identified to be the two dominant contributors to four out of five impact categories considered: biotic resource use, cumulative energy use, global warming, and acidification (Cao et al. 2011). Grow-out effluent was the major contributor to eutrophication, the remaining impact category of interest (Cao et al. 2011). In comparison to extensive ponds, intensive shrimp aquaculture systems are associated with higher waste nutrient concentrations in discharged effluents, which could deteriorate water quality in receiving waters through eutrophication (Páez-Osuna 2001).

While the extent of eutrophication impacts varies depending on capacity and nutrient profile of receiving waters, other land use impacts associated with shrimp aquaculture are more direct. Particularly, ecologically vital mangrove ecosystems have been lost through conversion to coastal shrimp farms, and agricultural soils have been damaged through salinization by inland shrimp pond effluents (Páez-Osuna 2001). Escapement of cultured organisms has also been identified as a major threat to biodiversity when species are not farmed in their native range, as escapees can become invasive, disrupting established ecosystem dynamics (Diana 2009).

Recirculating aquaculture systems may enable sustainable intensification

Pursuing sustainable intensification of aquaculture can enable balance between two important goals, namely expanding food supply to match growing demand while also keeping environmental impacts in check (Godfray et al. 2010). Recirculating aquaculture systems (RAS) have been identified as a technology that can achieve high production with minimal ecological impact (Martins et al. 2010). In RAS, rearing tanks or raceways are closed to the natural environment, in contrast to conventional pond systems. Whereas

intensive flow-through systems require high rates of water exchange to flush away excess nutrients, which can cause ecological impacts if discharged without treatment, water quality in RAS is instead maintained by continuous treatment and reuse of culture water. Ammonia is the dominant form of nitrogenous waste excreted by shrimp, and its un-ionized form is toxic to shrimp at very low concentrations; in an acute toxicity study for *L. vannamei*, un-ionized ammonia-N was estimated to be toxic above 0.12–0.16 mg-N/L within the salinity range of 15–35 ppt (Lin and Chen 2001). The fraction of total ammonia nitrogen (TAN) in the toxic un-ionized form is determined by equilibrium kinetics affected by pH, temperature, and salinity; the remaining component exists as ammonium ions. To prevent accumulation of ammonia in the culture water, RAS leverage microbial metabolisms to remove TAN in an integrated biofilter. Biofilters used for aquaculture are generally fixed film bioreactors, though these can be further categorized into a variety of configurations (Malone and Pfeiffer 2006). The basic principle is that solid media in the biofilter provides surface area that can be colonized by autotrophic microbes that carry out nitrification, a process through which ammonia is oxidized to nitrite then to nitrate in the presence of oxygen. Nitrite-N has been estimated to be toxic to *L. vannamei* above 6.1–25.7 mg-N/L within the salinity range of 15–35 ppt (Lin and Chen 2003). However, nitrite does not accumulate if microbes carrying out nitrite oxidation are established in the biofilter, as TAN undergoes complete nitrification to nitrate. During RAS operation, water continuously recirculates between culture tanks and the biofilter to ensure that TAN removal prevents accumulation of ammonia to toxic levels. Mutualistic interactions between the shrimp population and the microbial community are mediated through the connecting water flow, thereby avoiding discharge of culture water to the environment.

Arising from different aspects of their design and operation, RAS can offer many advantages toward environmental sustainability. Eutrophication impacts associated with conventional intensive aquaculture are abated by the lack of effluent discharge from RAS. Additionally, indoor RAS eliminates risk of ecological impacts from shrimp escapement as well as reduces risk of disease-related crop failure by providing a high level of biosecurity (Lotz 1997). Water use requirements are minimized through integrated filtration and reuse, and water resource limitations have been identified as a driver of RAS adoption (Gutierrez-Wing and Malone 2006). RAS operation also enables control of water quality parameters

such as temperature, dissolved oxygen, and pH to relatively precise optimal ranges, which can result in more efficient feed utilization than in open systems affected by diurnal fluxes (van Rijn 2013). However, exerting control of water quality conditions, running recirculation pumps, and maintaining adequate biofiltration are require their respective energy expenditures. As a result, the key disadvantage of RAS is that their higher energy requirements are associated with greater impacts in global warming, non-renewable resource depletion, and acidification (Ayer and Tyedmers 2009). While these energy use impacts should be kept in mind and used to drive improvements in RAS energy efficiency, the numerous benefits offered by RAS make it an attractive option for intensive shrimp aquaculture.

Low-salinity aquaculture can further enhance opportunities for RAS production

Whereas the previous discussions about system intensity, environmental impacts, and RAS use for whiteleg shrimp aquaculture are also generally applicable to other cultured species, the ability of *L. vannamei* to acclimate to a wide range of salinity levels presents a unique opportunity. Owing to their osmoregulation capacity, *L. vannamei* can be acclimated to grow at a wide range of salinities, from freshwater to 49 ppt (Bray et al. 1994, McGraw and Scarpa 2004). Brackish groundwater is found in many regions, including two-thirds of the US, and the opportunity to use this resource instead of relying on seawater enables shrimp aquaculture to be viable in a larger range of geographical contexts (Roy et al. 2010). Aside from expanding aquaculture capacity to inland regions, an environmental benefit of inland shrimp aquaculture development is the avoided use of sensitive coastal ecosystems. However, not all groundwater sources can support good *L. vannamei* production, as their suitability depends on ionic composition, which varies greatly between sources (Saoud et al. 2003). As a result, salt supplements may be required to achieve a suitable ionic composition for shrimp aquaculture. Due to their minimal water exchange, RAS do not benefit as much from water source flexibility and reduced salt costs compared to flow-through systems, as use of both water and salt additives would be lower without the need for continual replacement. However, these savings could still contribute towards greater RAS adoption. Additionally, operating at a lower salinity could better enable treatment of waste sludge produced in the system; whereas high salinity can inhibit microbe activity needed for

anaerobic digestion of sludge, it was found that a brackish sludge from RAS did not inhibit methanogenesis and could be processed through anaerobic digestion (Mirzoyan et al. 2008). Operating a freshwater RAS would further expand opportunities for waste reuse such as through land application (van Rijn 2013).

Systems modeling can be a valuable tool for RAS management

Given the trade-offs in production efficiency, resource use, pollution potential, etc. that govern environmental impacts arising from aquaculture, LCAs are a useful tool to compare different systems across a consistent set of sustainability metrics (Cao et al. 2013, Diana et al. 2013). To assess a system through LCA, a comprehensive set of data regarding quantity of inputs and outputs must first be determined, as these material and energy flows are what determine level of impact. Bioenergetics summarizes how energy consumed by an organism is transformed through metabolic processes, wherein any fraction not lost to feces, excretion, or respiration is incorporated as biomass growth. In modeling an RAS, bioenergetics can therefore be used to compute crop and waste outputs from feed inputs. Integrating this key component with equations describing biofiltration requirements as well as how the system is stocked and managed can inform the design and management of RAS through greater understanding of system dynamics and sustainability issues.

Research objectives

My pilot study aimed to evaluate an indoor RAS for grow-out of *L. vannamei* at low salinity. A pilot RAS was constructed and monitored over a long-term operational period to assess its capabilities and limitations. Metrics of interest addressed both shrimp production and biofilter function. Shrimp production metrics included growth rate, survival, yield, net production, and feed conversion ratio. Biofilter function was assessed through concentrations of N-species, specifically ammonia-N, nitrite-N, and nitrate-N. To better understand how the pilot RAS performed relative to other systems, shrimp production metrics obtained from this study were compared to those gathered from published literature. Pilot system data were also used to calibrate a simulation model with the goal of estimating inputs and outputs associated with stable operation of the pilot RAS.

Pilot Methods

RAS design and construction

The RAS was composed of six rearing tanks, each directly receiving water pumped from a sump tank while directly discharging water into a biofilter. Influent flow to each rearing tank was controlled by a ball valve. Water from each rearing tank was discharged through vertical standpipes, the height of which set water depth and thereby volume. Four of the rearing tanks each held 80 L, whereas the other two each held 530 L. All standpipes were covered with plastic mesh to exclude shrimp. To minimize footprint, the rearing tanks were stacked in three tiers, with four small tanks on a platform above two large tanks (Figure 1). The biofilter was sized to provide enough total ammonia nitrogen (TAN) removal capacity to maintain sufficiently low TAN concentrations in the RAS, resulting in a biofilter volume of 350 L. Water flowing from standpipes in each rearing tank was carried by gravity to an inlet on one end of the biofilter, and displaced water exited through an outlet on the other end. At the outlet, a short horizontal pipe discharged water from the biofilter into the sump tank. It was sized to accommodate water from one large rearing tank, providing a 440-L capacity, to avoid discharging water from the RAS when draining tanks to facilitate shrimp harvest. The sump tank was the only tank in which water level can vary due to evaporation and manual filling, and water level was maintained at between one-half and one-third of tank depth during standard operation. Water was continuously drawn from the sump tank to all rearing tanks by a 79.2-W pump (Deepwater Aquatics DC10 BLDC). All tanks were constructed from plywood board, their interior surfaces painted with epoxy paint (Pentair Aquatic Eco-Systems), and all edges made watertight through application of fiberglass and resin (3M Bondo). All pipes and fittings used in RAS plumbing were PVC, with joints solvent-welded with pipe cement (Oatey).

The biofilter was configured as a moving bed biofilm reactor (MBBR) filled to 65% tank volume with Kaldnes K1 biofilm carriers, which provide 500 m^2/m^3 of effective specific surface area. To seed the biofilter with microbes adapted for nitrification in salt water, approximately 35 L of wet sand was collected from the sand filter of a shark exhibit backwash recovery system at the Shedd Aquarium and placed into the RAS biofilter. Nitrification was established by daily addition of ammonium chloride for two months prior to

stocking the first batch of shrimp into RAS. Continuous aeration was provided by three circular air stones connected to a 7.5-W air pump (Tetra Whisper AP300).

Because rearing tanks were quite shallow, holding water 8” deep with 3” freeboard, shrimp were frequently lost from the system by jumping over the sides of rearing tanks. After five months of operation, an attempt was made to retain shrimp by securing plastic netting over the tanks. While this reduced the incidence of shrimp escapement, the netting was not able to prevent it completely. Subsequently, around eight months into RAS operation, custom-made screens were installed to enclose all rearing tanks. The screens were constructed from rigid plastic mesh (Pentair Aquatic Eco-systems) of 1/8” mesh size, secured on all sides to an aluminum frame clamped to the top of each tank. Mesh screens for small tanks each include an opening that allows access for feeding and taking measurements without needing to remove the screen. When not in use for tank access, these openings were covered with a flexible mesh fabric held secure by elastic cords. These screens successfully prevented shrimp from jumping out of rearing tanks.

Figure 1. Pilot-scale RAS with four small rearing tanks and two large rearing tanks in stacked configuration. Through recirculation, all rearing tanks directly discharge water into aerated biofilter containing Kaldnes K1 media and directly receive water from sump tank.

Water quality maintenance and monitoring

Water used in the RAS was Ann Arbor, MI municipal water that had been pretreated on site. Pretreatment included chloramine removal through granular activated carbon filtration, followed by passage through a trickling biofilter. Pretreated water filled a storage tank and was drawn for use as needed. When filling the RAS initially, commercial sea salt (Instant Ocean) was added to achieve 4 ppt salinity throughout the system. During operation, there was no routine discharge from the system. Evaporative losses were replaced by regular manual addition of water to the sump tank. To replace alkalinity and maintain desired water pH, sodium bicarbonate was added to the system as needed. Aquarium heaters (EHEIM) were used to maintain water temperatures around 27 °C; the small rearing tanks each employed one 75-W heater, while the large rearing tanks each employed one 300-W heater. Continuous aeration was provided in all rearing tanks by rectangular aquarium air stones connected to a compressed air source by flexible tubing.

DO, temperature, pH, and salinity were monitored daily using handheld meters. Temperature and salinity were measured with YSI model 30, pH was measured with Orion QuikChek pH meter, and DO was measured with YSI model 58. Water samples for analysis of nitrogen species were collected weekly from all rearing tanks containing shrimp, biofilter influent, biofilter effluent, and sump tank. Weekly collection of water samples from sump tank began on Day 185, when microbial solids from the biofilter were observed to be settling there. Samples were filtered through a mixed cellulose ester filter with pore size of 0.45 µm, collected in plastic Falcon tubes, and stored at -18 °C prior to analysis. Standard methods were used to quantify ammonium, nitrite, and nitrate (American Public Health Association et al. 2005). Ammonium was measured through a colorimetric assay in which phenol, hypochlorite, and sodium nitroprusside are added to samples containing ammonium to produce indophenol, a blue compound. Colorimetric determination of nitrite utilized the reaction of sulfanilamide and N-(1-naphthyl)-ethylenediamine dihydrochloride with nitrite to produce a pink azo dye. Ammonium and nitrite analyses were carried out in triplicate on microplates, with a reaction volume of 500 µL for ammonium and 200 µL for nitrite. On the microplate spectrophotometer, absorbance was measured at 640 nm for ammonium analysis and at 543 nm for nitrite analysis. Nitrate was quantified through ion chromatography using triplicate injections per sample. For all three nitrogen species, calibration curves were

generated by preparing standards at a series of known concentrations using ammonium chloride, sodium nitrite, or potassium nitrate in Milli-Q water containing 4 ppt Instant Ocean sea salt to better match the ionic composition of RAS water samples.

Shrimp rearing and assessment

Specific-pathogen-free *L. vannamei* post-larvae (PLs) were provided by Miami Aquaculture, shipped overnight from Miami, FL to Ann Arbor, MI. After allowing gradual temperature equilibration to nursery tank water, shrimp were transferred from their shipping bag into glass aquarium nursery tanks. Initially, nursery tank water had salinity matching the water in which PLs were shipped. After shrimp had spent one week in the nursery tanks, salinity acclimation to 4 ppt was conducted by replacing water slowly, such that the rate of salinity reduction did not exceed 1 ppt every 15 minutes. Water used for replacement was heated to match the temperature of nursery tank water. During stocking of shrimp into the RAS, shrimp were first netted in batches from the nursery tanks into a bucket, where videos were taken to enable subsequent counting by visual inspection. Then, shrimp were weighed in batches to determine initial weight before being placed into a small rearing tank.

During rearing, average wet weight of shrimp was estimated weekly. For each rearing tank, at least 10% of initial number stocked was used as sample size for weighing. Shrimp were netted from the rearing tank into temporary holding buckets containing water filled from the same rearing tank. Once enough had been netted, shrimp were weighed in batches. Each batch was enclosed in a thin mesh fabric tied with a rubber band, placed inside a plastic cup, and weighed on an analytical balance (Denver Instrument APX-100). The mass of the slightly wetted mesh fabric with the rubber band was recorded to be subtracted later, whereas the plastic cup was tared on the balance.

Shrimp were hand-fed commercial feed formulated for shrimp aquaculture containing 40% protein (Rangen Inc.). For initial batches, amount fed was gradually increased based on visual inspection of whether previously provided feed remained uneaten. Feeding method was improved for later batches, wherein shrimp weights measured weekly and assumed survival rate were used to estimate shrimp biomass in the rearing tanks. Feed provision was then calculated using by multiplying estimated shrimp biomass and appropriate feed rate for the current shrimp size according to a feeding table provided by Rangen Inc. (Table 1). Each

ration was divided evenly across two feedings per day, once in the morning and once in the evening. Feed particle size was increased with shrimp weight according to the Rangen feeding table (Table 1).

Table 1. Feeding table for *L. vannamei* production given by Rangen Inc., manufacturer of the commercial shrimp feed used.

DIETS	FEED PARTICLE SIZE*	AVG. SHRIMP SIZE (G)	FEED RATE (% BIOMASS/ DAY)	FEEDING FREQUENCY***	RECOMMENDED USE
	No. 0	PL 5 - PL 10**	80 - 40	4 - 6	
Shrimp Grower	No. 0 AND No. 1	0.1 - 0.25	40 - 20	4 - 6	Semi-intensive
45% Protein	No. 1 AND No. 2	0.25 - 0.05	20 - 15	4 - 6	Nursery
Post Larval Granules	No. 2 AND No. 3	0.5 - 1	15 - 10	4	Pond
	No. 3 AND No. 4	1 - 3	10 - 5	4	
	3/32"	3 - 8	5 - 4	3	
Shrimp Production	3/32"	8 - 12	4 - 2.5	3	Semi-intensive
25-40% Protein	3/32"	12 - 16	2.5 - 2.2	3	or Extensive
Pellets	3/32"	16 - 20	2.2 - 2.0	3	Pond Culture
	3/32"	>20	2	2 - 3	

To enable continuous RAS operation and regular harvests year-round, the four small rearing tanks and two large rearing tanks were used to implement the rotational stocking schedule illustrated in Figure 2. According to this schedule, each batch was stocked one-third of expected rearing time apart from the previous batch, and batches were harvested from the RAS at this same interval. During rearing, every batch spent the first two-thirds of expected rearing time in small tanks and the remaining one-third in large tanks. For RAS operation in this study, rearing time was initially expected to be three months, with two months in small tanks and one month in large tanks.

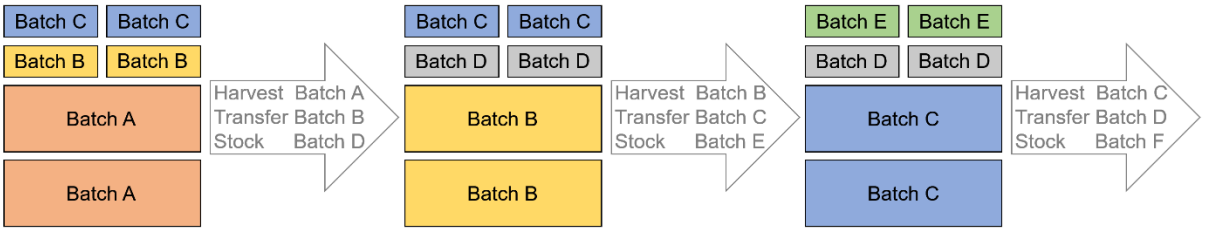

Figure 2. Diagram of rotational stocking schedule that utilized the four small rearing tanks and two large rearing tanks to accommodate three different batches concurrently. For the example batches shown here, Batch A was stocked earliest, followed by Batch B, C, D, E, and lastly F.

To better understand shrimp rearing at different stages in the RAS, average weight at time of transfer and number of shrimp transferred from small tanks to large tanks were recorded. A mesh net was secured onto the drainpipe at the bottom of the small tanks, thereby containing all shrimp as small tanks were emptied of water. Collected shrimp were then placed into buckets containing water from large rearing tanks, which was kept aerated by one aquarium air stone per bucket. At least 15% of transferred shrimp were weighed following normal procedure. Transfer was completed by hand-netting shrimp from the buckets into large tanks while keeping tally of how many were transferred.

When harvesting shrimp from the RAS, shrimp were netted from large tanks, weighed individually on an analytical balance, and chill-killed by submerging in salted ice water kept below 0 °C. To facilitate continued netting of shrimp as fewer remained, water was drained from the large tanks by allowing it through the biofilter to be collected in the sump tank. After all shrimp had been harvested, weighed, and killed, a count of the recorded weights gave the number of shrimp harvested.

System performance metrics calculation

For each batch reared, number of shrimp and mean weight at stocking, transfer, and harvest were recorded. These data were used, in conjunction with the number of days spent in the RAS and cumulative mass of feed provided, to compute metrics to describe shrimp production observed in this system. Microsoft Excel was used to organize data, carry out calculations, and graph results.

Survival was quantified through two metrics:

$$percent\ survival\ (\%) = 100 \times \frac{number\ of\ shrimp\ harvested}{number\ of\ shrimp\ stocked}$$

$$weekly\ percent\ mortality\ (\%/wk) = \frac{100 - percent\ survival}{days\ in\ RAS} \times 7\frac{days}{wk}$$

Gross yield was estimated by:

$$yield\ \left(\frac{kg}{m^2 - month}\right) = \frac{mass\ of\ shrimp\ harvested}{area\ of\ one\ large\ rearing\ tank} * \frac{1}{days\ in\ RAS} \times \frac{365.25\ d/yr}{12\ month/yr}$$

Net production was estimated as:

$$net\ production\ (kg) = shrimp\ biomass\ harvested - shrimp\ biomass\ stocked$$

where $shrimp\ biomass\ (kg) = mean\ weight * number\ of\ shrimp$

Shrimp density, both numerical and biomass, were calculated:

$$numerical\ density\ \left(\frac{shrimp}{m^2}\right) = \frac{number\ of\ shrimp}{area\ of\ tank}$$

$$biomass\ density\ \left(\frac{kg}{m^2}\right) = \frac{shrimp\ biomass}{area\ of\ tank}$$

Feed conversion ratio (FCR) describes how efficiently feed provided was converted to harvested shrimp biomass:

$$FCR = \frac{cumulative\ mass\ of\ feed\ provided}{net\ production}$$

Rate of shrimp growth during rearing was quantified by growth rate, specific growth rate (SGR), and daily growth coefficient (DGC). DGC was originally developed to model growth of salmonids in hatcheries (Iwama and Tautz 1981), but has been found to also appropriately model growth of shrimp at constant temperature (Bureau et al. 2000).

Growth rate, both absolute and relative to weight, models linear growth:

$$growth\ rate\ (g/d) = \frac{mean\ weight - initial\ mean\ weight}{days\ in\ RAS}$$

$$growth\ rate\ (\%wt/d) = \frac{100 \times (mean\ weight - initial\ mean\ weight)/mean\ weight}{days\ in\ RAS}$$

Alternatively, SGR corresponds to an exponential growth model:

$$SGR = 100 \times \frac{\ln(mean\ weight) - \ln(initial\ mean\ weight)}{days\ in\ RAS}$$

DGC corresponds to a growth model based on the cubic root of weight:

$$DGC = 100 \times \frac{(mean\ weight)^{1/3} - (initial\ mean\ weight)^{1/3}}{days\ in\ RAS}$$

Shrimp production literature comparison

Data reported in 17 studies of *L. vannamei* culture in different systems were compared to production results from this current study. Encompassed within the 17 literature studies are 75 experimental shrimp growth runs which were categorized into five culture system types: RAS, low-discharge, flow-through, cage culture, and biofloc system (Table 2). To represent production in my RAS, only data from Batch 4, 5, and 6 were included for comparison, as these batches better reflect production that can be achieved in the system, while earlier batches were impacted by problematic feeding and containment of shrimp. The two cohorts of Batch 4 were considered as separate growth runs, so production in the current study was represented by a total of four runs.

Table 2. Five types of shrimp culture systems for which shrimp production data was reported in the corresponding references. Number of growth runs for each system type and number of runs contributed by each reference are indicated. Note that three references are listed for more than one system type.

Culture System Type	Reference Citation	Study ID	Number of Runs
Current Study RAS (N=4)	n/a	0	4
RAS (N=19)	Appelbaum et al. 2002	1	2
	Araneda et al. 2008	2	3
	Browdy and Moss 2005	3	4
	Esparza-Leal et al. 2010b	4	3
	Ray and Lotz 2017	5	1
	Ray et al. 2017	6	1
	Samocha et al. 2004	7	2
	Sowers et al. 2006	8	3
Low-discharge (N=41)	Bray et al. 1994	9	7
	Cuvin-Aralar et al. 2009	17	1
	Esparza-Leal et al. 2009	10	5
	Esparza-Leal et al. 2010a	11	16
	Fóes et al. 2016	12	2
	Mena-Herrera et al. 2006	13	6
	Patnaik and Samocha 2009	14	4
Flow-through (N=9)	Otoshi et al. 2006	15	4
	Moss et al. 1992	16	5
Cage culture (N=4)	Cuvin-Aralar et al. 2009	17	4
Biofloc system (N=2)	Ray and Lotz 2017	5	1
	Ray et al. 2017	6	1

For shrimp growth runs, rearing conditions and shrimp production results reported in the cited studies were compiled and graphed in Microsoft Excel. These data included experiment duration, salinity, temperature, numerical stocking density, type of feed, initial weight, final weight, percent survival, and FCR. Additional production metrics were computed, namely biomass stocking density, growth rate, SGR, DGC, thermal-unit growth coefficient (TGC), percent mortality, and yield. When experiment duration was reported in weeks, it was multiplied by seven to represent duration in days.

Biomass stocking density was computed from numerical density and initial weight reported:

$$biomass\ stocking\ density\ \left(\frac{g}{m^2}\right) = initial\ weight * stocking\ density$$

Metrics describing rate of growth were calculated using initial weight, final weight, and experiment duration; for TGC, temperature expressed in units of ºC is an additional factor:

$$growth\ rate\ (g/d) = \frac{final\ weight - initial\ weight}{experiment\ duration}$$

$$SGR = 100 \times \frac{\ln(final\ weight) - \ln(initial\ weight)}{experiment\ duration}$$

$$DGC = 100 \times \frac{(final\ weight)^{1/3} - (initial\ weight)^{1/3}}{experiment\ duration}$$

$$TGC = 1000 \times \frac{(final\ weight)^{1/3} - (initial\ weight)^{1/3}}{experiment\ duration * temperature}$$

Weekly percent mortality rate was calculated using percent survival and experiment duration:

$$weekly\ percent\ mortaility\ rate\ (\%/wk) = \frac{100 - percent\ survival}{experiment\ duration} \times 7\ \frac{days}{wk}$$

Gross yield was calculated using stocking density, percent survival, final weight, and experiment duration:

$$yield\ \left(\frac{kg}{m^2 - month}\right) = \frac{stocking\ density * percent\ survival}{100} * \frac{final\ weight}{1000\frac{g}{kg}} * \frac{1}{experiment\ duration} \times \frac{365.25\ d/yr}{12\ month/yr}$$

Pilot Results

Six batches of shrimp were reared over the course of 366 days of RAS operation between December 2016 and December 2017 (Table 3). Operation was terminated after a die-off event beginning around Day 362 which left virtually no surviving shrimp in Batch 5 and 6.

Table 3. All batches of shrimp reared in the RAS as summarized by which rearing tanks they occupied and initial number of shrimp stocked. Batch 1, 2, and 4 were each split into two cohorts reared in separate tanks. Batch 3 contained one cohort which was not transferred into a large rearing tank. Batch 5 and 6 were each considered to contain one cohort, because shrimp stocked into two small tanks were combined into the same large tank at transfer.

Batch ID	Tanks Occupied	Initial Number Stocked		Batch ID	Tanks Occupied	Initial Number Stocked
Batch 1	ST1 → MT	565		Batch 4	ST1 → BT	234
	ST2 → BT	821			ST2 → MT	235
Batch 2	ST1 → MT	517		Batch 5	ST1 → BT	444
	ST2 → BT	517			ST2 → BT	444
Batch 3	ST4	308		Batch 6	ST3 → MT	443
					ST4 → MT	443

Water quality in rearing tanks

There was a downward trend in DO concentrations, with later batches having lower mean DO than earlier ones (Table 4, Figure 3). Mean water temperature for Batch 1 was around 26 ºC, whereas later batches were reared at 27–28 ºC. Initially, mean pH for Batch 1 was around 8.0; after it dropped to around 7.5, regular additions of sodium bicarbonate were used to maintain pH at that level for Batch 4, 5, and 6. Mean salinity was between 3.8 ppt and 4.1 ppt for all batches reared.

Table 4. Mean and standard deviation of DO, temperature, pH, and salinity readings collected daily within rearing tanks occupied by each batch. Tanks that comprise a cohort are indicated by pattern of shading. For DO and temperature, minimum and maximum observed values are also included.

	Dissolved Oxygen (mg/L)			**Temperature (°C)**			**pH**	**Salinity (ppt)**
	Mean ± SD	Min.	Max.	Mean ± SD	Min.	Max.	Mean ± SD	Mean ± SD
Batch 1 ST1	7.6 ± 0.2	7.2	8.0	24.5 ± 0.5	23.8	26.8	8.3 ± 0.1	4.1 ± 0.1
Batch 1 MT	6.9 ± 0.7	4.1	8.1	25.9 ± 1.1	23.7	28.3	7.8 ± 0.3	3.9 ± 0.1
Batch 1 ST2	7.4 ± 0.2	6.9	7.9	25.8 ± 0.4	24.9	27.4	8.3 ± 0.1	4.1 ± 0.1
Batch 1 BT	6.9 ± 0.8	2.3	8.1	25.8 ± 1.1	23.5	28.1	7.8 ± 0.3	3.9 ± 0.1
Batch 2 ST1	6.4 ± 1.0	4.2	8.4	26.7 ± 1.0	24.8	28.6	7.7 ± 0.3	3.8 ± 0.2
Batch 2 MT	5.7 ± 0.7	3.3	7.0	27.9 ± 0.4	26.5	28.7	7.5 ± 0.1	3.9 ± 0.2
Batch 2 ST2	5.9 ± 1.3	2.9	8.3	27.7 ± 0.9	25.6	29.5	7.7 ± 0.3	3.9 ± 0.2
Batch 2 BT	5.9 ± 0.6	5.0	6.9	27.7 ± 0.4	26.5	28.5	7.5 ± 0.1	3.9 ± 0.2
Batch 3 ST4	5.7 ± 1.0	3.9	7.8	27.6 ± 0.7	25.6	28.6	7.6 ± 0.2	3.8 ± 0.2
Batch 4 ST1	5.7 ± 0.7	4.3	7.0	27.9 ± 0.3	26.9	28.5	7.5 ± 0.1	3.9 ± 0.2
Batch 4 BT	5.7 ± 0.4	4.8	6.5	27.7 ± 0.4	26.9	28.4	7.5 ± 0.1	4.0 ± 0.1
Batch 4 ST2	5.5 ± 0.8	4.3	7.0	28.3 ± 0.3	27.0	28.8	7.5 ± 0.1	3.9 ± 0.2
Batch 4 MT	5.3 ± 0.5	4.3	6.9	27.9 ± 0.4	27.0	28.6	7.5 ± 0.1	4.0 ± 0.1
Batch 5 ST1	5.4 ± 0.6	3.8	7.0	27.9 ± 0.5	26.0	28.8	7.5 ± 0.1	4.0 ± 0.1
Batch 5 ST2	5.2 ± 0.6	3.8	6.7	28.4 ± 0.7	26.7	29.5	7.5 ± 0.1	4.0 ± 0.1
Batch 5 BT	5.2 ± 0.9	3.1	7.3	27.3 ± 0.6	26.1	28.2	7.4 ± 0.1	4.1 ± 0.2
Batch 6 ST3	5.6 ± 0.5	4.4	6.4	27.0 ± 0.5	25.9	28.0	7.5 ± 0.1	4.1 ± 0.1
Batch 6 ST4	5.7 ± 0.5	4.3	6.8	27.7 ± 0.8	26.1	29.0	7.5 ± 0.1	4.1 ± 0.1
Batch 6 MT	4.9 ± 0.7	3.7	6.5	27.6 ± 0.4	26.6	28.4	7.4 ± 0.1	4.1 ± 0.2

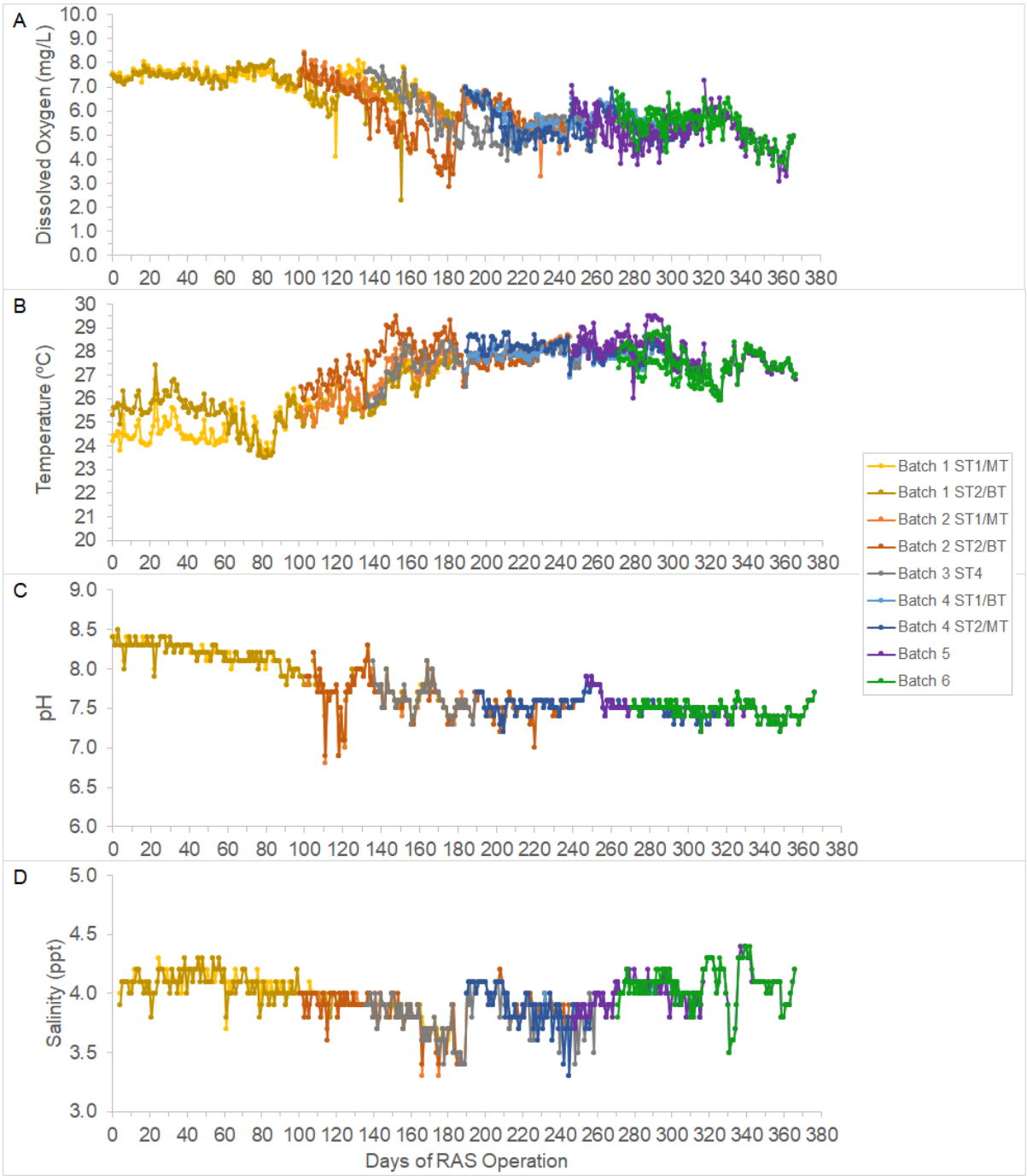

Figure 3. Daily values for (A) DO (mg/L), (B) temperature (°C), (C) pH, and (D) salinity (ppt) in rearing tanks over 366 days of RAS operation. Data are displayed by cohort.

Concentration of ammonium and nitrite in water samples taken from rearing tanks indicated mean ammonium in Batch 1, 2, 3, and 4 tanks did not exceed 0.64 mg-N/L (Table 5). However, when Batch 5 and Batch 6 were concurrently in the large rearing tanks, ammonium had increased from around 1 mg-N/L to 40 mg-N/L over the course of the final

month of system operation. No accumulation of nitrite was observed; mean nitrite in the rearing tanks did not exceed 0.18 mg-N/L during RAS operation.

Table 5. Mean and standard deviation of ammonium and nitrite concentrations measured in water samples collected weekly from rearing tanks occupied by each batch. Tanks that comprise a cohort are indicated by pattern of shading.

	Ammonium (mg-N/L)	Nitrite (mg-N/L)			Ammonium (mg-N/L)	Nitrite (mg-N/L)
	Mean ± SD	Mean ± SD			Mean ± SD	Mean ± SD
Batch 1 ST1	0.05 ± 0.05	0.01 ± 0.01		Batch 4 ST1	0.61 ± 0.50	0.16 ± 0.07
Batch 1 MT	0.16 ± 0.18	0.16 ± 0.16		Batch 4 BT	0.60 ± 0.39	0.13 ± 0.10
Batch 1 ST2	0.07 ± 0.06	0.01 ± 0.02		Batch 4 ST2	0.58 ± 0.55	0.15 ± 0.06
Batch 1 BT	0.13 ± 0.11	0.15 ± 0.15		Batch 4 MT	0.64 ± 0.44	0.13 ± 0.11
Batch 2 ST1	0.12 ± 0.08	0.11 ± 0.11		Batch 5 ST1	0.63 ± 0.41	0.14 ± 0.11
Batch 2 MT	0.52 ± 0.49	0.14 ± 0.06		Batch 5 ST2	0.67 ± 0.48	0.15 ± 0.11
Batch 2 ST2	0.12 ± 0.09	0.11 ± 0.11		Batch 5 BT	6.48 ± 8.16	0.18 ± 0.08
Batch 2 BT	0.54 ± 0.57	0.13 ± 0.06		Batch 6 ST3	0.75 ± 0.38	0.17 ± 0.09
Batch 3 ST4	0.40 ± 0.47	0.11 ± 0.07		Batch 6 ST4	0.74 ± 0.43	0.17 ± 0.10
				Batch 6 MT	7.40 ± 8.14	0.17 ± 0.07

Water quality in biofilter and sump tank

Alongside daily monitoring of rearing tank water quality, the same parameters were recorded at the biofilter influent, biofilter effluent, and in the sump tank. Over the course of operation, DO decreased from around 8 mg/L to below 2 mg/L at the biofilter effluent and sump and below 1 mg/L at the biofilter influent. Temperature was raised from around 24 ºC at the start of operation to 27–28 ºC by the end. Initial pH was around 8.4 and gradually dropped to 7.5, at which point it was maintained by regular sodium bicarbonate addition. Salinity was maintained around 4 ppt.

Ammonium, nitrite, and nitrate concentrations in water samples collected from the biofilter were similar across samples taken on the same day, and nitrate was analyzed only at the biofilter effluent. Mean ammonium at the biofilter effluent was 0.07 ± 0.07 mg-N/L from the start of operation until Day 200, before increasing to 0.62 ± 0.45 mg-N/L from Day 200 to Day 335 (Figure 5). During the last month of operation, ammonium increased from around 0.5 mg-N/L on Day 335 to over 40 mg-N/L on Day 364. Mean nitrite at biofilter effluent was 0.11 ± 0.10 mg-N/L over the course of RAS operation. Nitrate concentration was initially

around 5 mg-N/L, increased to a maximum of 47 mg-N/L observed on Day 149, and then decreased to around 2 mg-N/L on Day 244. From then until end of system operation, average nitrate was 1.8 ± 0.7 mg-N/L.

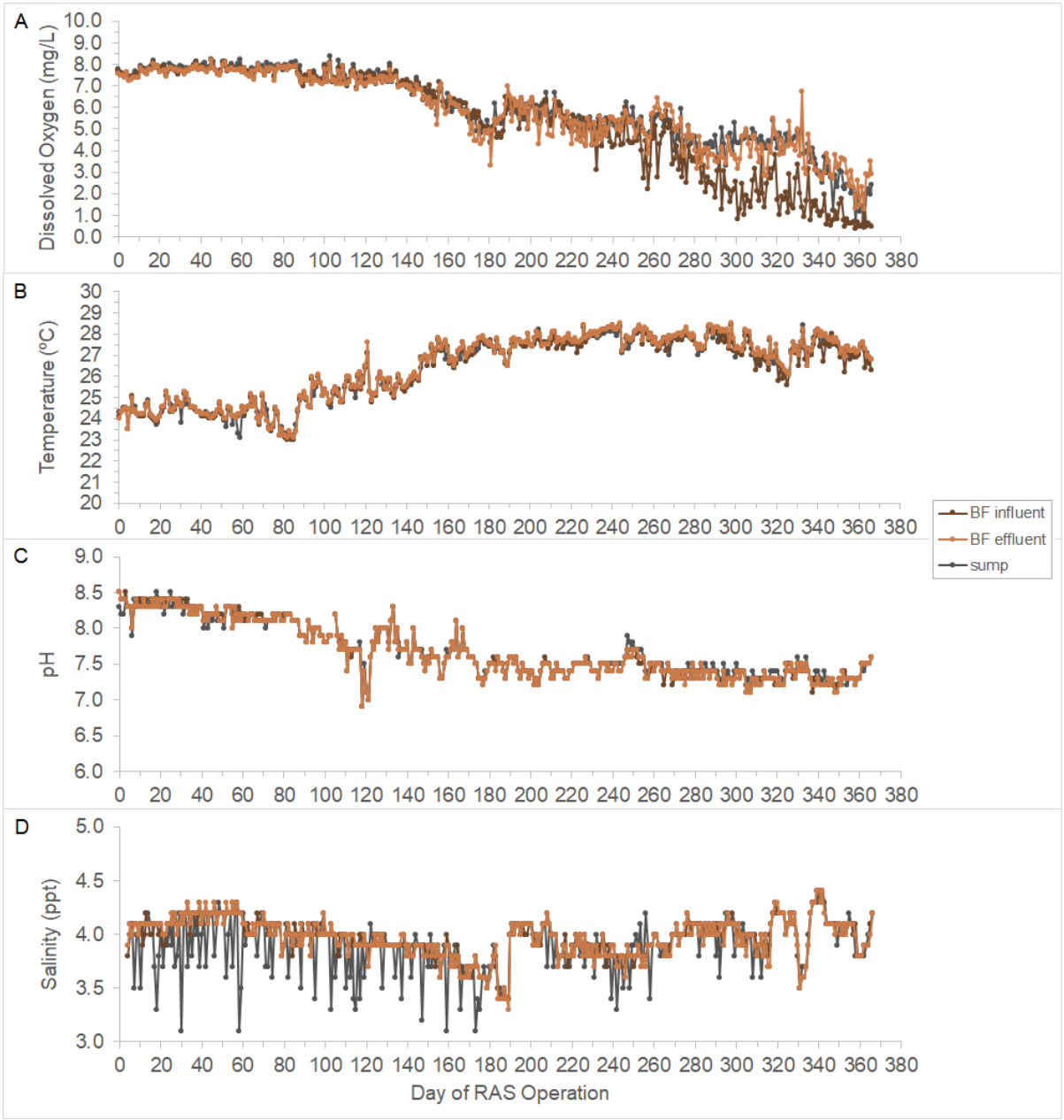

Figure 4. Daily values for (A) DO (mg/L), (B) temperature (ºC), (C) pH, and (D) salinity (ppt) at the biofilter influent, biofilter effluent, and sump tank over 366 days of RAS operation.

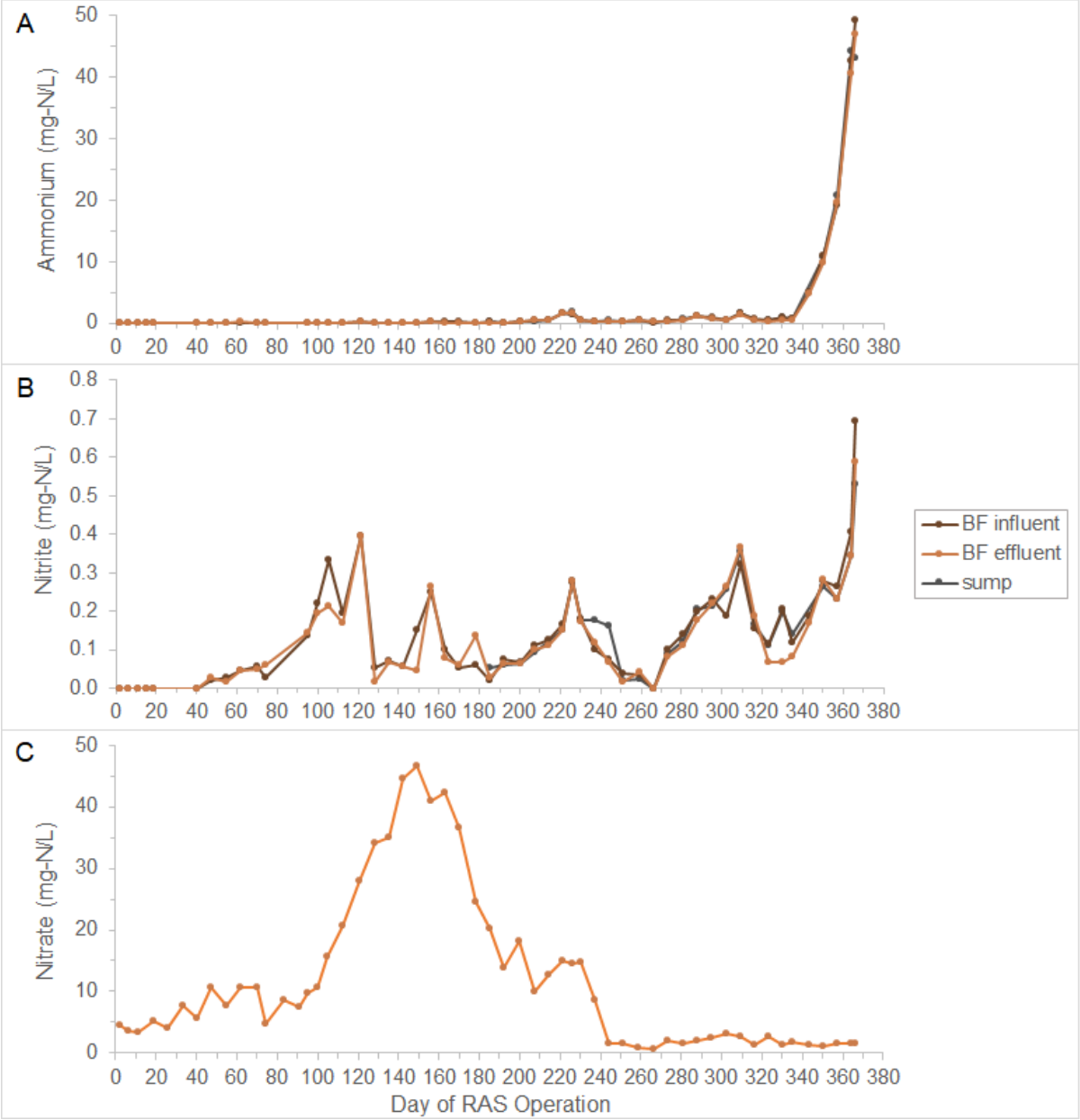

Figure 5. Concentration of (A) ammonium, (B) nitrite, and (C) nitrate measured in water samples collected weekly from the biofilter and sump tank during RAS operation. Nitrate was analyzed only in biofilter effluent samples. Sump tank water samples were collected and analyzed for ammonium and nitrite starting on Day 185.

During RAS operation, the biofilter media was colonized by brown biofilms growing on the available surfaces. Similar brown microbial biomass was also suspended in the surrounding water. In addition, an anoxic layer of black sludge was created as solids settled at the bottom of the biofilter.

Shrimp production metrics

The growth curves in Figure 6 describe the pattern of growth of cohorts, generated from weekly weighing of reared shrimp. Figure 6A is referenced to number of days since the RAS first began operation to illustrate when batches were stocked relative each other, whereas Figure 6B is referenced to number of days each batch has spent in the RAS to show differences in rearing duration and growth rate between different batches. One exception to note is that the Batch 2 ST1/MT cohort was not weighed while in the small tank. While the target for average shrimp weight at harvest was 20 g, only Batch 1 and 4 were reared to this size, with Batch 1 cohorts harvested at 20.4 ± 2.8 g and 21.6 ± 3.1 g and Batch 4 cohorts harvested at 21.0 ± 3.6 g and 20.3 ± 3.2 g. For logistical reasons, Batch 2 cohorts were harvested at 15.2 ± 4.4 g and 17.2 ± 4.0 g and Batch 3 was harvested at 14.2 ± 2.5 g. Batch 5 and 6 were concurrently lost to the die-off event after reaching an estimated 13.2 ± 2.1 g and 10.2 ± 1.4 g, respectively. Comparing the two batches that reached the target harvest weight of 20 g, Batch 1 needed 178 days in the RAS while Batch 4 needed only 126 days (Figure 6B). To consider growth of all batches by comparing when each reached 10 g, Batch 4 did so in the shortest duration, followed by Batch 6, Batch 5, Batch 3, Batch 2, and Batch 1.

Survival of shrimp over the course of rearing in RAS was calculated using two metrics, percent survival and weekly percent mortality (Figure 7). For Batch 5 and 6, survival metrics are based on estimates of how many survived until immediately before the die-off event. Percent survival was lowest in Batch 1 at 7.1% and 4.3%. It was 22.5% and 18.6% in Batch 2 and 25.0% in Batch 3. Higher survival was obtained in Batch 4 at 58.1% and 55.3%. For Batch 5 and 6, estimated hypothetical survival immediately before the die-off event was 50.7% and 63.0%, respectively (Figure 7A). Weekly percent mortality was highest in Batch 3 at 4.2%/wk. It was similar for Batch 1 and 2, with 3.6%/wk and 3/7%/wk for Batch 1 and 3.8%/wk and 4.0%/wk for Batch 2. Batch 4 had the lowest mortality rate at 2.3%/wk and 2.5%/wk. For Batch 5 and 6, the estimated hypothetical weekly percent mortality rates were 3.1%/wk and 3.0%/wk, respectively (Figure 7B).

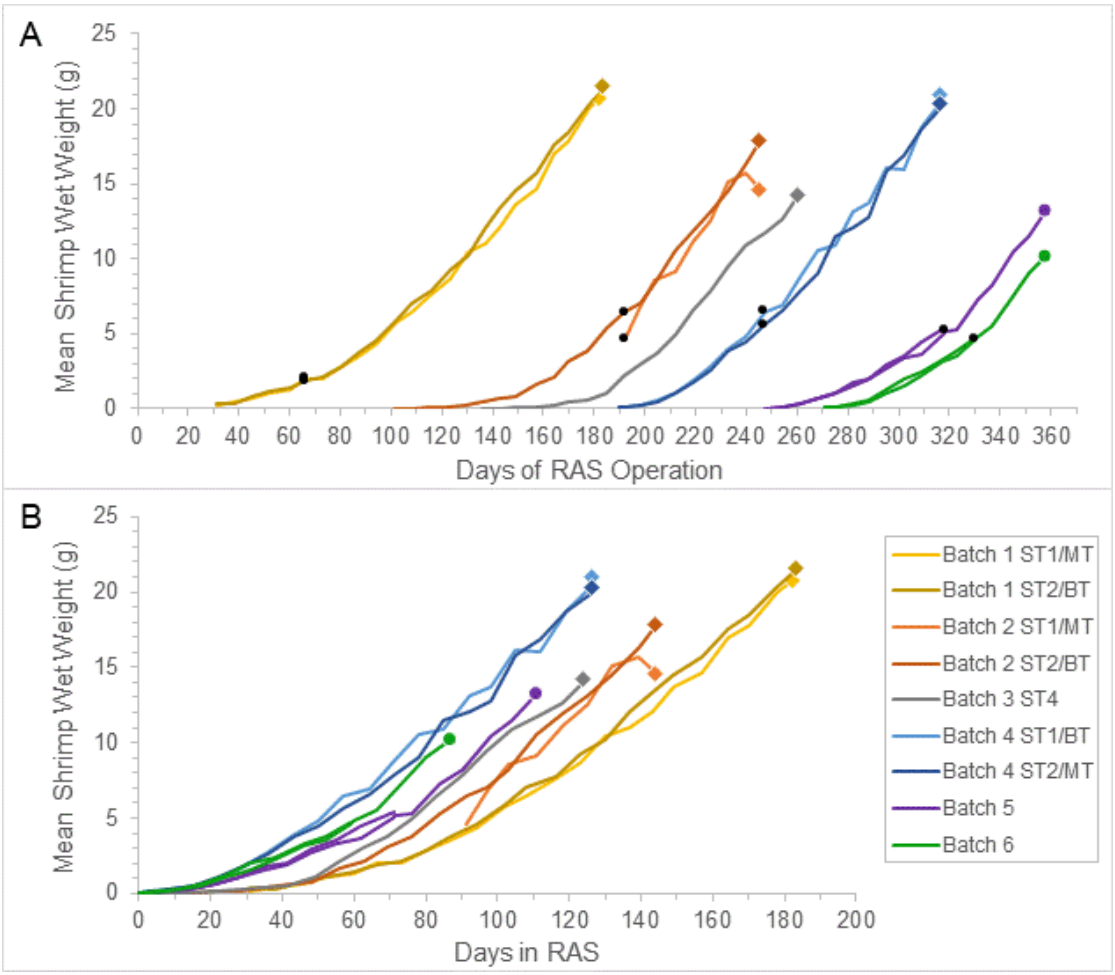

Figure 6. Growth curves generated from weekly weighing of at least 10% of shrimp in each tank. Mean wet weight (g) is plotted against (A) days since operation of RAS began and (B) days since initial stocking for each batch. Black points indicate the first weights measured after transfer into large rearing tanks. Harvest weights are indicated by diamond markers; for Batch 5 and 6, round markers indicate the last mean weights recorded prior to die-off.

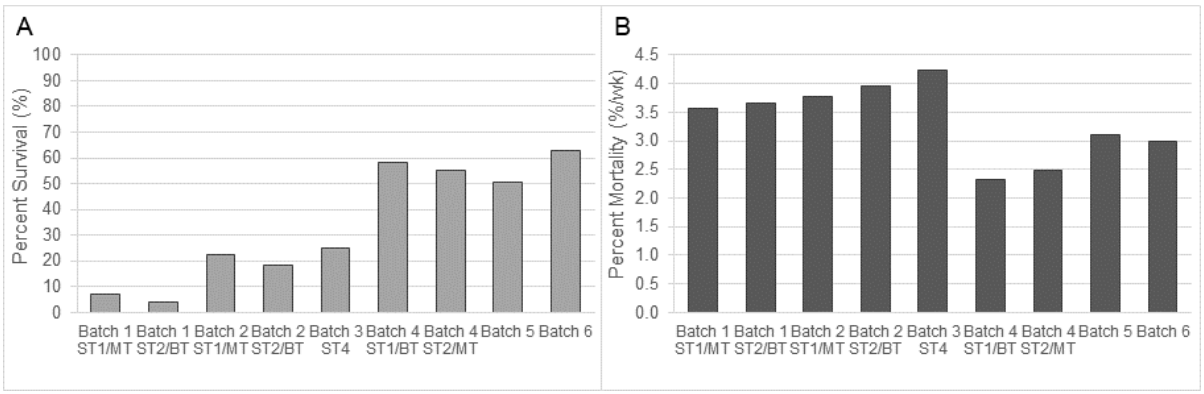

Figure 7. Shrimp survival as described by (A) percent survival (%) and (B) weekly percent mortality (%/wk). For Batch 5 and 6, hypothetical survival metrics are based on estimates of how many survived until immediately before die-off event.

As a function of stocking density, harvest weight, survival, and growth rate, yield varied for the batches reared (Figure 8). Yield was calculated relative to area of one large tank, except for Batch 3, which was calculated relative to small tank area. To reflect the space-saving benefit of stacked rearing tanks, Figure 8B shows yield for batches relative to the area of one large tank even if two cohorts were harvested from two large tanks concurrently. Therefore, combined yields for Batch 1, 2, and 4 were 0.10 kg/m^2-month, 0.28 kg/m^2-month, and 0.51 kg/m^2-month, respectively (Figure 8B), around twice as high in each case as yield of its cohorts considered separately (Figure 8A). For Batch 3, 4, 5, and 6, yield exceeded 0.5 kg/m^2-month (Figure 8B).

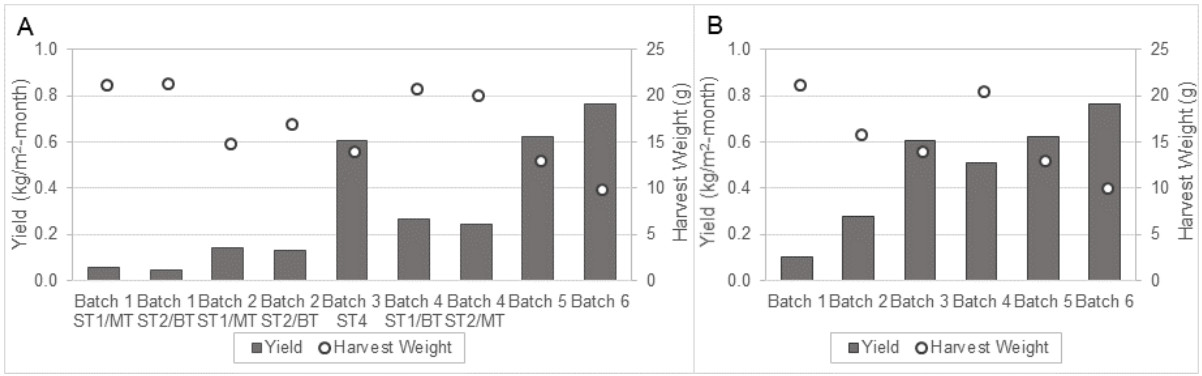

Figure 8. Yield (kg/m^2-month) at harvest shown alongside mean harvest weight achieved (g). Metrics are presented (A) for individual cohorts where possible and (B) as combined into whole batches for more direct comparison. For Batch 5 and 6, hypothetical yields immediately before the die-off event were estimated.

FCR was relatively low in Batch 2, 4, 5, and 6, ranging between 1.72 in Batch 4 and 2.13 in Batch 2. FCR was 3.06 for Batch 1 and 4.54 in Batch 3 (Figure 9).

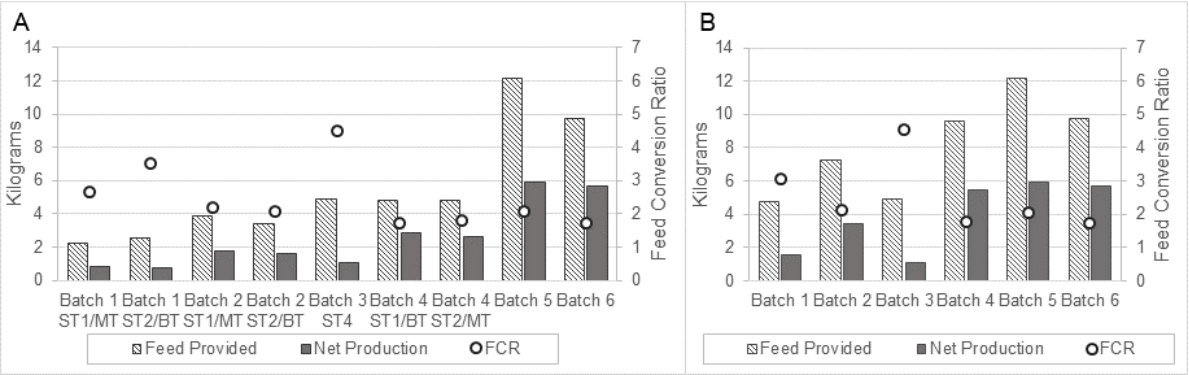

Figure 9. FCR calculated from feed provided (kg) and net production of shrimp (kg) from stocking to harvest. Metrics are presented (A) for individual cohorts where possible and (B) as combined into whole batches for more direct comparison. For Batch 5 and 6, net production and FCR before the die-off event were estimated.

Comparison of rearing in small versus large tanks

Based on shrimp weight at transfer and number of shrimp transferred from small to large rearing tanks, survival, net production, and FCR were compared between the two types of rearing tanks. Because transfer weight and number of shrimp transferred were not accurately measured for Batch 1, it was excluded from these comparisons. Batch 3 was also excluded, as it had remained in a small tank without transfer.

One difference between rearing in small versus large tanks is shrimp density. Each large tank has around six times the area as each small tank, and therefore both numerical and biomass density were reduced during transfer. For Batch 5 and 6, cohorts from two small tanks were combined into the same large tank, resulting in a three-fold reduction in density during transfer; other batches had a six-fold reduction. Numerical densities at transfer and harvest depend on number of shrimp stocked and survival during rearing, and biomass densities depend additionally on growth rate. For all batches, numerical density showed a continually decreasing trend with increasing mortalities, whereas biomass density relative to the same tank increased due to shrimp growth (Table 5, Table 6). Biomass density in small tanks at transfer was higher than in large tanks at harvest (Table 6).

Percent survival at the time of transfer was quite similar to percent survival at harvest, indicating that a greater percentage of mortalities occurred in small tanks compared to large tanks. Survival at harvest relative to shrimp transferred was between 82.6% to 97.0% across Batch 2, 4, 5, and 6 (Figure 10A). Weekly percent mortality rate was higher during the period when smaller shrimp were reared in small tanks compared to the entire duration of grow-out (Figure 10B).

Table 5. Numerical density (shrimp/m^2) at stocking, transfer, and harvest. Numerical density in small tanks is number of shrimp divided by tank area of 0.44 m^2, and numerical density in large tanks is number of shrimp divided by tank area of 2.61 m^2.

	Stocking Density in Small Tank	Transfer Density in Small Tank	Transfer Density in Large Tank	Harvest Density in Large Tank
Batch 1 ST1/MT	1273	estimated 167	estimated 28	15
Batch 1 ST2/BT	1849	estimated 284	estimated 48	13
Batch 2 ST1/MT	1164	302	51	44
Batch 2 ST2/BT	1164	223	38	37
Batch 3 ST4	694	173*	n/a	n/a
Batch 4 ST1/BT	527	329	56	52
Batch 4 ST2/MT	529	333	57	50
Batch 5 ST1/BT	1000	685	209	172
Batch 5 ST2/BT	1000	543		
Batch 6 ST3/MT	998	709	233	214
Batch 6 ST3/MT	998	660		

*As Batch 3 remained in ST4 for the entirety of rearing, 173 shrimp/m^2 is its harvest density in small tank.

Table 6. Biomass density (kg/m^2) at stocking, transfer, and harvest. Biomass density in small tanks is biomass divided by tank area of 0.44 m^2, and biomass density in large tanks is biomass divided by tank area of 2.61 m^2.

	Stocking Density in Small Tank	Transfer Density in Small Tank	Transfer Density in Large Tank	Harvest Density in Large Tank
Batch 1 ST1/MT	0.059	estimated 0.26	estimated 0.043	0.33
Batch 1 ST2/BT	0.086	estimated 0.44	estimated 0.075	0.29
Batch 2 ST1/MT	0.016	1.51	0.26	0.67
Batch 2 ST2/BT	0.014	1.47	0.25	0.63
Batch 3 ST4	0.010	2.46*	n/a	n/a
Batch 4 ST1/BT	0.028	2.02	0.34	1.09
Batch 4 ST2/MT	0.021	1.86	0.32	1.01
Batch 5 ST1/BT	0.029	3.43	1.08	2.28
Batch 5 ST2/BT	0.032	2.91		
Batch 6 ST3/MT	0.040	3.21	1.07	2.18
Batch 6 ST3/MT	0.041	3.07		

*As Batch 3 remained in ST4 for the entirety of rearing, 2.46 kg/m^2 is its harvest density in small tank.

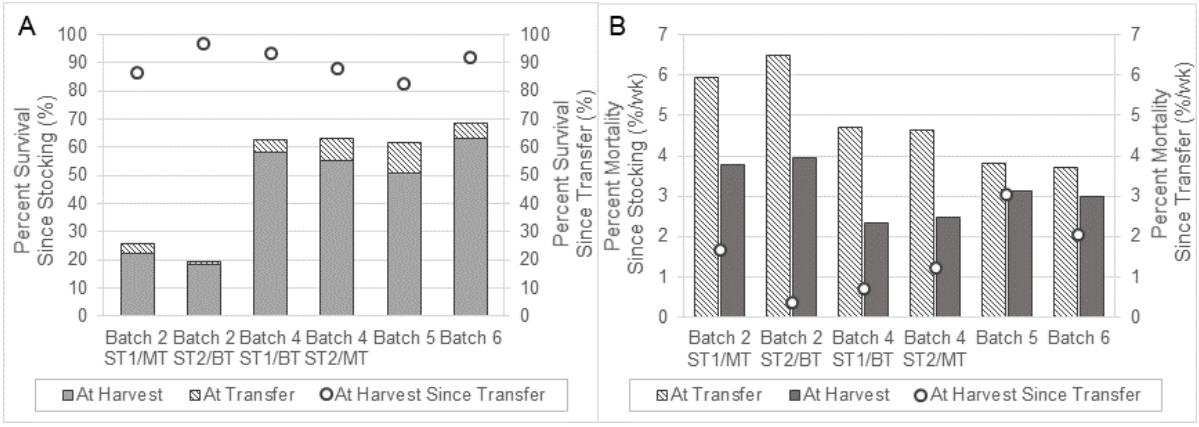

Figure 10. Comparison of (A) percent survival (%) and (B) weekly percent mortality rate (%/wk) at transfer and at harvest. Points represent survival or mortality rate in large tanks alone, calculated with respect to number of shrimp transferred. For Batch 5 and 6, hypothetical survival metrics are based on estimates of how many survived until immediately before the die-off event.

Another difference between shrimp reared in small tanks and large tanks was their body weight. Mean wet weight at time of transfer was between 4.6 g and 6.6 g across Batch 2, 4, 5, and 6 (Figure 11). For the timing of transfer and harvest employed with these batches, net production in large tanks was higher than in their corresponding small tank (Figure 11). Rate of net production was 1.8 to 2.5 times higher in large tanks than in small tanks (Figure 12).

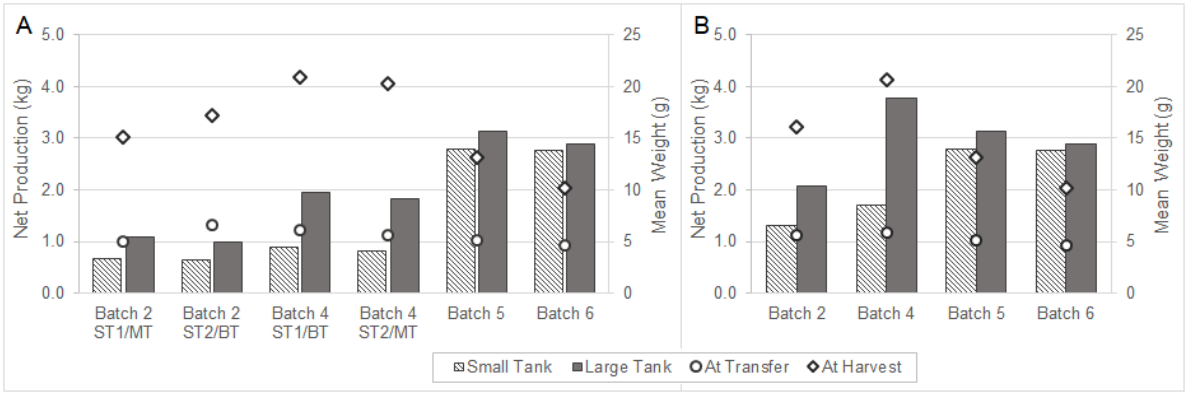

Figure 11. Comparison of net production (kg) in small versus large rearing tanks, shown alongside mean shrimp weight at transfer and at harvest. Metrics are presented (A) for individual cohorts where possible and (B) as combined into whole batches for more direct comparison. For Batch 5 and 6, net production before the die-off event was estimated.

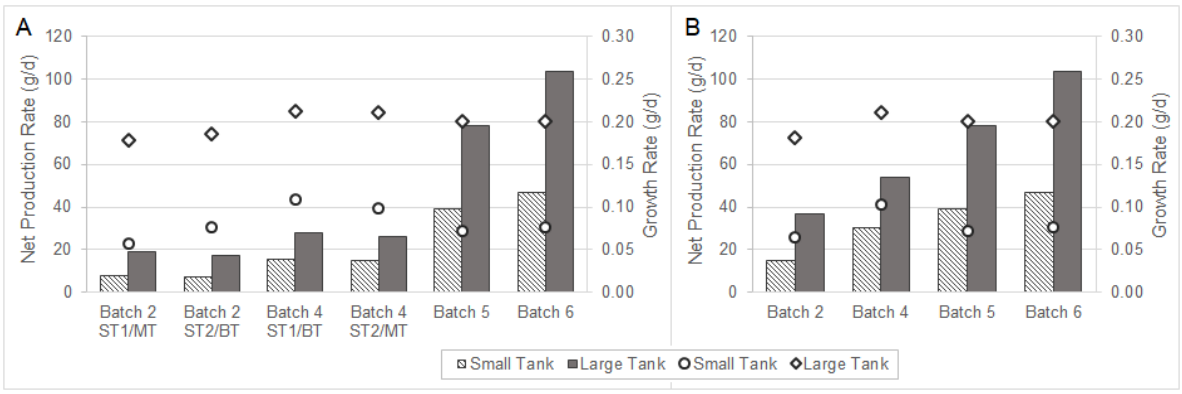

Figure 12. Comparison of net production rate (g/d) in small versus large rearing tanks, shown alongside growth rate (g/d) of shrimp reared in the two types of tanks. Metrics are presented (A) for individual cohorts where possible and (B) as combined into whole batches for more direct comparison. For Batch 5 and 6, net production before the die-off event was estimated.

FCR was between 10% and 21% lower in large tanks than small tanks for Batch 2, 4, 5, and 6 (Figure 13).

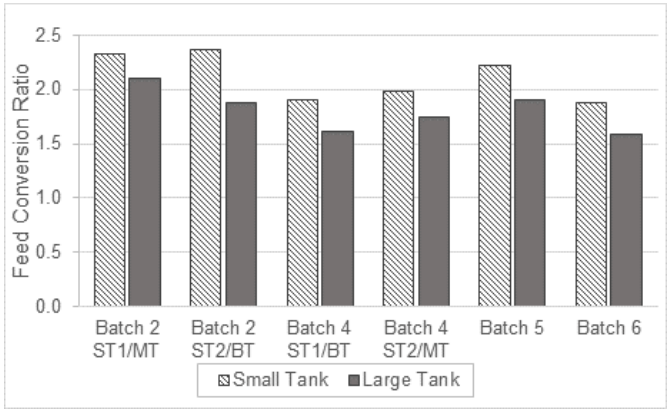

Figure 13. Comparison of FCR in small versus large rearing tanks. For Batch 5 and 6, FCR before the die-off event was estimated.

Shrimp growth parameters

Shrimp growth during grow-out in RAS was described by growth rate, SGR, and DGC. As these parameters vary with initial weight, and accurate initial weights at stocking were not obtained for Batch 1, it was excluded from growth parameter calculations. For the other batches reared, growth parameters were calculated for and plotted against shrimp weights recorded weekly relative to initial weight (Figure 14). While growth rate in grams per day increased with increasing shrimp weight, growth rate in percent of weight per day

decreased. Similarly, SGR also decreased with increasing weight. Compared to SGR, DGC did not vary with shrimp weight as much; for Batch 4, maximum SGR was more than 4 times the minimum SGR, whereas maximum DGC was less than 2 times the minimum DGC.

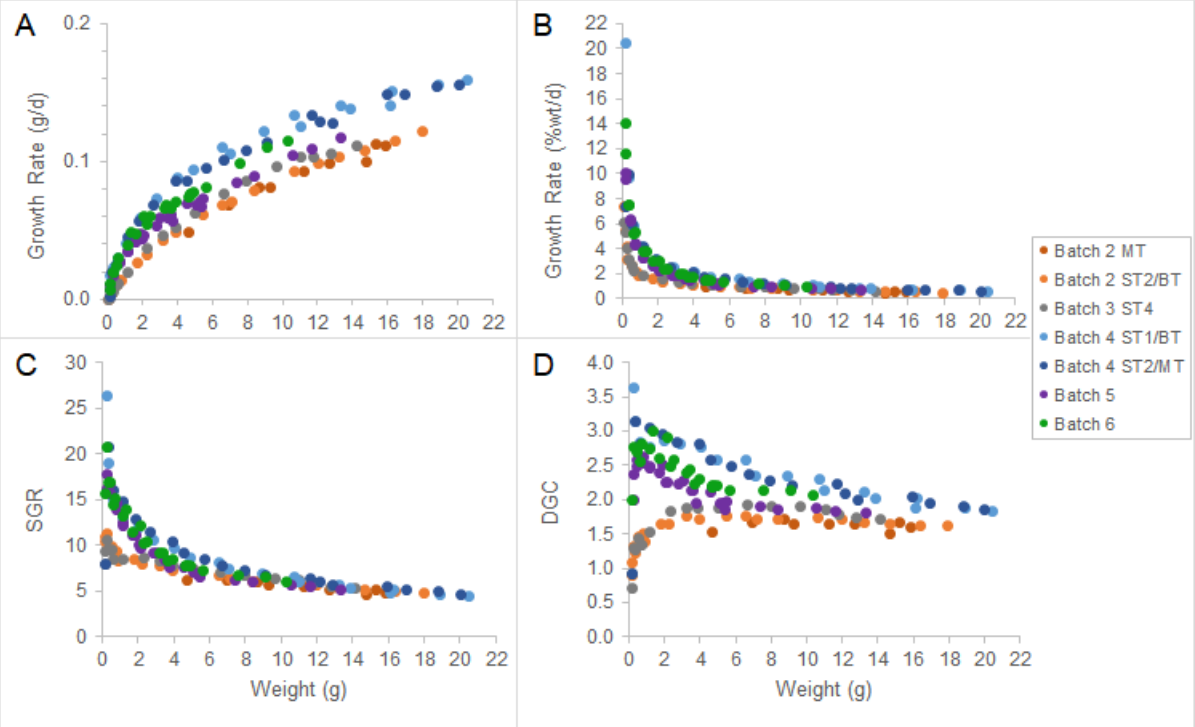

Figure 14. (A) Growth rate (g/d), (B) growth rate (% weight/d), (C) SGR, and (D) DGC calculated for corresponding weight (g) with respect to initial weight.

Comparison of shrimp production with experimental systems from literature

Rearing condition and shrimp production data compiled from literature studies are graphed alongside the same metrics from my current study in Figure 15–24. For all literature comparison graphs, marker colors correspond to the culture system types indicated in Table 2. For graphs sorting metrics by Study ID, Table 2 shows the reference citations corresponding to each ID. Note that not all data points may be visible due to overlap. Most metrics have 75 values graphed, with a few exceptions as follows. Initial weight was not reported in one study, giving a total of 69 reference values for initial weight as well as biomass stocking density, SGR, TGC, and DGC, which could not be calculated without initial weight. FCR was only reported in 10 of the 17 studies cited, giving a total of 33 reference values.

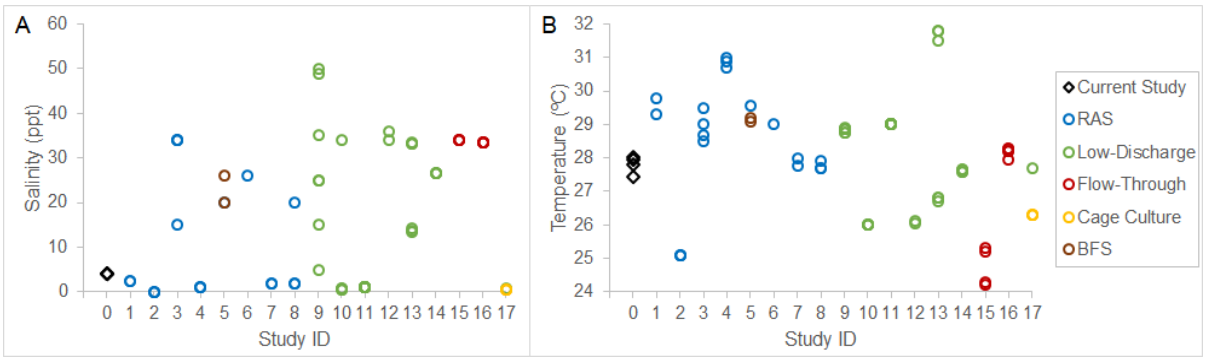

Figure 15. Range of reported (A) salinity (ppt) and (B) temperature (ºC) conditions at which shrimp were cultured.

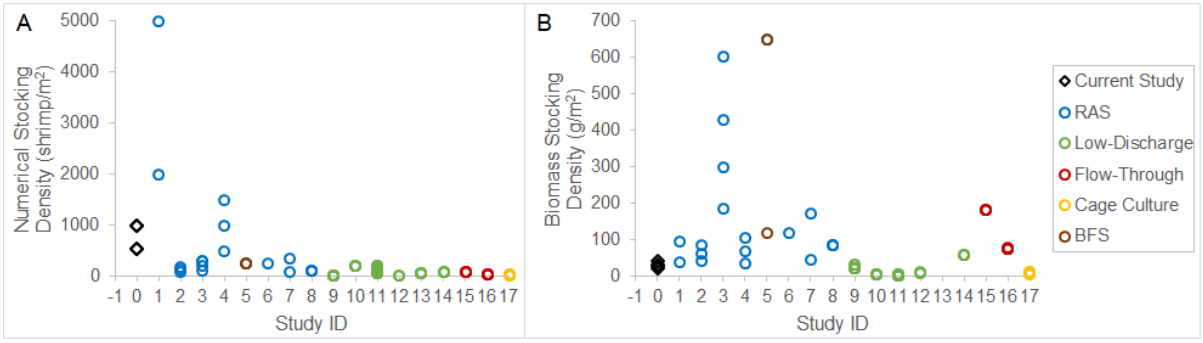

Figure 16. (A) Reported numerical stocking density (shrimp/m^2) and (B) calculated biomass stocking density (g/m^2) of shrimp growth runs.

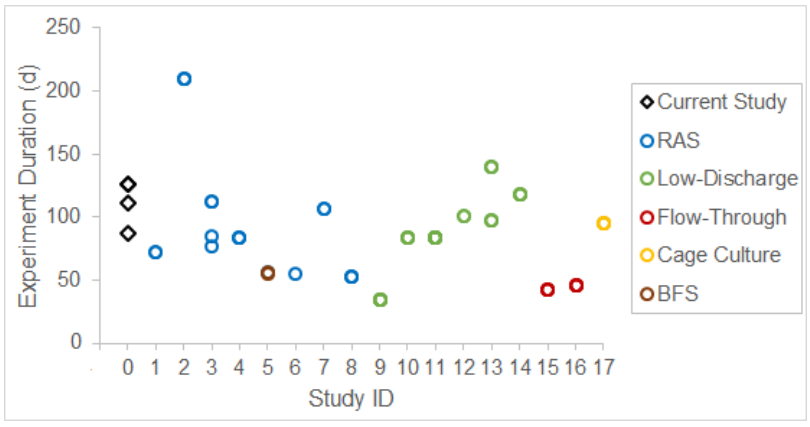

Figure 17. Reported duration (d) of shrimp growth runs.

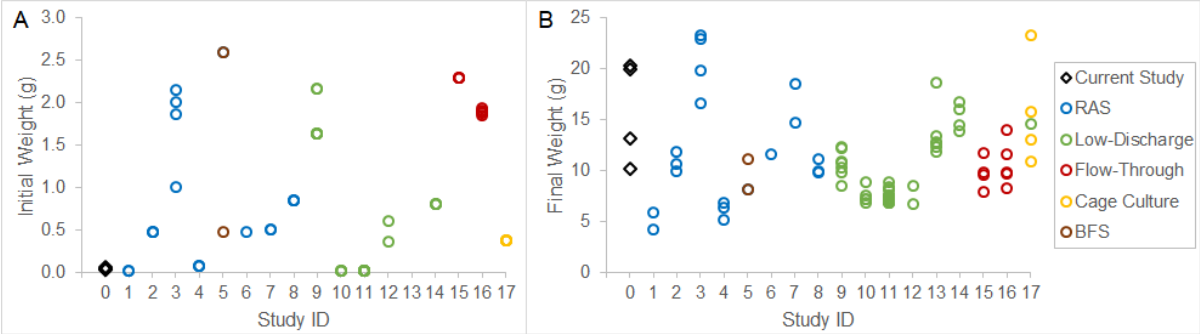

Figure 18. Reported mean (A) initial shrimp weight (g), (B) final shrimp weight.

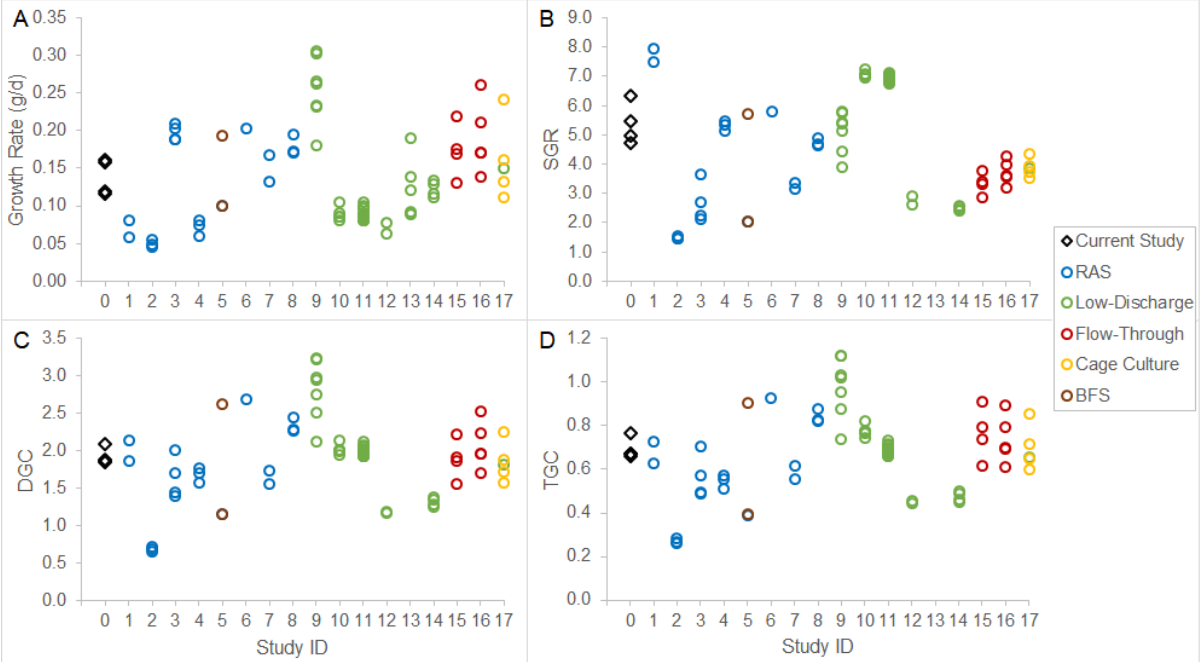

Figure 19. Overall (A) growth rate (g/d), (B) SGR, (C) DGC, and (D) TGC calculated using initial weight, final, weight, and experiment duration.

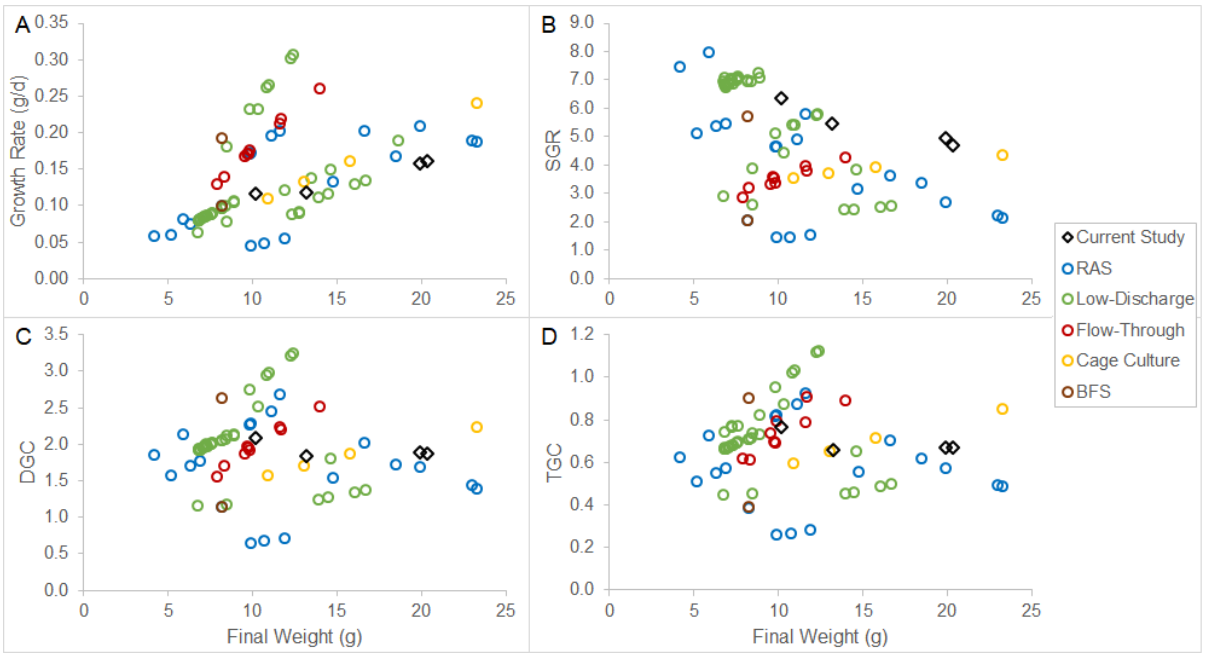

Figure 20. Overall calculated (A) growth rate (g/d), (B) SGR, (C) DGC, and (D) TGC versus reported final weight (g).

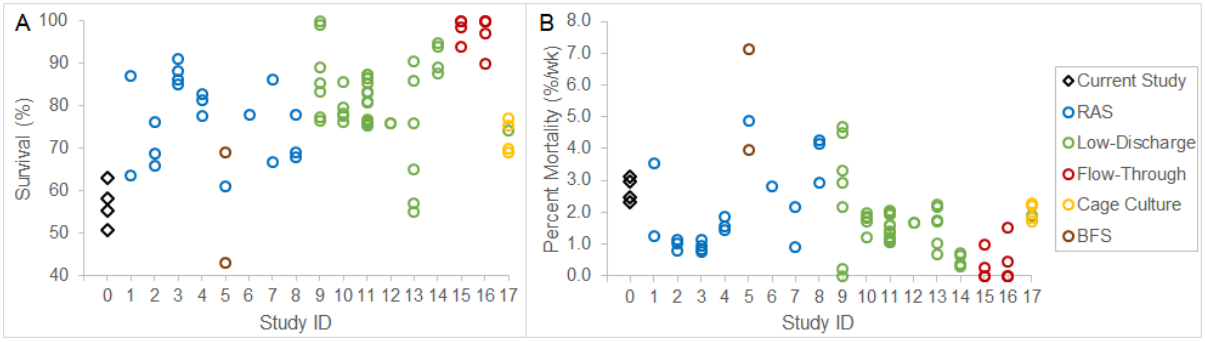

Figure 21. (A) Percent survival (%) reported and (B) weekly percent mortality rate (%/wk) calculated using percent survival and experiment duration.

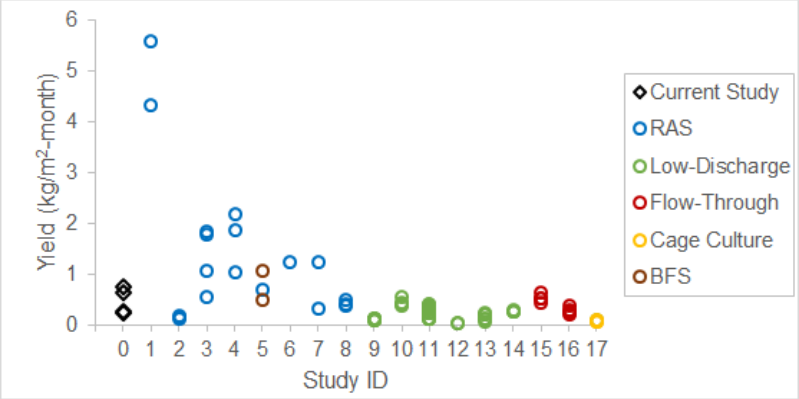

Figure 22. Yield (kg/m^2-month) calculated using reported stocking density, percent survival, final weight, and experiment duration.

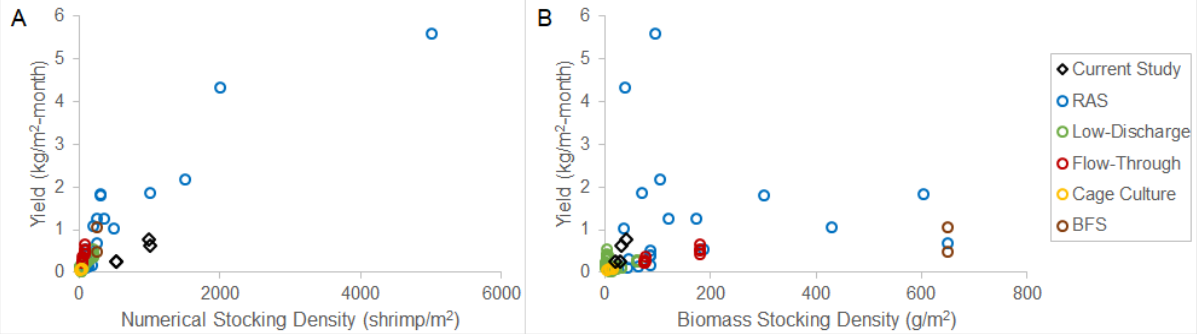

Figure 23. Calculated yield (kg/m^2-month) versus (A) reported numerical stocking density (shrimp/m^2) and (B) calculated biomass stocking density (g/m^2).

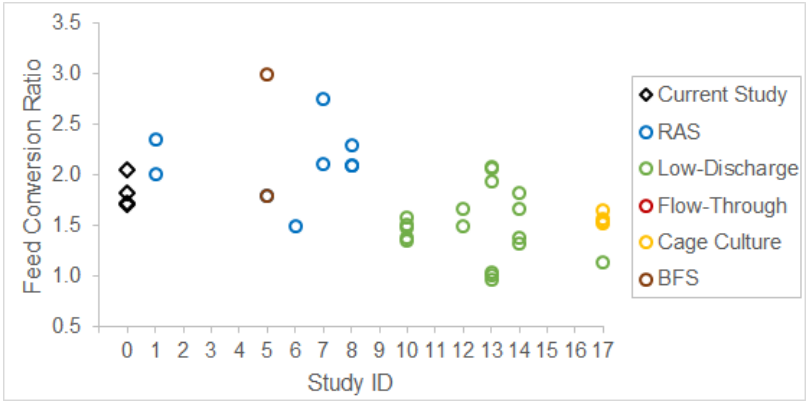

Figure 24. Reported FCR values.

Pilot Discussion

Shrimp production improved with better system management

The following discussion of shrimp production across different batches will be based on a hypothetical harvest of Batch 5 and 6 on Day 357, the day when shrimp were weighed for the last time preceding the die-off event. The last mean weight measured was used as harvest weight, while number of shrimp harvested was estimated as the number of shrimp corpses collected on Day 366, after the die-off event. In turn, all production metrics based on harvest conditions are hypothetical for Batch 5 and 6. Through this hypothetical harvest, I can approximate the rearing progress that was made prior to the die-off event and can thereby compare production across all six batches.

Though only Batch 1 and 4 were reared until the target harvest weight of 20 g, the other batches also achieved marketable sizes, at between 10 g and 16 g (Figure 6). Growth was faster, and survival was higher in Batch 4, 5, and 6 than in Batch 1, 2, and 3 (Figure 6B; Figure 7). These improvements were due to, at least in large part, adjustments in different aspects of system management. For Batch 1, 2, and the first six weeks for Batch 3, amount of feed provided each day was gradually increased based on visual inspection of whether previously provided feed remained uneaten. The feeding method was improved for Batch 4, 5, and 6 by estimating current shrimp biomass from weekly weight measurements in conjunction with expected survival rate, so that feed could be provided according to the manufacturer's feeding table. When comparing amount fed for earlier versus later batches, it became evident that Batch 1, 2, and 3 had been severely underfed, which likely caused slower growth and a higher mortality rate due to starvation. Apart from underfeeding, another factor contributing to much slower growth in Batch 1 is that average water temperature was around 2 ºC lower compared to other batches reared (Table 4). This temperature difference occurred because fewer heaters were in the RAS when fewer rearing tanks contained shrimp. Within the range of 20–30 ºC, *L. vannamei* growth is directly correlated to temperature when not limited by feed availability (Wyban et al. 1995, Ponce-Palafox et al. 1997). Another improvement to the system was the installation of rigid screens to enclose rearing tanks, which prevented shrimp in Batch 4, 5, and 6 from jumping out of rearing tanks as they had in earlier batches. After adjusting feeding methods and installing

containment screens, survival rates more than doubled compared to the first three batches (Figure 7A).

In addition to faster growth and higher survival, the last three batches reared had relatively low FCR: 1.76 in Batch 4, 2.06 in Batch 5, and 1.72 in Batch 6 (Figure 9B). This improved FCR was likely enabled in large part by increased survival in these batches. With fewer shrimp dying before harvest, FCR would reflect better feeding efficiency, because all shrimp that die before harvest represent a waste of the feed they had consumed during rearing. However, a fraction of this consumed feed could be retained, as dead shrimp were not removed from rearing tanks, and their embodied nutrients were consumed by other shrimp. Batch 3 had the highest FCR at 4.54, more than double that of Batch 4, 5, and 6. This especially high FCR likely resulted from the change in feeding procedure partway through its rearing period. After being underfed during the initial six weeks of culture, a large fraction of shrimp had likely already died in that period. However, in the subsequent effort to feed according to feeding table, shrimp biomass remaining in the tank was overestimated, leading to overfeeding and a corresponding elevated FCR.

Stacked tanks and rotational stocking contribute to higher yield in RAS

Yield is a measure of production that accounts for how much area and time are required, with higher yields indicating more intensive farming. One feature of the RAS design is that rearing tanks are stacked vertically, thus reducing system footprint. To reflect this benefit, yields for batches reared were calculated relative to the area of one large tank even if two cohorts were harvested from two tanks concurrently. Yields presented in Figure 8 do not account for biofilter and sump tank footprint, which is around 1.32 m^2 in combined area. Yields calculated relative to total system footprint instead would be 34% lower for all batches except Batch 3. For this batch, yield was calculated relative to area of a small rearing tank, so including biofilter and sump tank area would reduce yield by 75%.

Another aspect of RAS design is the capacity for rotational stocking and harvest, wherein the six rearing tanks enable three batches to be reared concurrently. A distinction should therefore be made between yield of individual batches and yield of the overall RAS. Over the 366-day operational period, a total of 23.2 kg of shrimp were harvested. With respect to area of a large rearing tank, this harvested biomass corresponds to an overall RAS

yield of 8.9 kg/m^2-yr or 0.74 kg/m^2-month. In contrast, the mean of yields calculated for the six batches individually is 0.48 kg/m^2-month (Figure 8). That yield of the overall RAS is higher than mean yield across individual batches is an outcome of rotational stocking and harvest, because yield corresponding to an individual batch does not account for any growth progress in concurrently reared batches.

Production metrics tended to be better in large tanks than small tanks

Except for Batch 3, all batches first occupied small rearing tanks then large rearing tanks. Shrimp weight at transfer and number of shrimp transferred were not accurately measured for Batch 1, but production could be compared between small and large tanks for Batch 2, 4, 5, and 6. Differences between small and large tanks were consistent across batches. The most distinct difference was in survival; most of the reduction in survival occurred while shrimp were in small tanks, with 82.6% to 97.0% of shrimp transferred to large tanks surviving until harvest (Figure 10A). FCR was consistently marginally lower in large tanks compared to small tanks (Figure 13) despite the tendency of FCR to increase with shrimp size, suggesting that higher survival in the large tanks enabled lower FCR.

Net production was higher in large tanks than small tanks, indicating that a greater fraction of total net production took place after the transfer of shrimp (Figure 11). While survival and growth rate are factors, how net production is distributed across small and large tanks reflects most directly the timing of shrimp transfer and harvest. As an illustration of this, large tank net production for Batch 4, which grew to the greatest harvest weight, was 122% higher than small tank net production. For Batch 6, which grew to the least weight, net production in the large tank was only 5% greater than in the small tanks. As long as shrimp growth rate is positive, net production increases with additional time spent in a rearing tank. Normalizing by time spent in each tank, daily rate of net production gives a clearer comparison of production in small versus large tanks. Net production rate was consistently higher in the large tanks, ranging from 1.8 to 2.5 times the rate in small tanks (Figure 12). This trend seems to reflect the faster absolute growth rate of larger shrimp compared to smaller shrimp (Figure 12, Figure 14A), with additional influence from the observed disparity in survival during rearing in large versus small rearing tanks.

Lower survival in small tanks may result from several factors

Comparing shrimp production before and after the implementation of an improved feeding procedure, I found that underfeeding of shrimp in Batch 1, 2, and 3 seemed to contribute to low survival in those batches, in conjunction with insufficient containment of shrimp. It is likely that management of feeding could be further improved to attain higher survival in future batches reared in the RAS. For Batch 4, 5, and 6, feed ration for shrimp in small tanks ranged from 80% of biomass upon stocking to around 4.6–4.8% of estimated shrimp biomass near time of transfer. Compared to actual transfer biomass, Batch 4 was slightly overfed right before transfer, while Batch 5 and 6 were slightly underfed, as referenced to the Rangen feeding table. During rearing in small tanks, feed amounts were calculated weekly by estimating an 80% survival from stocking to transfer, assuming survival decreases linearly, and projecting mean shrimp weight for each following week based on previously measured shrimp weights. Because it was only possible to base ration calculations on an estimate of current shrimp biomass dependent on multiple uncertain factors, there was much room for error in calculating how much feed to provide, thereby creating the possibility of underfeeding. To assess whether decreases in survival were due to insufficient feed provision, future experiments could compare survival in Batch 4, 5, and 6 against survival in batches given more feed at several successively higher levels. Because overfeeding decreases FCR and exerts additional nutrient loading on the system, it is important to determine how much feed is just enough for optimal survival and growth.

Another possible reason for the difference in survival between small and large rearing tanks is that high shrimp densities can impose a negative effect on survival. A primary difference in rearing conditions before and after transfer is higher shrimp density in small tanks. Numerical density was highest at initial stocking into small tanks and then decreased due to mortalities and increase in tank area at transfer (Table 5). Biomass density was also highest in the small tanks, though at transfer rather than at stocking (Table 6). While numerical density was very high at stocking, corresponding biomass density was miniscule due to the small shrimp size at that point. Compared to numerical density, biomass density likely relates more directly to density-dependent mortality, as it accounts for number as well as size of shrimp. Experiments could be done in my RAS to examine the possibility that that

high densities experienced by shrimp when in small tanks may contribute to the greater reduction in survival observed especially when crowding intensifies as shrimp approach the 4.6- to 6.6-g transfer weight. Assuming biomass density does impact survival, transferring shrimp to large tanks during rearing seems to be an effective way to reduce mortalities by reducing biomass density six-fold through additional tank area.

There is some literature evidence that survival is negatively correlated to stocking density. In a 210-day growth trial of *L. vannamei* in a freshwater RAS, percent survival significantly decreased with increasing stocking density, with 76.1% survival in the 90 shrimp/m^2 treatment versus 65.9% survival in the 180 shrimp/m^2 treatment (Araneda et al. 2008). In a study of *L. vannamei* culture in semi-closed RAS at a series of stocking densities from 28.4 to 281.4 shrimp/m^2, Williams et al. (1996) found 95% survival at lower densities and around 82% survival at higher densities after 49 days, though the effect was not statistically significant. However, the same study did demonstrate a significant inverse relationship between stocking density and survival for *L. setiferus* (Williams et al. 1996). Esparza-Leal et al. (2010b) found survival after 84 days was 77.6% for shrimp stocked at 1500/m^2, compared to 82.8% for shrimp stocked at 500/m^2, but this difference was not significant. In a 12-week study of shrimp growth in tanks of low-salinity well water at different stocking densities, there were no significant differences in survival for shrimp cultured at 50, 100, 150, and 200 shrimp/m^2 (Esparza-Leal et al. 2010a). Literature studies do not converge on a consistent relationship between survival and stocking density, possibly due to differences in culture system and other aspects of rearing management. Another limitation is that biomass density is not quantified in these studies, and considering only numerical density fails to account for potential conflating effects of shrimp size, as biomass density is not analyzed for relationship to survival.

By nature of the rotational stocking and transfer schedule, another key difference between small versus large tanks is shrimp weight. For Batch 2, 4, 5, and 6, mean shrimp weight at transfer was 4.6–6.6 g (Figure 11). It is possible that smaller shrimp are inherently less likely to survive than larger shrimp, thereby causing lower survival in small tanks in the presence of environmental factors to which smaller shrimp are more sensitive. Size-specific mortality has been documented for an ornamental shrimp species, the banded coral shrimp *Stenopus hispidus*, through a tagging study in their natural ecosystem (Chockley and St.

Mary 2003). Though predation is a source of mortality in the wild but not applicable to shrimp reared in my RAS, there is evidence for size-dependent mortality in cultured organisms. Mortality-weight relationships were developed for fish using data from literature studies of both natural ecosystems and aquaculture, and a stronger negative correlation between fish weight and mortality was found in aquaculture than in natural ecosystems (Lorenzen 1996).

From my RAS, there is some evidence that handling of shrimp during weighing may negatively impact survival. Of the two Batch 2 cohorts, one was sampled and weighed weekly, whereas the other was not weighed between stocking and transfer. The weighed cohort, Batch 2 ST2, had a survival of 19.1% at transfer and a weekly mortality rate of 6.5%/wk in the small tank. The un-weighed cohort, Batch 2 ST1, had a survival of 25.9% and a weekly mortality rate of 6.0%/wk (Figure 10). These differences were larger between Batch 2 cohorts than between cohorts of the other batches, which were all weighed weekly (Figure 10). Batch 2 cohorts were fed the same amount as each other, and they were both underfed, limiting the ability to generalize an interpretation of the observed survival disparity. Because all cohorts were weighed weekly after transfer to large tanks, no comparison can be made between weighed and un-weighed cohorts for larger shrimp, and there is therefore no evidence that larger shrimp are more resistant than smaller shrimp to mortality associated with handling.

Production metrics were within ranges reported in literature

Shrimp growth runs cited from the literature were conducted at a range of rearing conditions. Salinity in cited runs ranged from 0–50 ppt, reflecting the euryhaline nature of *L. vannamei* (Figure 15A). Compared to the mean salinity of 15 ppt in cited runs, the 4 ppt level used in my RAS is on the lower end of brackish treatments. Range of temperature was 24–32 ºC, with temperatures in my RAS falling right around the mean of 28 ºC (Figure 15B). Shrimp stocking density in cited runs was between 10–5,000 shrimp/m^2, with the majority of runs employing much lower stocking densities than used in my RAS (Figure 16). Duration of growth runs ranged from 35–210 days in cited studies; my grow-outs of Batch 4 and 5 were among the longest, as only 16 of 75 reference runs exceeded 100 days (Figure 17). Correspondingly, shrimp in my study started at around 0.04 g, at the lower end of the range

of cited initial weights, and grew to a higher mean weight than that of cited studies (Figure 18). Specifically, shrimp in cited runs grew from 0.02–2.60 g to 4.2–23.3 g. Production in each study system is influenced by these rearing parameters, so it is difficult to directly compare production metrics from my study to those from cited studies in a quantitatively rigorous way. Therefore, my focus is to develop a general idea of how production in my RAS compares to production in other types of culture systems by identifying qualitative patterns.

From Figure 14, which shows different growth rate metrics versus shrimp weight, absolute growth rate increases with increasing shrimp weight, while SGR decreases. In comparison, DGC does not vary as much, but some effect from weight does occur (Figure 14D). Given these relationships and the broad range of final weights in cited studies, growth rate metrics were graphed against final weight to facilitate comparison between different studies (Figure 20). Growth in Batch 4, 5, and 6 was higher than in most RAS runs from the literature, especially for shrimp grown to around the same size. Among the other culture system types, some runs had higher growth, and some had lower growth compared to this current study. Overall, my RAS is demonstrated to support growth rates similar to those reported in other studies. However, survival in my RAS was lower than in most cited studies. Survival in literature runs ranged from 40–100% with a mean of 80.2%, much higher than the mean 57% survival in my study (Figure 21A). To account for varying experiment durations, weekly percent mortality rate was also compared, revealing a generally similar pattern of better survival in most cited studies than in my RAS (Figure 21B). Literature mortality rates ranged from 0–7.1%/wk with a mean of 1.8%/wk, less than the mean 2.7%/wk mortality rate in my study. As previously discussed, most mortalities occurred during rearing in my RAS when shrimp were in small tanks, with survival in the large tanks alone ranging from 83–93% in Batch 4, 5, and 6 (Figure 10). While weighing frequency varied across studies, there were no trends between weighing frequency and weekly percent mortality rate. Shrimp were weighed weekly, as in my study, in 47% of literature growth runs. The other half of reference growth runs weighed less frequently, either only at the beginning and end of the experiment or with more days between weighings. Of these runs, some had higher mortality, while others had lower mortality than observed in this study. So, less frequent weighing did not clearly correlate with lower mortality rates. However, it is possible that differences in when and how shrimp are sampled and handled during weighing

could exert relatively small effects on mortality that are obscured by other factors. Future efforts focused on improving shrimp survival will be essential to making production in my RAS more comparable to what has shown to be possible in reference systems.

A limitation to comparing yield across studies as a metric of system productivity is that differences in final weight (Figure 18B) can translate the same yield into different amounts of value generated. Keeping this caveat in mind, yield in my RAS ranged from 0.24–0.76 kg/m^2-month, lower than mean yield in RAS studies cited but higher than that in low-discharge tanks and ponds (Figure 22). In cited RAS studies, mean ± SD of yield was 1.34 ± 1.44 kg/m^2-month; if the two very high values in Appelbaum et al. (2002) are excluded, mean yield is 0.91 ± 0.68 kg/m^2-month. Meanwhile, in low-discharge systems, mean yield is 0.23 ± 0.13 kg/m^2-month. This difference in yield could be partly attributed to a difference in stocking density, as RAS tends to employ more intensive rearing than other systems (Figure 16). Generally, there is a direct relationship between stocking density and yield (Figure 23), and studies comparing treatments of differing numerical stocking density had higher yield in higher-density treatments (Appelbaum et al. 2002, Samocha et al. 2004, Browdy and Moss 2005, Mena-Herrera et al. 2006, Araneda et al. 2008, Cuvin-Aralar et al. 2009, Esparza-Leal et al. 2010b, 2010a). In both Esparza-Leal et al. studies, this pattern was statistically significant. To visualize the effect of stocking density, Figure 23 shows yield plotted versus both numerical and biomass stocking density. Because yield was not directly reported in most cited studies, it was calculated using stocking density, percent survival, and final weight, assuming that stocking density and yield would be normalized by the same tank, pond, or cage area. It appears that yields of batches in my RAS were not as high as expected given the high stocking densities used, and this may reflect the relatively low survival observed in my RAS (Figure 23).

Our ability to compare FCR across studies is more limited than for other parameters, as it was reported in only 10 of the 17 cited studies. Additionally, methodology for determining rations and providing feed varied between studies, and while all studies used commercial feeds, protein contained therein ranged from 35–50%. FCR in my RAS ranged from 1.70–2.06, lower than mean FCR in other RAS studies but higher than mean FCR in low-discharge systems (Figure 24). Specifically, mean FCR was 2.12 ± 0.38 in cited RAS studies and 1.49 ± 0.34 in cited low-discharge systems. Because the low-discharge systems

were tanks, lined ponds, or earthen ponds either outdoor or in a greenhouse, natural productivity could develop and contribute to the diet of shrimp reared in these systems. For example, in one study, there were between 43,000–854,000 phytoplankton/mL measured in outdoor rearing tanks, with diatoms making up the majority of phytoplankton observed (Bray et al. 1994). The presence of diatoms has been shown to enhance shrimp growth, with growth rates 89% higher in unfiltered pond water compared to clear well water (Moss et al. 1992). By deriving nutrition needed for growth from natural production, shrimp require less nutritional input from formulated feed, thereby enabling reductions in FCR compared to RAS environments that do not support natural production.

Low ammonium was maintained for most of RAS operation

For around 11 months of operation, sufficient ammonium removal was achieved in the RAS biofilter, maintaining average ammonium levels below 1 mg-N/L in most rearing tanks (Table 5). Li et al. (2007) found that for *L. vannamei* acclimated to 3 ppt salinity, no mortalities occurred during 96 h of exposure to ammonia-N concentrations up to 4 mg-N/L. Because un-ionized ammonia is toxic to shrimp, whereas ammonium is not, it is useful to understand this toxicity threshold in terms of un-ionized ammonia concentration. The toxicity assay carried out by Li et al. (2007) had experimental conditions of temperature=29 ºC and pH=8.3. Applying a temperature-corrected pK_a value of 9.135, the TAN concentration of 4 mg-N/L corresponds to 0.51 mg-N/L of un-ionized ammonia at pH=8.3. For my RAS, most rearing tanks had an average pH between 7.8 and 7.3 (Table 4). For this pH range, the 0.51 mg-N/L ammonia toxicity threshold corresponds to between 12.4 and 38.2 mg-N/L of ammonium. For most of RAS operation, observed ammonium concentration remained below 1.7 mg-N/L (Figure 5A), much lower than the expected ammonia toxicity threshold.

Water samples analyzed for N-species concentration were collected before shrimp were given the second feeding of the day, around 8–10 hours after the first feeding. Samples collected from rearing tanks, biofilter influent and effluent, and the sump tank on the same day had approximately the same N-species concentrations. Though nitrification in the biofilter prevented accumulation of ammonium week to week, conversion kinetics were not characterized. To gain understanding of how ammonium fluctuates relative to shrimp feeding schedule and hydraulic behavior within the RAS, ammonium should be measured in a series

of samples collected at different time points after feeding and in different locations in the system. Results quantifying peak ammonium levels after feeding could confirm whether nitrification is able to remove excreted ammonium quickly enough to prevent toxic peak ammonia concentrations after feeding. In turn, this could inform better management; for example, if shrimp were found to be exposed to toxic peak ammonia levels, it may be advantageous to stagger when different rearing tanks are fed, instead of feeding all tanks at the same time.

Ammonium accumulation was observed leading up to shrimp die-off event

In the last month of operation, ammonium increased from around 0.5 mg-N/L on Day 335 to over 43 mg-N/L on Day 366 (Figure 5A). The die-off event which left virtually no surviving shrimp occurred around Day 362, when ammonium concentrations would have been approaching 40 mg-N/L. At that time, temperature in the large rearing tanks containing Batch 5 and 6 was 27.7 ºC, and pH was 7.5. In these conditions, ammonium concentration of 40 mg-N/L corresponds to 0.82 mg-N/L of un-ionized ammonia, exceeding the threshold for toxicity found by Li et al. (2007) and suggesting that the die-off event was due to ammonia toxicity. Failure of the biofilter to prevent the rapid accumulation of ammonia could be attributed to a few interrelated factors. Starting around Day 270, when DO was 3.6 mg/L at the influent and 5.0 mg/L at the effluent, biofilter DO steadily decreased, reaching 0.5 mg/L and 2.9 mg/L, respectively on Day 366 (Figure 4A). At lower depths of the biofilter, the microbial biomass was black in color, in contrast to lighter brown biomass present closer to the surface. From these observations, there seemed to be excessive microbial biomass accumulation which reduced available DO and created anoxic zones in the biofilter.

Because oxygen is required for nitrification at a ratio of 3.43 mg O_2 to 1 mg ammonia-N and 1.14 mg O_2 to 1 mg nitrite-N (Chen et al. 2006), failure of the biofilter to prevent ammonium accumulation in the last month of operation seems to be caused by nitrification rate becoming DO-limited instead of ammonium-limited. Based on a review of how DO affected nitrification activity in several conditions, Chen et al. (2006) noted that minimum DO needed for reliable nitrification is between 0.6 and 3.4 mg/L. This range is consistent with DO in my system as it dropped below the concentration needed to support reliable nitrification. Mean biofilter DO during the month of ammonium accumulation was

0.9 ± 0.5 mg/L at the influent and 2.9 ± 0.7 mg/L at the effluent. In contrast, for the preceding month when ammonium levels had been stable, mean biofilter DO was 2.2 ± 0.9 mg/L at the influent and 4.2 ± 0.8 mg/L at the effluent.

During the last month of system operation, pH tended to decrease, and addition of sodium bicarbonate every day or two was necessary to maintain relatively stable pH. This implies that nitrification was not completely inhibited, as alkalinity was still being consumed in the RAS. The tendency of pH to decrease may also indicate that alkalinity was low and therefore unable to buffer changes in pH. Mean pH in the last month of operation was 7.3 ± 0.1, and the lowest pH observed was 7.1 (Figure 4C). A study evaluating nitrifying biofilm activity at varying initial alkalinity levels found 45 mg/L as $CaCO_3$ to be the minimum alkalinity that did not impair nitrification rates (Biesterfeld et al. 2003). Leading up to the die-off event, nitrification in my RAS could have been limited by insufficient alkalinity, but it is hard to conclude without having measured alkalinity in the water samples collected.

Hydrogen sulfide and low DO could also have contributed to system destabilization

Hydrogen sulfide was detected in the system through its strong smell, which was released upon disruption of black sludge settled in the biofilter. Sulfate in commercial salt and mineralized from organic sulfur in feed and feces can be converted to hydrogen sulfide by sulfate-reducing microbes in anoxic conditions. Presence of hydrogen sulfide has been shown to inhibit nitrification in biofilms (Æsøy et al. 1998). In my RAS, hydrogen sulfide and low DO conditions both could have contributed to the inhibition of nitrification rates, leading to ammonia accumulation and shrimp die-off. Hydrogen sulfide may also have impacted shrimp survival directly, as it is toxic to aquatic animals (Avnimelech and Ritvo 2003). In a toxicity study on *L. vannamei*, the LC_{50} value of sulfide was determined to be 4254.8 µg/L, and exposure to a sublethal concentration of 425.5 µg/L was also associated with significantly lower survival after 21 days compared to control (Li et al. 2017). However, since hydrogen sulfide was produced at the bottom of the RAS biofilter, shrimp in the rearing tanks may not have been exposed to it. Additionally, because the die-off event occurred around when ammonia became elevated to a toxic concentration, ammonia toxicity was probably a larger factor in the shrimp mortalities than sulfide toxicity.

Nitrate removal was observed after initial period of accumulation

While anoxic zones in the RAS biofilter caused serious issues that led ultimately to the loss of two batches of shrimp, a potentially beneficial aspect is that the anoxic conditions enabled denitrification. High nitrate levels can occur in zero-exchange RAS that employ only nitrifying biofilters, as ammonium is continually excreted and converted to nitrate, which accumulates if there is no removal mechanism (van Rijn et al. 2006). Though toxicity of ammonia is of greater concern in aquaculture, chronic exposure to elevated nitrate has been found to impact *L. vannamei* production. In a 42-day study comparing shrimp reared at four different nitrate concentrations, survival, final mean weight, and final overall biomass were significantly lower at 425 mg-N/L of nitrate than in the 35-mg-N/L control. These production metrics were not significantly different for an intermediate 220-mg-N/L nitrate treatment compared to the control (Kuhn et al. 2010). When examining the interaction between nitrate toxicity and salinity, Kuhn et al. (2010) found that deleterious effects caused by culturing in 440 mg-N/L of nitrate were more severe at 2 ppt than at 9 or 18 ppt, suggesting that nitrate is more toxic at lower salinities. In my RAS, nitrate reached a peak concentration of 47 mg-N/L on Day 149 after an initial period of accumulation. Subsequently, nitrate concentrations gradually decreased, reaching around 2 mg-N/L on Day 244 and remaining near that level for the rest of RAS operation (Figure 5C). Had anoxic zones enabling nitrate reduction not developed at the bottom of the biofilter, it is possible that nitrate could have accumulated enough to affect shrimp production, particularly at 4-ppt salinity culture.

Continued improvements are needed to address issues arising with long-term operation

Though production in Batch 4, 5, and 6 was comparable to reference systems in the literature, Batch 5 and 6 could not be harvested as edible shrimp due to the die-off event caused by water quality issues following sludge accumulation in the system. Future operation of the RAS will only be possible in conjunction with operational changes to prevent sludge accumulation in the biofilter. Though the biofilter was configured as a MBBR with a filling of 65% by plastic biofilm carriers, most carriers did not move freely within the reactor, a defining feature of the MBBR configuration (Ødegaard et al. 1994). Typically, a grid of diffusers at the tank bottom both provide aeration and promote circulation of biofilm carriers (McQuarrie and Boltz 2011). In my biofilter, there was some biofilm carrier movement in the

water column directly above the three air stones. But most carriers remained stationary, with water flowing through the biofilter media. Because the air stones did not enable much water circulation, the relatively stagnant hydraulics allowed solids to accumulate at the bottom of the tank, creating conditions for anoxic sludge formation. To enable shrimp production over a longer period than was achieved in this study, a future iteration of the RAS should implement a more robust biofilter aeration system. In addition to preventing sludge formation and consequent inhibition of nitrification, ensuring adequate levels of oxygen and sufficient mixing promotes higher ammonium removal rates over the course of operation (Kamstra et al. 2017). Allowing the biofilm carriers to move freely would also address another issue with biofilter design experienced in this run, wherein carriers near the pipe connecting the biofilter and sump tank would partially block water from exiting the biofilter. As a result, if system recirculation rate was too high, water would overflow from the biofilter instead of flowing into the sump tank for recirculation. To avoid loss of water from the system, the pump used for recirculation of water was adjusted to the highest speed that would not cause overflows from the biofilter, resulting in a biofilter effluent flowrate of 0.29 L/s, around 25 m^3/d. Ideally, flowrates should be designed for ammonium removal from rearing tanks rather than be limited by overflow concerns. Future iterations of the biofilter, in which outlet pipe clogging is no longer an issue, will enable improved control of system flowrates.

Starting around Day 185 of system operation during this current study, suspended solids migrated from the biofilter into the sump tank, where they then settled. The solids seemed to primarily be microbial biomass, forming flocs along the walls and at the bottom of the sump tank. Air stones were placed in the sump tank to promote movement of the settled microbial flocs into rearing tanks. The motivation for this was to make the microbial flocs available for consumption by shrimp, as shrimp grown with biofloc culture can have better growth and FCR compared to shrimp grown in clear water (Xu and Pan 2012, Xu et al. 2012). A drawback to the presence of microbial flocs in the rearing tanks is that additional aeration is required, as enough oxygen must be provided for microbial respiration in addition to shrimp respiration. In my RAS, when Batch 5 and 6 were in the large rearing tanks, the water in those tanks was more turbid than in previous batches, indicating higher concentrations of microbes. More air stones were needed to maintain DO concentrations

above 5 mg/L compared to previous batches; instead of two per tank, Batch 5 and 6 each used seven air stones in their large rearing tanks.

In future operation, if circulation of water is improved in the biofilter through more rigorous aeration, microbial solids which had previously settled at the bottom would instead remain suspended. Consequently, these solids would flow into the biofilter to a greater degree than observed in my current study. To prevent development of anoxic sludge, management of the RAS will need to include removal of these solids from the biofilter. If they are directly pumped into the rearing tanks to contribute to shrimp diet, much more aeration would need to be provided in the rearing tanks. Otherwise, a mechanism can be developed to remove solids from the system, by either modifying the sump tank or adding a mechanical filter for solids removal to the RAS treatment train.

Waste streams from RAS operation could become resources

If future operation will involve removal of solids from the system, this will be a continuous waste stream requiring environmentally-sound disposal. To enhance sustainability of the RAS, the ideal treatment process would avoid negative environmental impacts of discharging nutrient-rich sludge while simultaneously generating value from this waste stream. In a 35-day feeding trial in a clear-water indoor RAS, good growth and survival were observed in shrimp fed diets with microbial floc replacing different fractions of fish meal (Kuhn et al. 2009). Microbial floc was produced in sequencing batch reactors processing wastewater from tilapia farm effluent with sugar added as a growth substrate, and the floc was settled, siphoned out, air-dried, and ground into powder that could be incorporated to the feed formulation (Kuhn et al. 2009). In my RAS, characterization of the solids produced in the system can inform what processing is required to generate material appropriate as feed supplements for shrimp reared in the system. Another option for sludge management is anaerobic digestion, which can treat both freshwater and brackish RAS sludge by reducing sludge volume and generating biogas, which could in turn contribute to system energy demands (Mirzoyan et al. 2010).

Another waste stream from RAS operation is the exoskeletons shrimp shed when they molt. In my system, these discarded shells would accumulate on the mesh covering rearing tank standpipes, requiring frequent manual removal to avoid water overflowing from the

rearing tanks. Shrimp shells can be treated to extract chitin, and crab and shrimp shells are currently the main commercial sources of this material, which has applications in food processing and in the biomedical and pharmaceutical fields (Rinaudo 2006). Chitosan, a derivative of chitin, has a broad range of applications in agriculture, water treatment, food, cosmetics, and pharmaceutics (Rinaudo 2006). Shrimp shells serving as feedstock for the extraction of these economically valuable materials are typically generated by the food processing industry. RAS culture of shrimp could perhaps become a valuable source of shrimp shells, as several shrimp molt multiple times over the course of rearing, producing several shells per shrimp in addition to the one removed from harvested shrimp during standard processing.

Model Description

Stocking pattern, shrimp bioenergetics, waste production, and biofilter function were combined in a model to represent operation of the pilot-scale RAS (Figure 25).

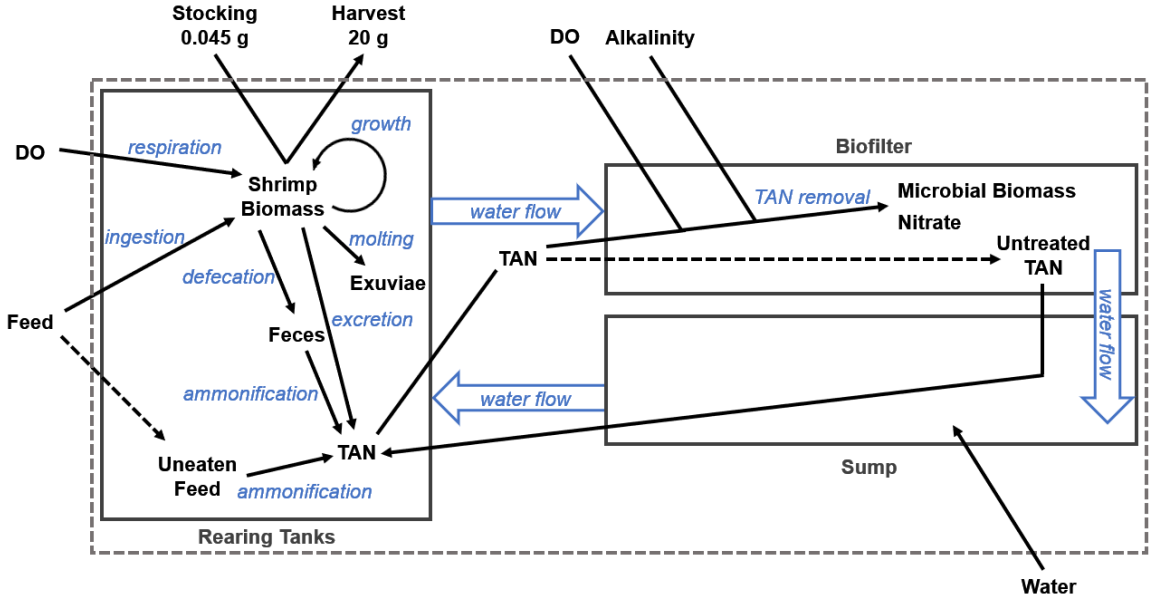

Figure 25. Conceptual model of material components and interrelating processes considered. RAS system boundary is indicated by the dotted outline.

Stocking pattern

To model rotational stocking, transfer, and harvest enabled by the six tanks of the pilot-scale RAS, rearing tanks were modeled as three components. Each batch reared always occupies two tanks simultaneously (Figure 2), so components represent the three batches that can be reared concurrently. Specifically, Component A represents rearing in two of the small tanks, Component B represents rearing in the other two small tanks, and Component C represents rearing in the two large tanks. Initial number of shrimp is zero for all components. For Component A and B, number of shrimp increases by stocking and decreases by mortality and transfer to Component C:

```
Number_of_Shrimp_A(t) = Number_of_Shrimp_A(t - dt) + (Stocking_A - Mortality_A - Transfer_A_to_C) * dt
        INIT Number_of_Shrimp_A = 0
INFLOWS:
        Stocking_A = PULSE(Number_Stocked_per_Batch, 0, 2*Rearing_Duration_Unit)
OUTFLOWS:
        Mortality_A = Number_of_Shrimp_A*Mortality_Rate_Small_Tank_A
        Transfer_A_to_C = PULSE(Number_of_Shrimp_A, 2*Rearing_Duration_Unit, 2*Rearing_Duration_Unit)
```

```
Number_of_Shrimp_B(t) = Number_of_Shrimp_B(t - dt) + (Stocking_B - Mortality_B - Transfer_B_to_C) * dt
        INIT Number_of_Shrimp_B = 0
INFLOWS:
        Stocking_B = PULSE(Number_Stocked_per_Batch, Rearing_Duration_Unit, 2*Rearing_Duration_Unit)
OUTFLOWS:
        Mortality_B = Number_of_Shrimp_B*Mortality_Rate_Small_Tank_B
        Transfer_B_to_C = PULSE(Number_of_Shrimp_B, 3*Rearing_Duration_Unit, 2*Rearing_Duration_Unit)
```

For Component C, number of shrimp increases by transfer from Component A and B and decreases by mortality and harvest:

```
Number_of_Shrimp_C(t) = Number_of_Shrimp_C(t - dt) + (Transfer_A_to_C + Transfer_B_to_C - Mortality_C - Harvest) * dt
        INIT Number_of_Shrimp_C = 0
INFLOWS:
        Transfer_A_to_C = PULSE(Number_of_Shrimp_A, 2*Rearing_Duration_Unit, 2*Rearing_Duration_Unit)
        Transfer_B_to_C = PULSE(Number_of_Shrimp_B, 3*Rearing_Duration_Unit, 2*Rearing_Duration_Unit)
OUTFLOWS:
        Mortality_C = Number_of_Shrimp_C*Mortality_Rate_Large_Tank
        Harvest = PULSE(Number_of_Shrimp_C, 3*Rearing_Duration_Unit, Rearing_Duration_Unit)
```

In all components, stocking, transfer, and harvest are controlled by pulse functions of the form PULSE (quantity, time of first pulse, time interval). To maintain regular rotation schedule, rearing time in small tanks must be twice that in large tanks. In the model, rearing duration unit is defined as one-third of total rearing duration, and shrimp occupy small tanks for two rearing duration units and large tanks for one rearing duration unit.

Shrimp bioenergetics

To model shrimp growth during rearing, energy budget values were collected from five studies describing *L. vannamei* bioenergetics as $Q_C = Q_G + Q_F + Q_U + Q_E + Q_R$, wherein energy consumed (Q_C) is partitioned into energy deposited in growth (Q_G), lost as feces (Q_F), excreted as nitrogenous waste (Q_U), shed as exuviae (Q_E), and expended during respiration (Q_R) (Wang et al. 2004, Zhu et al. 2004, Yan et al. 2007, Feng et al. 2008, Su et al. 2010). All cited studies employed the same procedure to estimate these six components of the energy budget. Energy embodied in feed, feces, exuviae, and shrimp, at their initial and final weight, were measured using a bomb calorimeter. Energy excreted as nitrogenous waste was estimated through a nitrogen balance by quantifying nitrogen content of feed, feces, exuviae, and shrimp. Energy expended during respiration was calculated from the other terms of the bioenergetics equation. In all cited studies, energy budget values were reported as a percentage of consumed energy, for example G/C and F/C. For most studies, values were

reported numerically; however, values from the Yan et al. study were estimated from bar graphs.

All studies reported significant differences in energy allocation among different experimental treatments. Energy budget values corresponding to rearing conditions most similar to those in the pilot-scale RAS were selected for a total of eight sets of reference energy budget values. Table 7 summarizes rearing conditions corresponding to the selected values graphed in Figure 26.

Table 7. Temperature (ºC), salinity (ppt), percent protein in feed (%), and initial and final shrimp weights (g) corresponding to energy budget values referenced from cited studies. Conditions for Batch 4 reared in pilot-scale RAS are included for comparison.

Label	Study	Temperature (ºC)	Salinity (ppt)	Feed Protein (%)	Initial Weight (g)	Final Weight (g)
I	Yan et al. 2007	28	0.2	29	0.28	1.6
II		28	11	29	0.28	1.8
III	Wang et al. 2004	25	4	45	0.63	2.60
IV		25	4	35	0.63	3.39
V	Feng et al. 2008	25	20	43	0.8	2.94
VI	Su et al. 2010	25	20	43	0.8	1.78
VII		30	20	43	0.8	3.43
VIII	Zhu et al. 2004	25	30	42	5.44	8.45
Current Study		28	4	40	0.45	20.7

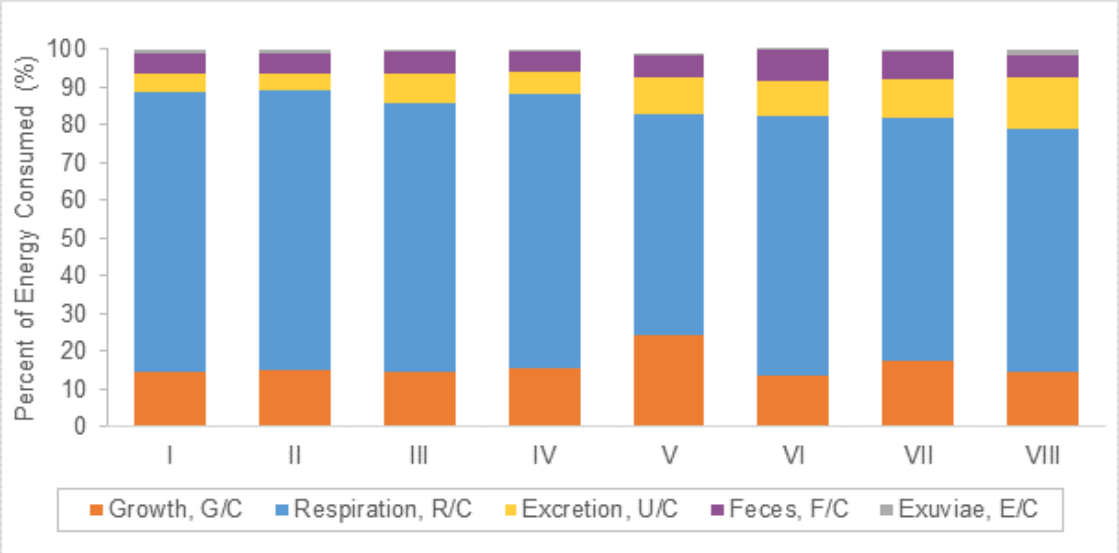

Figure 26. Eight sets of *L. vannamei* energy budget values reported across five studies. Energy towards growth, respiration, excretion, feces, and exuviae were reported as a percentage of energy consumed.

These literature values were the basis for representing the bioenergetics of shrimp reared in the pilot-scale RAS (Table 8). Model values of energy lost through excretion, feces, and exuviae were set to the mean literature values. To match actual growth observed in Batch 4, a model growth fraction of 21.2% of consumed energy was needed; this value was indirectly calibrated through adjustment of the respiration fraction. All model values fall within their respective literature range (Table 8).

Table 8. For each component of the *L. vannamei* energy budget, mean and range across cited studies are shown alongside the value used in my model and a brief explanation. All energy budget values are expressed as a percentage of consumed energy.

	Literature Mean ± SD	Literature Range	Model Value	Explanation of Model Value
Growth, G/C (%)	16.3 ± 3.4	13.8–24.3	21.2	computed as 100 - R/C - F/C - U/C - E/C
Respiration, R/C (%)	68.5 ± 5.7	58.5–74.4	63.7	calibrated against Batch 4 growth
Excretion, U/C (%)	8.2 ± 3.0	4.8–13.3	8.2	mean of literature values
Feces, F/C (%)	6.0 ± 1.1	5.0–8.2	6.0	
Exuviae, E/C (%)	0.9 ± 0.4	0.3–1.5	0.9	

In modeling shrimp bioenergetics using these values, I assume that the fraction of consumed energy allocated to each component remains constant over the range of shrimp sizes between stocking and harvest weight. However, the absolute levels of energy vary over the course of rearing with changes in total energy consumed, which is determined according to size-dependent feed rates as recommended by the feed manufacturer. Referencing the Rangen feeding table (Table 1), feed rates were graphed against corresponding mean shrimp weight, and power functions were used to fit available points in two segments (Figure 27).

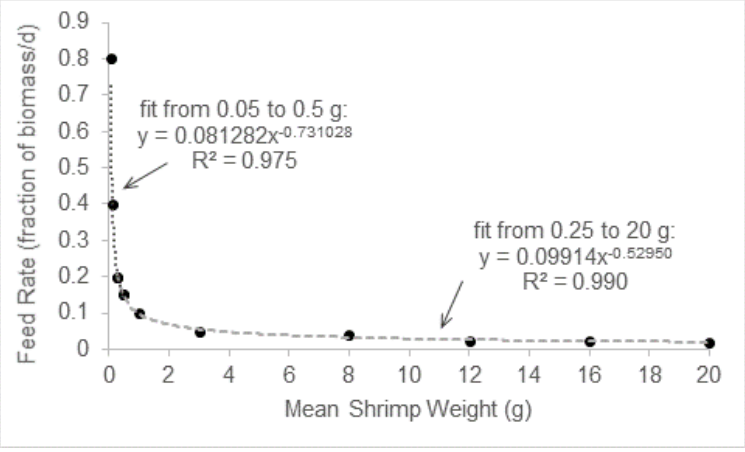

Figure 27. Feed rate (fraction of biomass/d) versus mean shrimp weight (g) from Rangen feeding table, with power function fit equations and R^2 values.

To model how much feed is ingested by shrimp reared, feed rate for shrimp smaller than 0.25 g was determined by coefficients from the first fit equation, while that for shrimp 0.25 g and larger was determined by the second set of coefficients:

```
Feed_Rate_A = IF (Mean_Weight_per_Shrimp_A>0)
        THEN Rangen _Fit_Constant_A*(Mean_Weight_per_Shrimp_A^Rangen_ Fit_Exponent_A) ELSE 0

Rangen_Fit_Constant_A = IF (Mean_Weight_per_Shrimp_A<0.25) THEN 0.081282 ELSE 0.09914
Rangen_Fit_Exponent_A = IF (Mean_Weight_per_Shrimp_A<0.25) THEN -0.731028 ELSE -0.5295
```

Amount of feed present in rearing tanks increases with provision and decreases with ingestion, with any remaining feed considered uneaten. Feed ingested is modeled as the product of shrimp biomass and corresponding feed rate; however, if provision is smaller than this value, only the provided feed would be ingested:

```
Feed_A(t) = Feed_A(t - dt) + (Provision_A - Ingestion_A - Uneaten_A) * dt
        INIT Feed_A = 0
INFLOWS:
        Provision_A = Shrimp_Biomass_A*Feed_Rate_A
OUTFLOWS:
        Ingestion_A = MIN(Shrimp_Biomass_A*Feed_Rate_A, Provision_A)
        Uneaten_A = IF (Provision_A>Ingestion_A) THEN Feed_A ELSE 0
```

Ingested feed is converted to consumed energy by factoring in the energy content of the feed:

```
Consumed_QC_A = Ingestion_A*Feed_Energy_Content
```

Energy allocated to growth is the corresponding fraction of consumed energy (Table 8):

```
Growth_QG_A = Growth_Fraction*Consumed_QC_A
```

In turn, energy allocated to growth is converted to increasing mean shrimp weight via energy content embodied in shrimp, which was referenced from literature values (Table 9). Since consumed energy and all its ensuing allocations are that of all the shrimp in each rearing tank component, collective increase in shrimp weight is divided by number of shrimp to obtain weight gain per shrimp each day:

$$(growth)\frac{g/shrimp}{d} = \frac{(energy\ for\ growth)\frac{kJ}{d} * \frac{1}{(shrimp\ energy\ content)\ kJ/g}}{(number\ of\ shrimp)\ shrimp}$$

To represent simultaneous transfer and restocking of shrimp, it was necessary to modify this growth model to prevent growth carried over from the previous batch from being assigned to the new batch. Pulse functions were incorporated to subtract an arbitrary large number from the growth rate to ensure zero growth at time of each transfer. Additional pulse functions

reset mean shrimp weights to zero and add in either initial stocking weight or transfer weight during transfer of shrimp between small and large rearing tank compartments.

Mean shrimp weight in Component A and B starts at a set initial stocking weight of 0.045 g, resetting to this value with each transfer and restocking:

```
Mean_Weight_per_Shrimp_A(t) = Mean_Weight_per_Shrimp_A(t - dt) +
                                    (Growth_A + From_Stocking_A - Transfer_Reset_A) * dt
        INIT Mean_Weight_per_Shrimp_A = 0.045
INFLOWS:
        Growth_A = SAFEDIV((Growth_QG_A/Shrimp_Energy_Content), Number_of_Shrimp_A) +
                PULSE(-10, 2*Rearing_Duration_Unit, 2*Rearing_Duration_Unit)
        From_Stocking_A = PULSE(Stocking_Weight, 2*Rearing_Duration_Unit, 2*Rearing_Duration_Unit)
OUTFLOWS:
        Transfer_Reset_A = PULSE(Mean_Weight_per_Shrimp_A, 2*Rearing_Duration_Unit, 2*Rearing_Duration_Unit)
```

```
Mean_Weight_per_Shrimp_B(t) = Mean_Weight_per_Shrimp_B(t - dt) +
                                    (Growth_B + From_Stocking_B - Transfer_Reset_B) * dt
        INIT Mean_Weight_per_Shrimp_B = 0.045
INFLOWS:
        Growth_B = SAFEDIV((Growth_QG_B/Shrimp_Energy_Content), Number_of_Shrimp_B) +
                PULSE(-10, 3*Rearing_Duration_Unit, 2*Rearing_Duration_Unit)
        From_Stocking_B = PULSE(Stocking_Weight, 3*Rearing_Duration_Unit, 2*Rearing_Duration_Unit)
OUTFLOWS:
        Transfer_Reset_B = PULSE(Mean_Weight_per_Shrimp_B, 3*Rearing_Duration_Unit, 2*Rearing_Duration_Unit)
```

In Component C, mean shrimp weight is set to the transfer weight whenever shrimp are transferred into the large tanks. From there, mean weight increases with growth and is ultimately reset at each harvest:

```
Mean_Weight_per_Shrimp_C(t) = Mean_Weight_per_Shrimp_C(t - dt) +
                                    (Growth_C + From_Transfer - Harvest_Reset_C) * dt
        INIT Mean_Weight_per_Shrimp_C = 0
INFLOWS:
        Growth_C = IF (Number_of_Shrimp_C>0)
                THEN (Growth_QG_C/Shrimp_Energy_Content)/Number_of_Shrimp_C ELSE 0
        From_Transfer = PULSE(Transfer_Weight, 2*Rearing_Duration_Unit, Rearing_Duration_Unit)
OUTFLOWS:
        Harvest_Reset_C = PULSE(Mean_Weight_per_Shrimp_C, 3*Rearing_Duration_Unit, Rearing_Duration_Unit)
```

Waste production

As with energy allocated to growth, energy in lost in feces, excretion, exuviae, and respiration are each their respective fractions of consumed energy (Table 8):

```
Feces_QF_A = Feces_Fraction*Consumed_QC_A
Excretion_QU_A = Excretion_Fraction*Consumed_QC_A
Exuviae_QE_A = Exuviae_Fraction*Consumed_QC_A
Respiration_QR_A = Respiration_Fraction*Consumed_QC_A
```

To integrate these values into my understanding of the RAS, each is expressed in terms of mass by applying corresponding energy contents taken from literature values (Table 9):

```
Feces_A = Feces_QF_A/Feces_Energy_Content
Excretion_A = Excretion_QN_A/Ammonia_Energy_Content
Evuviae_A = Exuviae_QN_A/Exuviae_Energy_Content
Shrimp_Respiration_Rate_A = Respiration_QR_A/Oxycalorific_coefficient
```

Feces and any uneaten feed generated comprise solid wastes formed in each tank. All solid waste is considered to degrade through ammonification unless manually removed:

```
Solid_Wastes_A(t) = Solid_Wastes_A(t - dt) + (Waste_Formation_A - Manual_Removal_A - Ammonified_A) * dt
        INIT Solid_Wastes_A = 0
INFLOWS:
        Waste_Formation_A = Uneaten_A+Feces_A
OUTFLOWS:
        Manual_Removal_A = 0
        Ammonified_A = Solid_Wastes_A
```

Solid wastes are considered to undergo ammonification such that all embodied nitrogen becomes TAN dissolved in the water. Nitrogen content is estimated by assuming both uneaten feed and feces to consist of 40% protein and then applying the Jones factor suggested for meats, 6.25 (Jones 1941):

$$(ammonification)\frac{mg\ N}{d} = (solids\ ammonified)\frac{g\ solids}{d} * \left(1000\frac{mg}{g}\right) * \left(0.40\ \frac{g\ protein}{g\ solids}\right) * \left(\frac{1}{6.25\ \frac{g\ protein}{g\ N}}\right)$$

In rearing tanks, TAN increases by excretion from shrimp, ammonification of solid wastes, and potentially flow from sump, while the only TAN removal is by flow to the biofilter:

```
Tank_TAN_A(t) = Tank_TAN_A(t - dt) +
                (Excretion_A + Ammonification_A + Sump_to_Tank_TAN_A - Tank_to_BF_TAN_A) * dt
        INIT Tank_TAN_A = 0
INFLOWS:
        Excretion_A = Excretion_QU_A/Ammonia_Energy_Content
        Ammonification_A = Ammonified_A*1000*Feed_Protein_Fraction/Nitrogen_to_Protein_Conversion
        Sump_to_Tank_TAN_A = Sump_TAN*Flowrate_Sump_to_Tank_A/Flowrate_BF_to_Sump
OUTFLOWS:
        Tank_to_BF_TAN_A = Flowrate_Sump_to_Tank_A*Tank_TAN_Conc_A
```

Amount of TAN is expressed as mass, in mg of N. Dividing each by volume of water in its corresponding tank (Table 9) gives TAN concentrations. To assess what fraction of TAN in each rearing tank is in the toxic un-ionized form, the model considers effects of pH, temperature, and salinity. Ammonium dissociation in water can be represented as follows:

$$NH_4^+ + H_2O \rightleftarrows NH_3 + H_3O^+$$

The equilibrium constant associated with this process, i.e. the acid dissociation constant of ammonium, K_a, is defined by the ratio of product to reactant activities:

$$K_a = \frac{\{NH_3\}\{H_3O^+\}}{\{NH_4^+\}a_w}$$

Activity of each component can be expressed as the product of its molar concentration and an activity coefficient:

$$K_a = \frac{\gamma_{NH_3}[NH_3]\gamma_{H_3O^+}[H_3O^+]}{\gamma_{NH_4^+}[NH_4^+]a_w} = \left(\frac{[NH_3][H_3O^+]}{[NH_4^+]}\right)\left(\frac{\gamma_{NH_3}\gamma_{H_3O^+}}{\gamma_{NH_4^+}a_w}\right)$$

In pure water, activity coefficients are equal to 1, making activity and concentration equal. So, dissociation constant in pure water, K_a^w, is the ratio of product to reactant concentrations:

$$K_a^w = \frac{[NH_3][H_3O^+]}{[NH_4^+]}$$

However, activity coefficients decrease with increasing ionic strength of the surrounding aquatic environment, so dissociation constant would differ between pure water and saline water. An empirical expression for dissociation constant in saline water, pK_a^s, was developed to reflect disparity in dissociation constants arising from differing ionic strengths:

$$pK_a^s = pK_a^w + (0.1552 + 0.0003142\,t)\,I$$

where t is temperature in ºC and I is ionic strength in mol/kg (Khoo et al. 1977).

Molal ionic strength of seawater can be related to salinity in units of ppt, $S‰$, through an empirical expression (Whitfield 1974):

$$I = \frac{19.9273\,S‰}{1000 - 1.005109\,S‰}$$

Temperature is a key factor affecting dissociation constants, and an empirical expression describing how pK_a^w varies with temperature can be applied:

$$pK_a^w = 0.09018 + \frac{2729.92}{T}$$

where T is temperature in K (Emerson et al. 1975), and $T(\mathrm{K}) = t(°\mathrm{C}) + 273.15$.

Combining the above equations gives an overall expression relating K_a^s to temperature in ºC and salinity in ppt:

$$pK_a^s = 0.09018 + \frac{2729.92}{(t+273.15)} + (0.1552 + 0.0003142\,t)\left(\frac{19.9273\,S‰}{1000 - 1.005109\,S‰}\right)$$

Using this temperature-dependent and salinity-adjusted dissociation constant, un-ionized ammonia concentration can be calculated from known TAN concentration at any given pH:

$$K_a^s = \frac{[NH_3][H_3O^+]}{[NH_4^+]} = \frac{[NH_3][H_3O^+]}{TAN - [NH_3]} \quad \rightarrow \quad [NH_3] = \frac{TAN}{1 + \frac{[H_3O^+]}{K_a^s}} = \frac{TAN}{1 + 10^{pK_a^s - pH}}$$

These relationships were used in the model to calculate unionized ammonia concentration in each rearing tank using TAN concentration, temperature, salinity, and pH as inputs. Equations shown for Component A are the same for Component B and C:

```
Corrected_pKa_A = 0.09018+(2729.92/((Tank_Temperature_A+273.15)))+
                  (0.1552+0.0003142*Tank_Temperature_A)*((19.9273*RAS_Salinity)/(1000-1.005109*RAS_Salinity))
Tank_NH3_N_Conc_A = Tank_TAN_Conc_A/(1+10^(Corrected_pKa_A-Tank_pH_A))
```

Biofilter function

Hydraulic flows connecting the rearing tanks, biofilter, and sump are modeled to represent recirculation of water through the system. Each of these compartments is considered a continuous stirred-tank reactor with uniform TAN concentration. Amount of TAN entering each tank per day is calculated as follows:

$$(TAN\ to\ tank)\frac{mg\ N}{d} = (flowrate\ into\ tank)\frac{L}{d} * (TAN\ concentration\ in\ previous\ tank)\frac{mg\ N}{L}$$

Similarly, amount of TAN leaving each tank per day is:

$$(TAN\ from\ tank)\frac{mg\ N}{d} = (flowrate\ out\ of\ tank)\frac{L}{d} * (TAN\ concentration\ in\ tank)\frac{mg\ N}{L}$$

For the rearing tanks and sump, flowrate of water into each tank is equal to flowrate out, as the latter results from displacement by the former. Flowrate into small rearing tanks, large rearing tanks, and from the biofilter to sump were measured in the pilot RAS and extrapolated to daily flowrates (Table 9). As Component A and B each contain two small rearing tanks, and Component C contains two large tanks, flowrates are doubled accordingly:

```
Flowrate_Sump_to_Tank_A = 2*Flowrate_Small_Tank
Flowrate_Sump_to_Tank_B = 2*Flowrate_Small_Tank
Flowrate_Sump_to_Tank_C = 2*Flowrate_Large_Tank
```

Initially, there is no TAN in rearing tanks, biofilter, or sump tank. TAN arising from shrimp metabolism in rearing tanks is carried to the biofilter, and biofilter TAN accordingly increases with flows from all three rearing tank components. Biofilter TAN decreases with TAN removal, with rate of TAN removal constrained either by amount of TAN present or by TAN removal capacity provided by the biofilter. If TAN present surpasses removal capacity available, then TAN cannot be completely removed, and remaining untreated portion would leave through flow to the sump:

```
BF_TAN(t) = BF_TAN(t - dt) +
              (Tank_to_BF_TAN_A + Tank_to_BF_TAN_B + Tank_to_BF_TAN_C - TAN_Removal - BF_to_Sump_TAN) * dt
            INIT BF_TAN = 0
INFLOWS:
            Tank_to_BF_TAN_A = Flowrate_Sump_to_Tank_A*Tank_TAN_Conc_A
            Tank_to_BF_TAN_B = Flowrate_Sump_to_Tank_B*Tank_TAN_Conc_B
            Tank_to_BF_TAN_C = Flowrate_Sump_to_Tank_C*Tank_TAN_Conc_C
OUTFLOWS:
            TAN_Removal = MIN(BF_TAN, TAN_Removal_Capacity)
            BF_to_Sump_TAN = Flowrate_BF_to_Sump*BF_TAN_Conc
```

To avoid un-ionized ammonia in rearing tanks accumulating to toxic levels, the biofilter should be designed to provide sufficient capacity such that TAN removal is never constrained by biofilter capacity, i.e. all TAN present in the biofilter is removed instead of flowing to the sump. Therefore, design TAN removal capacity is set equal to the maximum amount of TAN present in the biofilter over the course of model simulation (Table 9).

Removal of TAN from water circulating through the RAS occurs as TAN is used in the biofilter to support microbial metabolism, including respiration and cell synthesis. In biofilters used in RAS, the autotrophic nitrifying microbes present convert TAN to nitrate and use TAN for cell synthesis, whereas heterotrophic microbes remove TAN only through cell synthesis. Through analysis of the stoichiometry of these metabolic reactions, factors were derived to express the mass of oxygen and alkalinity consumed for each gram of TAN removed (Ebeling et al. 2006). These factors were incorporated into the model to estimate the oxygen and alkalinity requirements associated with simulated TAN removal (Table 9).

To consider possible inhibition of TAN removal within the biofilter that reduces TAN removal capacity, a capacity reduction term is factored in:

```
TAN_Removal_Capacity = Design_TAN_Removal_Capacity*(1-TAN_Removal_Capacity_Percent_Reduction/100)
```

Default value of the capacity reduction term is 0, representing no reduction of design TAN removal capacity. In this case, complete TAN removal results in no outflow of TAN from the biofilter. If capacity reduction is introduced, a portion of TAN would remain untreated and flow from the biofilter into the sump. This inflow increases sump TAN, which would in turn decrease with flows to rearing tanks:

```
Sump_TAN(t) = Sump_TAN(t - dt) + (BF_to_Sump_TAN - Sump_to_Tanks_TAN) * dt
            INIT Sump_TAN = 0
INFLOWS:
            BF_to_Sump_TAN = Flowrate_BF_to_Sump*BF_TAN_Conc
OUTFLOWS:
            Sump_to_Tanks_TAN = Flowrate_BF_to_Sump*Sump_TAN_Conc
```

Table 9. Input parameters used in model with brief description, set value and units, and any relevant references and rationale.

Parameter	Description	Value	Units	References/Rationale
Rearing_Duration_Unit	Unit defined as one-third of rearing time	42	days	One-third of 126-day rearing time of Batch 4
Number_Stocked_per_Batch	Number of shrimp stocked per batch	470	unitless	Number stocked in Batch 4
Death_Rate_Small_Tank	Fraction of shrimp dying each day in small and large rearing tanks	0.00604	per day	Based on Batch 4 survival before and after transfer
Death_Rate_Large_Tank		0.00139		
Respiration Fraction	Fractions of consumed energy allocated to each aspect of bioenergetics	0.637	unitless	Calibrated to match rearing time of Batch 4 via growth
Excretion Fraction		0.082		Based on literature values; refer to Table (Wang et al. 2004, Zhu et al. 2004, Yan et al. 2007, Feng et al. 2008, Su et al. 2010)
Feces Fraction		0.060		
Exuviae Fraction		0.009		
Rangen _Fit_Constant_A	Parameters for power functions relating feed rate to mean shrimp weight	0.081282; then 0.09914	unitless	Based on feeding table values from Rangen, using one set of fit parameters for shrimp under 0.25 g and another set for larger shrimp; refer to Figure
Rangen_ Fit_Exponent_A		-0.731028; then -0.5295		
Stocking_Weight	Shrimp weight when stocked into RAS	0.045	g/shrimp	Approximate initial weight of Batch 4
Transfer_Weight	Shrimp weight at transfer	9.95	g/shrimp	Generated from model simulation
Feed_Energy_Content	Energy embodied in feed, shrimp, feces, ammonia-N, and exuviae used to convert between energy allocation and corresponding material mass	17.6	kJ/g dry weight	Mean of literature values (Pascual et al. 2004, Zhu et al. 2004, Kuhn et al. 2009)
Shrimp_Energy_Content		5.2	kJ/g wet weight	Mean of literature values (Jiménez-Yan et al. 2006, Venero et al. 2007, Hu et al. 2008)
Feces_Energy_Content		7	kJ/g dry weight	Experimental value corresponding to dietary protein level most representative of model (Pascual et al. 2004)
Ammonia_Energy_Content		0.0249	kJ/mg N	Converted from 5.94 cal/mg (Elliott and Davison 1975)
Exuviae_Energy_Content		6.34	kJ/g dry weight	Experimental value of *Penaeus monodon* exuviae (Sarac et al. 1994)
Oxycalorific_Coefficient	Energy of oxygen used for respiration	13.4	kJ/g O_2	Converted from 3.20 cal/mg O_2 for ammoniotelic animals (Elliott and Davison 1975)
Feed_Protein_Fraction	Fraction by mass of protein in feed	0.40	g protein/g solids	Rangen feed provided to Batch 4 contained 40% protein
Nitrogen_to_Protein_Conversion	Fraction by mass of nitrogen in protein	6.25	mg N/g protein	Approximated by Jones factor
Flowrate_Small_Tank	Flowrate in and out of each small tank	2400	L/day	Estimated using flowrates measured in pilot RAS
Flowrate_Large_Tank	Flowrate in and out of each large tank	7700		
Flowrate_BF_to_Sump	Flowrate from biofilter to sump	25000		
Small_Tank_Volume	Volume of water in small tank, large tank, biofilter, and sump	80	L	Estimated from pilot RAS rearing tank dimensions and standpipe heights
Large_Tank_Volume		530		
BF_Volume		334		Estimated from BF dimensions and outflow pipe height
Sump_Volume		238		Estimated from sump dimensions and usual water level
Water_Replacement	Water replacing evaporative losses	50	L/d	Estimated from pilot RAS conductivity data
Design_TAN_Removal_Capacity	TAN removal capacity biofilter must provide for complete TAN removal daily	34154	mg N/L	Generated from model simulation; equal to maximum value of biofilter TAN over entire simulation runtime

Electricity requirement

Electrical equipment required for operation of the RAS include a pump to recirculate water, a regenerative blower to provide aeration through air stones, heaters to maintain desired water temperature, and lights to implement desired light-dark cycle. To estimate daily energy needed to operate these electrical components, the wattage of one unit of each device was multiplied by its time in use each day; subsequently multiplying by number of units gave total energy needed per day for each component (Table 10).

Table 10. Electrical components required for RAS operation and their corresponding wattage, time in use, number of units, and energy needed.

Component	Wattage (W/unit)	Time in Use (h/d)	Energy Needed (kWh/d/unit)	No. of Units	Total Energy Needed (kWh/d)
Pump	79.2	24	1.9	1	1.9
Air blower	200	24	4.8	1	4.8
Small heaters	75	24	1.8	4	7.2
Large heaters	300	24	7.2	2	14.4
LED lights	17	12	0.2	8	1.6

Calibration to pilot RAS

Several model inputs were calibrated using data collected from operation of the pilot RAS. Rearing conditions and performance of Batch 4 were used to set relevant model parameters, namely rearing duration unit, number stocked per batch, mortality rates, respiration fraction, stocking weight, feed protein fraction, tank temperature, and tank pH (Table 9). Additionally, flowrates of water recirculation as well as tank volumes were set to match the pilot RAS (Table 9).

Simulation specifications

The model was constructed in Stella Professional version 1.4.3 (Isee Systems Inc., Lebanon, New Hampshire) and solved using Euler integration method. Simulations were run using days as the time unit, from start time of 0 days to stop time of 367 days. Delta time, the time between each calculation during simulation, was set to 1.0 days such that each model parameter is evaluated once per day simulated.

Simulation Results

Stocking pattern

The model represents ideal implementation of the rotational stocking schedule, which can be visualized by tracking mean shrimp weight and number of shrimp in the three rearing tank compartments over the course of simulation runtime (Figure 28). Batches are stocked to small tanks, alternating between Component A or B, every 42 days. Each batch is then transferred to Component C large tanks 84 days after stocking and ultimately harvested 125 days after stocking.

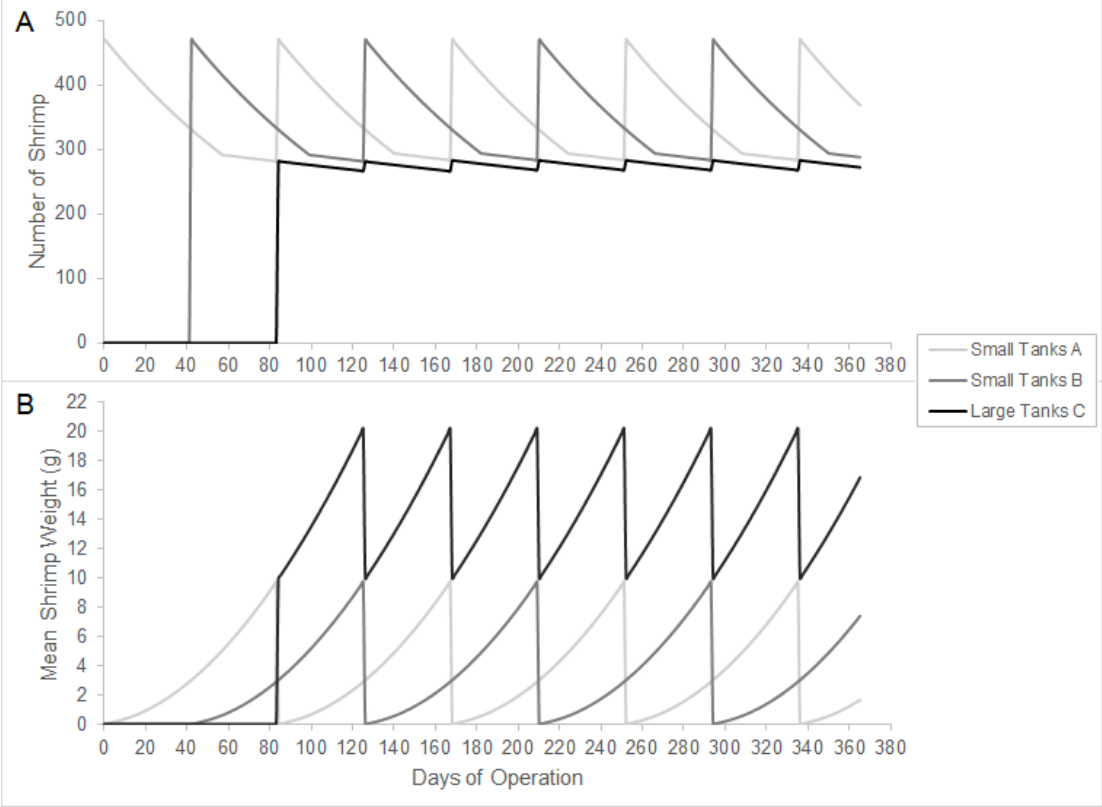

Figure 28. Model outputs of (A) mean shrimp weight (g) and (B) number of shrimp in the three rearing tank compartments during 365-day simulated RAS operation.

Shrimp production

All batches are modeled identically, so shrimp production metrics are presented for one characteristic batch. In Batch 4, 469 shrimp were stocked, 294 transferred, and 266 harvested; in the model, 470 shrimp were stocked, 281 transferred, and 266 harvested (Figure

29). Batch 4 was transferred from small to large rearing tanks on Day 56, whereas the modeled transfer was on Day 84. As a result, percent survival and weekly percent mortality rate were slightly different between experimental and model batches when considered for small and large tanks separately, though the model was calibrated to match experimental survival of 56.7% over the full rearing duration (Figure 30).

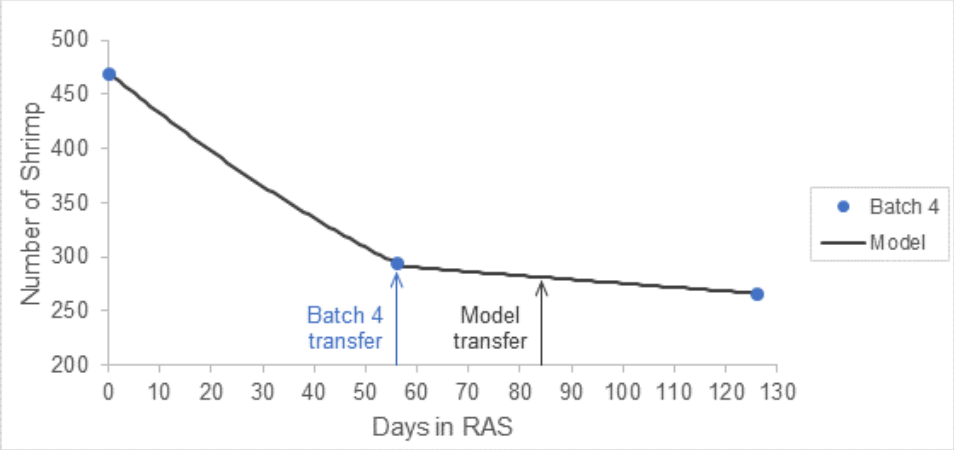

Figure 29. Number of shrimp per batch on each day reared in RAS, with three experimental points from Batch 4 and daily values generated by the model.

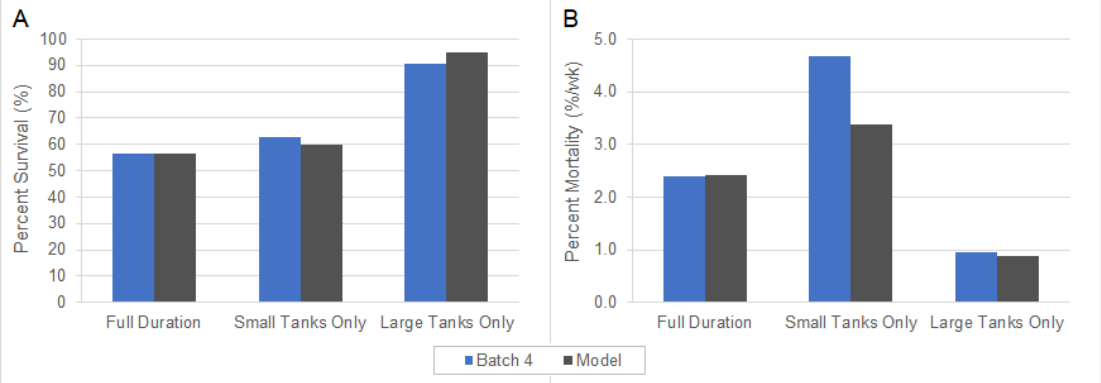

Figure 30. Comparison of Batch 4 and model (A) percent survival (%) and (B) weekly percent mortality rate (%/wk) for full rearing duration and small and large tanks separately.

Mean weight of shrimp in each batch was modeled to increase from 0.045 g at stocking to 9.95 g at transfer and ultimately to 20 g at harvest. The pattern of daily weights generated by the model generally matched the experimental growth curves from Batch 4 data (Figure 31). Experimental growth curves are more similar in shape to the bioenergetics

model curve than those generated from linear growth rate, SGR, and DGC growth models (Figure 31). Trends in growth rate metrics calculated from simulated shrimp weights generally matched those observed experimentally (Figure 32).

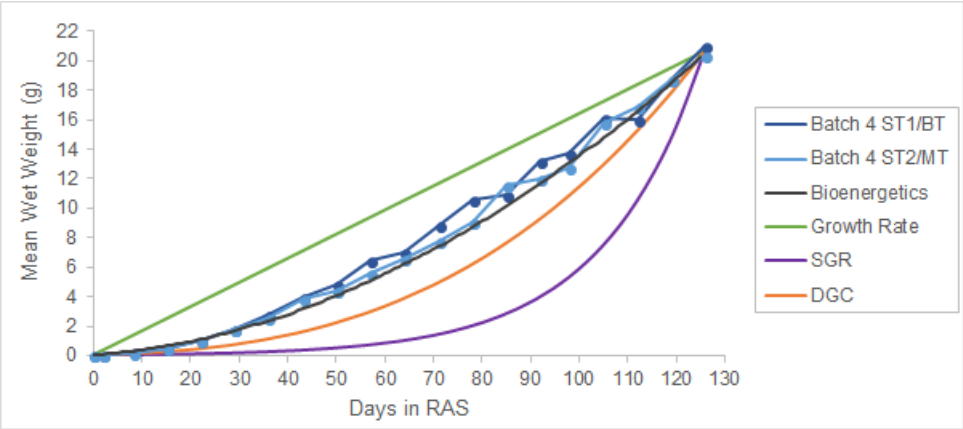

Figure 31. Growth curves observed for Batch 4 cohorts reared in pilot RAS (Figure 6B) and theoretical curves generated by bioenergetics, linear growth rate, SGR, and DGC growth models. In each case, mean wet weight (g) is plotted against days reared in RAS.

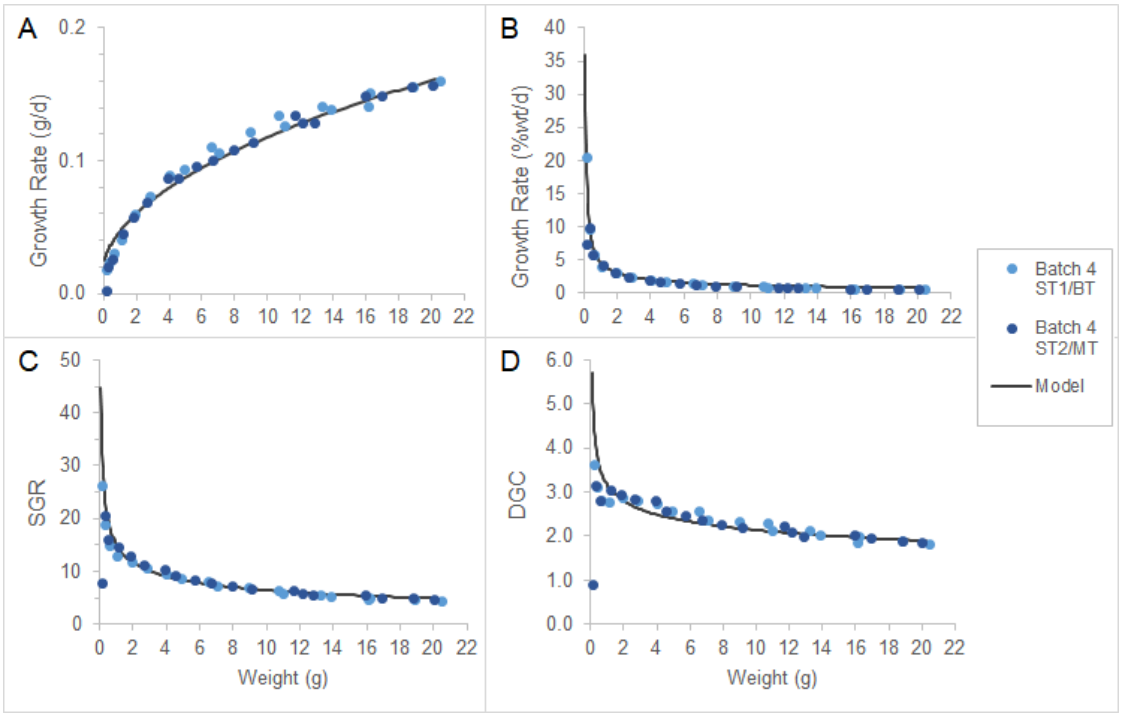

Figure 32. Comparison between Batch 4 values (Figure 14) and bioenergetics model output of (A) growth rate (g/d), (B) growth rate (% weight/d), (C) SGR, and (D) DGC at different weights (g) with respect to initial weight.

Shrimp density showed a different trend when expressed as numerical density than as biomass density (Figure 33). Whereas numerical density continually decreases with decreasing number of shrimp (Figure 29), biomass density continually increases despite mortalities due to the pattern of growth (Figure 31). In both cases, an instantaneous drop in shrimp density occurs when shrimp are transferred from small tanks to large tanks (Figure 33). The simulated trend in biomass density shows a maximum of 3.15 kg/m^2 relative to small tank area at transfer (Figure 33B), which is higher than the corresponding Batch 4 biomass density of 1.94 kg/m^2. This discrepancy arises because Batch 4 was transferred into large rearing tanks earlier than in the model.

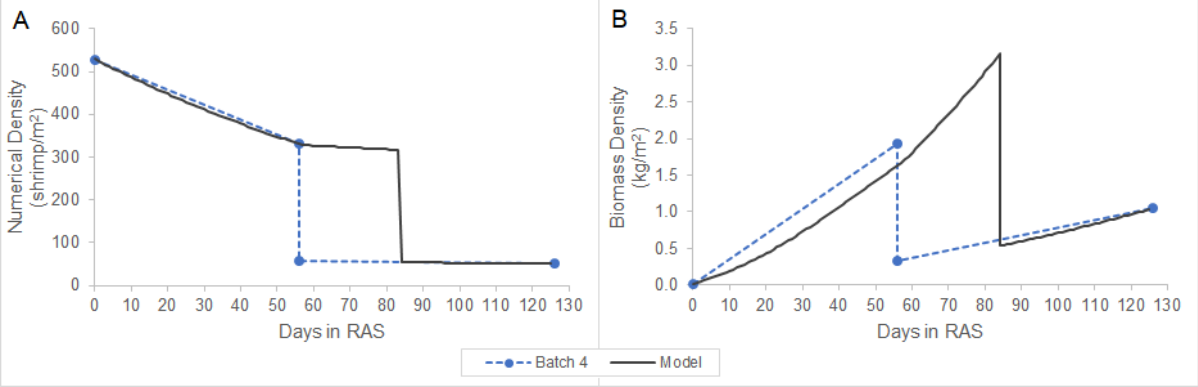

Figure 33. Comparison between Batch 4 data and modeled pattern of (A) numerical density (shrimp/m^2) and (B) biomass density (kg/m^2).

Net production of each batch was simulated to be 5.37 kg at harvest, only 2% lower than Batch 4 net production of 5.47 kg (Figure 9B) due to being calibrated indirectly through growth and mortality rate parameters. Meanwhile, cumulative feed provided had a model value of 8.45 kg at harvest, around 12% lower than the 9.63 kg of feed provided to Batch 4 (Figure 34A). FCR was correspondingly 11% lower in the modeled batch than in Batch 4 at 1.57 and 1.76, respectively. Plotting how much feed was provided each day over the course of rearing reveals that from Day 13 to Day 91, generally more feed was provided to Batch 4 than was modeled (Figure 34B).

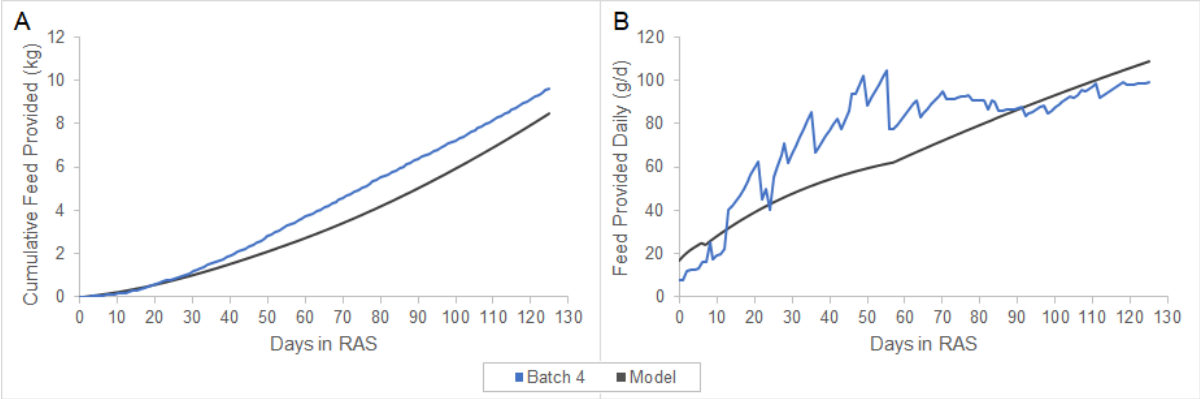

Figure 34. Comparison between Batch 4 data and modeled pattern of (A) cumulative feed provided (kg) and (B) feed provided daily (g/d) over the rearing period.

Over the year-long runtime, six batches were reared to 20 g (Figure 28B) with a final cumulative harvest of 32.4 kg. With respect to area of one large rearing tank, modeled yield for the first year of RAS operation was 12.4 kg/m^2-yr, with a yield of 0.50 kg/m^2-month for each batch reared. From Day 126 onwards, a harvest takes place every 42 days, because the RAS becomes fully occupied after the third batch is stocked on Day 82. From this point forward, eight batches can be harvested annually, and RAS yield would be 16.5 kg/m^2-yr.

Bioenergetic requirements and wastes

For each shrimp, metabolic rate increased with increasing shrimp weight, whereas larger shrimp had lower specific metabolic rate than smaller shrimp (Figure 35). Over the rearing period, 7.07 g of oxygen was cumulatively respired by each batch. Consistent with how bioenergetic allocation fractions were used in the model, respiration rate was a constant fraction of the rate at which feed was provided each day (Figure 36). Waste and exuviae production rates follow the same pattern with their respective fractions.

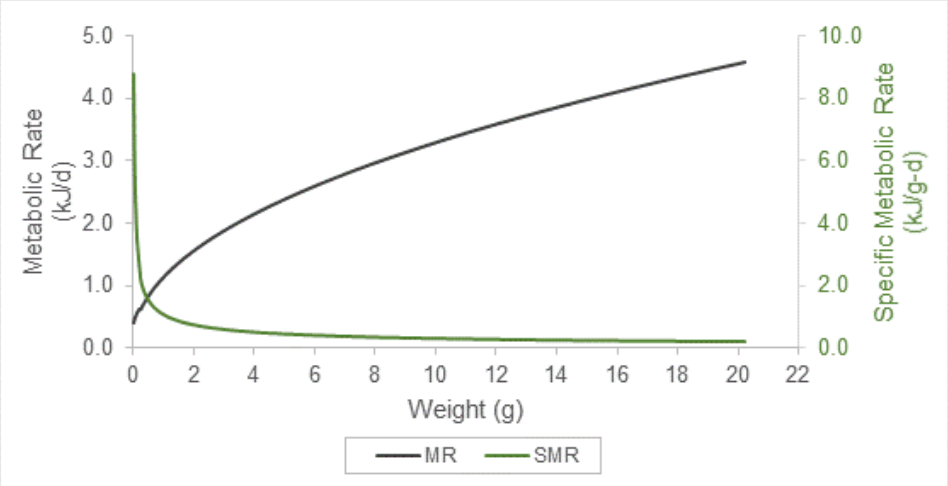

Figure 35. Model outputs of metabolic rate (kJ/d) of each shrimp and specific metabolic rate (kJ/g-d) versus shrimp weight (g).

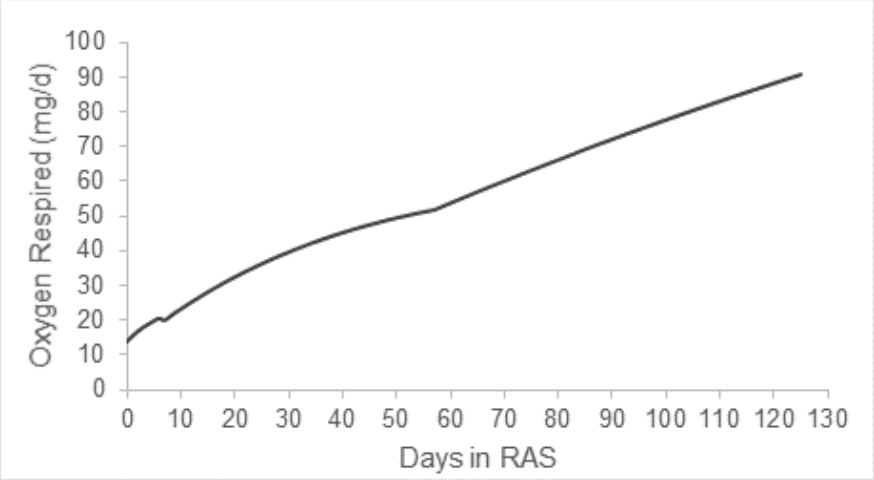

Figure 36. Modeled rate at which oxygen is respired (mg/d) by one batch on each day reared.

Over the rearing period, excretion accounted for around 86% of TAN production (Figure 37). In small tanks, TAN production increased to a maximum of 5.5 g-N/d during transfer; afterwards, TAN production continued to increase in the large tanks to a maximum of 7.4 g-N/d at harvest (Figure 38). When all rearing tanks are occupied, TAN production in large tanks made up around half of total TAN production, with a maximum combined TAN production of 16.6 g-N/d at each harvest (Figure 38).

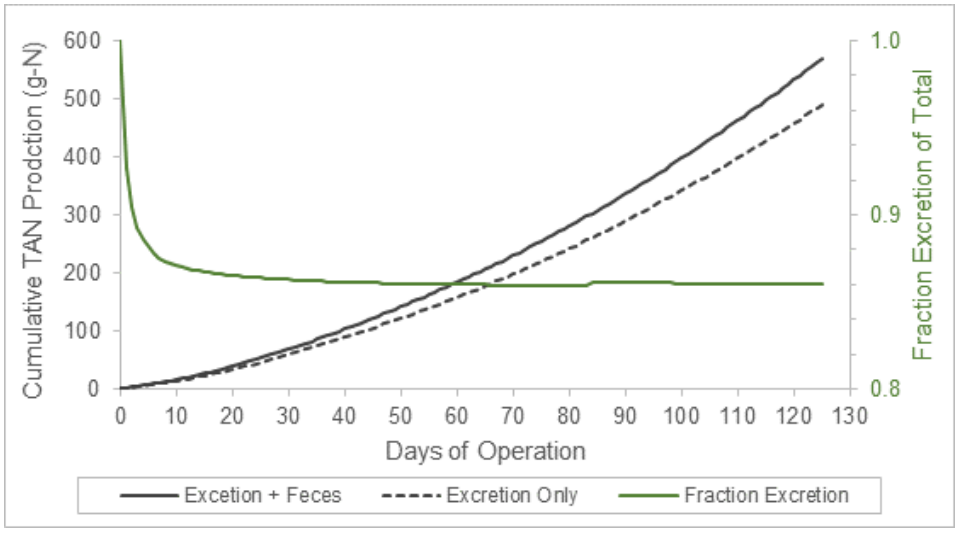

Figure 37. Cumulative TAN production (g-N) from (A) both excretion and feces and (B) excretion only. Fraction contributed by excretion is shown in green on the secondary axis.

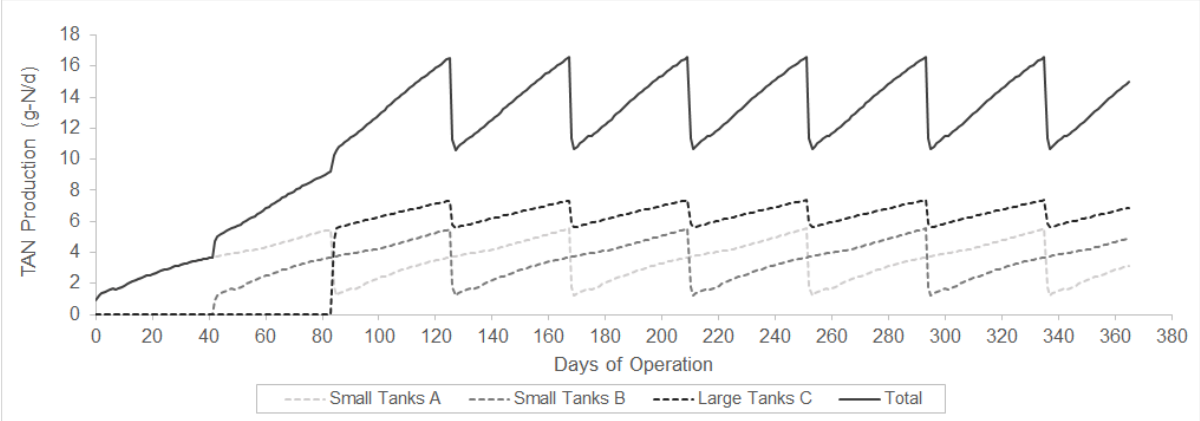

Figure 38. Daily TAN production in each rearing tank component and total TAN production across all rearing tanks.

Biofilter loading and function

TAN produced in the rearing tanks was modeled to flow into the biofilter in accordance with the TAN concentration and water flowrate for each compartment (Table 9). Amount of TAN from small rearing tanks increased to 10.9 g-N/d at transfer; after transfer, TAN discharge from large rearing tanks increased to 14.6 g-N/d immediately before harvest (Figure 39A). When all rearing tanks are occupied, flow of TAN from large tanks made up

around half of total TAN loading each day. Maximum amount of TAN in the biofilter was 33,085 mg-N (Figure 39B), which was used to set design TAN removal capacity (Table 9).

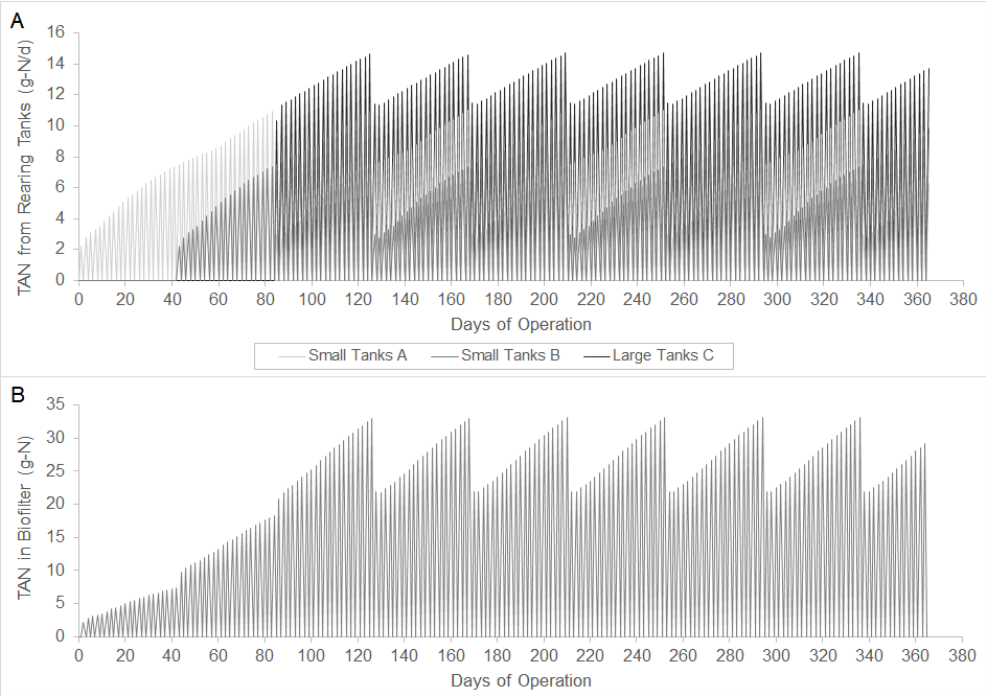

Figure 39. (A) TAN entering biofilter from each rearing tank component (g-N/d) and (B) total TAN present in biofilter (g-N) each day of simulation.

With no inhibition of this design TAN removal capacity, all TAN present in the biofilter is removed each day. Consequently, no TAN flows into the sump to then recirculate back to rearing tanks (Figure 40A). In this case, maximum un-ionized ammonia concentration is 0.72 mg-N/L in small tanks and 0.15 mg-N/L in large tanks (Figure 40B). However, when design TAN removal capacity was reduced by 25%, return of untreated TAN back to rearing tanks caused accumulation of un-ionized ammonia to greater than 9 mg-N/L in small tanks and 4.5 mg-N/L in large tanks (Figure 41).

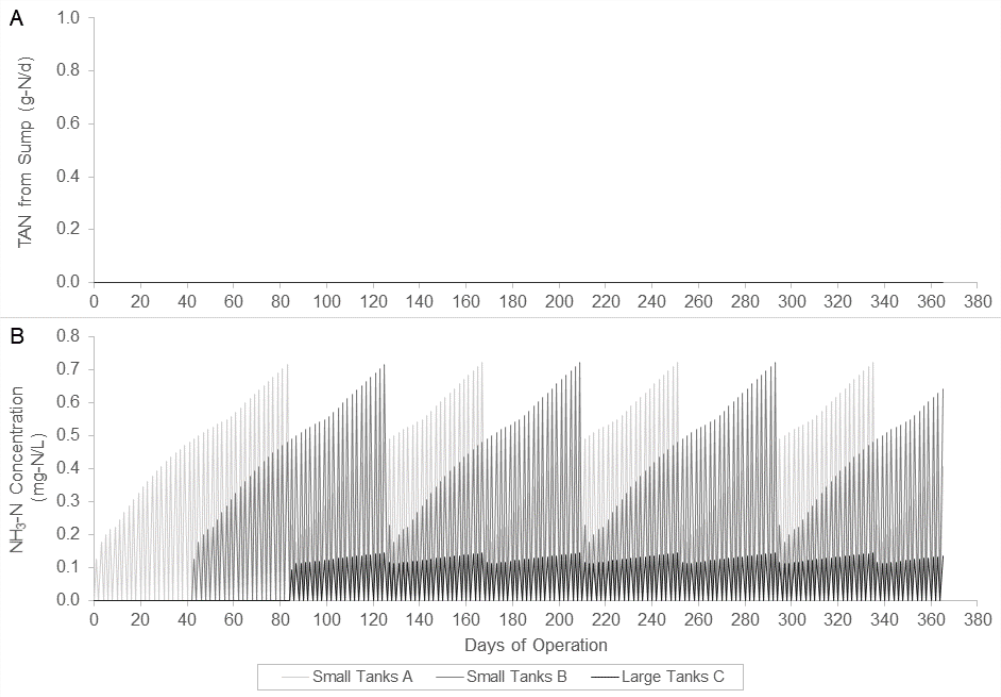

Figure 40. At design TAN removal capacity, (A) TAN recirculated to rearing tanks (g-N/d) and (B) un-ionized ammonia concentration (mg-N/L) in rearing tanks on each day simulated.

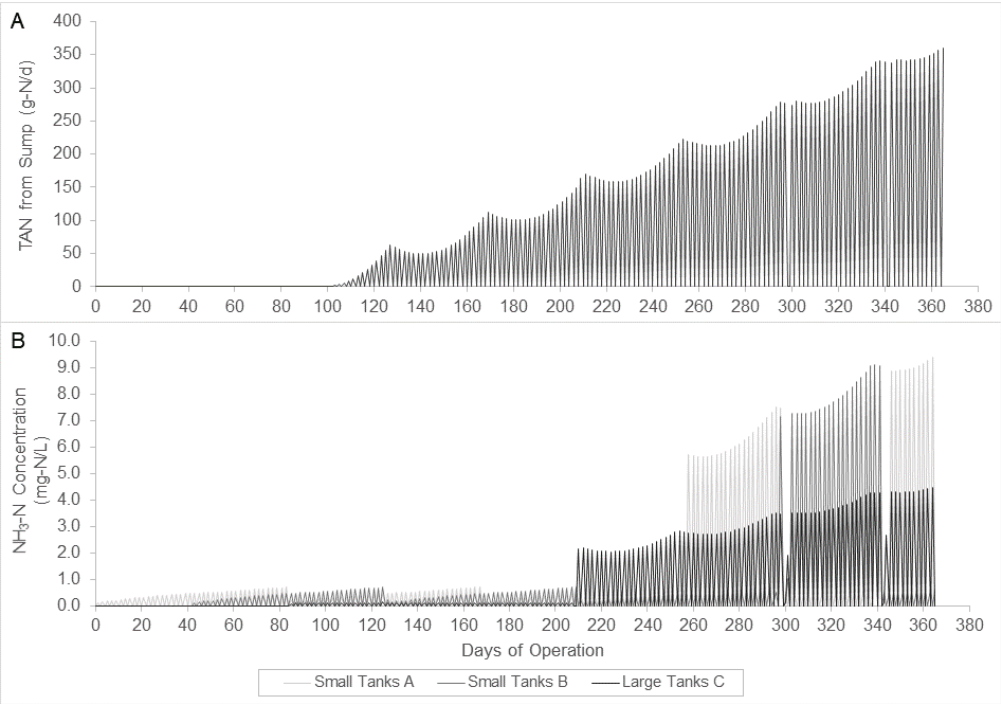

Figure 41. At 25%-reduction of design TAN removal capacity, (A) TAN recirculated to rearing tanks (g-N/d) and (B) un-ionized ammonia concentration (mg-N/L) in rearing tanks on each day of simulated.

Corresponding to the days with highest TAN loading, maximum oxygen needed is between 138 g/d and 156 g/d, and maximum alkalinity needed is between 118 g/d to 233 g/d (Figure 42). Autotrophic TAN removal requires around 10% less oxygen than heterotrophic TAN removal, but its alkalinity requirement is around two times higher than that of heterotrophic TAN removal (Figure 42).

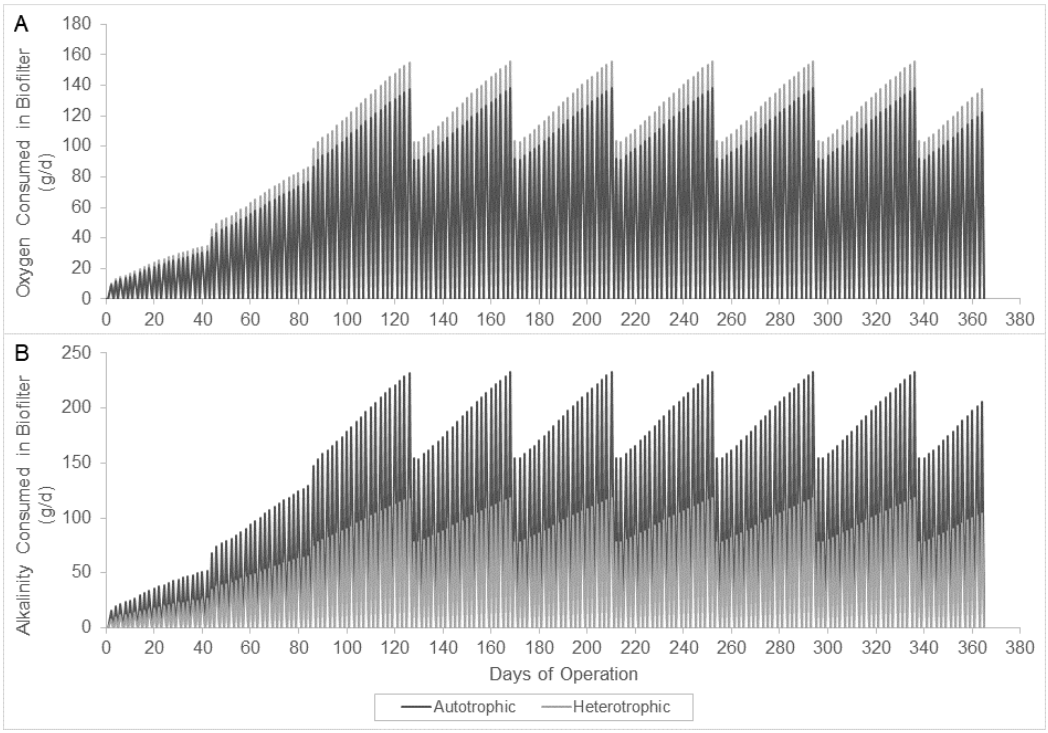

Figure 42. Amounts of (A) oxygen (g/d) and (B) alkalinity (g/d) consumed daily in the biofilter to carry out complete removal of TAN. Values corresponding to autotrophic and heterotrophic TAN removal are both shown.

Electricity requirement

A combined 30 kWh/d of electricity was needed to operate all electrical components listed in Table 10. The components making up the greatest fraction of electricity requirement were heaters, which needed 73% of total daily electricity requirement (Figure 43). Comparatively minor fractions of daily electricity requirement went into the other components, with the air blower, pump, and LED lights needing 16%, 6%, and 5%, respectively (Figure 43). Based on this value, electricity expenditure is 10,855 kWh annually, which corresponds to an electricity consumption index of 232 kWh/kg of shrimp harvested in the case of eight harvests per year.

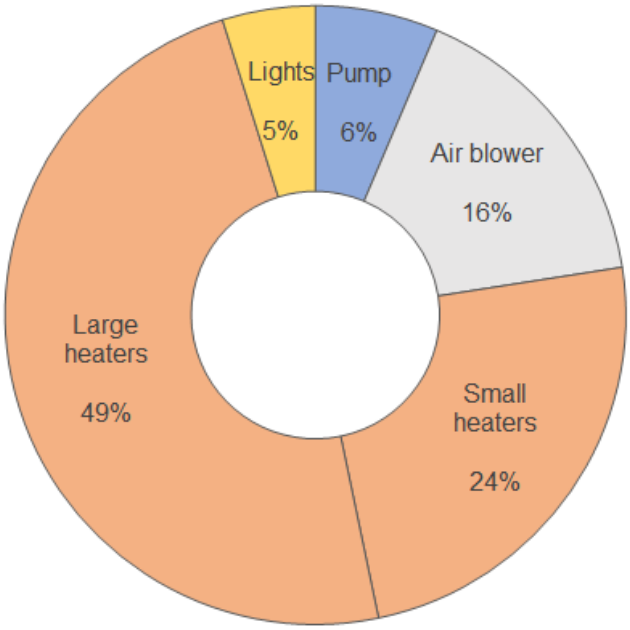

Figure 43. Percent of total daily electricity requirement used by electrical component type.

Model Discussion

Model represents stable operation of pilot RAS

Given operational issues during the pilot study resulting in high variability in performance between batches, the model was calibrated to the best-performing experimental batch, Batch 4 (Figure 6, Figure 7). To match rearing time required to grow Batch 4 to 20 g, fraction of consumed energy available for growth was calibrated through calibration of respiration fraction (Table 8). Growth curve generated by this model fit reasonably well with growth curves observed for Batch 4, representing observed growth more accurately compared to growth curves generated using linear growth rate, SGR, and DGC (Figure 31). Accordingly, growth rates generated by the bioenergetics model also fit well to those observed during rearing of Batch 4 (Figure 32).

Rotational stocking between four small rearing tanks and two large rearing tanks necessitates that exactly two-thirds of rearing time is spent in small tanks prior to transfer. Because each batch is modeled to grow from 0.045 g to 20 g in 126 days, transfer must occur on Day 84. This is inconsistent with Batch 4, which was transferred on Day 56 (Figure 29). During the pilot study, number of shrimp was counted only during stocking, transfer, and harvest (Figure 29). While mortality rate was observed to be higher in small tanks than in large tanks (Figure 30), the specific mortality patterns remain unknown. The model assumes that a constant fraction of the population dies each day, and two different fractions were used to achieve good fit with experimental data. A higher fraction was used until the population reached the number transferred in Batch 4; from then on, a lower fraction was used both for the remaining time in small tanks and for large tanks (Figure 29, Table 9). As a result, weekly percent mortality rate was higher for small tanks only in Batch 4 than in the model. Aside from this discrepancy, shrimp survival was generally consistent between the model and Batch 4 (Figure 30).

In real-world RAS operation, shrimp growth and survival are both sensitive to water quality and system management factors, so achieving identical growth patterns and 20-g harvest weight in every batch would require consistency in all aspects of the RAS over the course of its operation. The model does not consider possible variations between batches, instead aiming to approximate stable operation of the RAS in which production is similar

from batch to batch. Stable operation was not achieved in the pilot study, and variability in growth and survival were observed between different batches (Figure 6B, Figure 7). However, the model would be applicable to longer-term RAS operation in a commercial context, which would be expected to achieve more consistent and predictable batches than the one-year pilot trial.

Model could help improve feed management

Though growth and survival were modeled to match experimental results of Batch 4, discrepancies in feed provision arose (Figure 34), leading to 11% lower FCR in the modeled batch than in Batch 4. Though daily feed provision was calculated as the product of shrimp biomass and biomass-dependent feed rate (Figure 27) in both cases, the model benefits from always having perfect information. Specifically, number of shrimp and their mean weight, and thereby shrimp biomass, are known on each day simulated by the model. In contrast, assumptions were needed when estimating shrimp biomass for Batch 4 feeding calculations. Because shrimp were counted only at stocking, transfer, and harvest, number of shrimp present on any given week was estimated by assuming linear decline towards a predicted harvest population. But, while actual survival over the rearing period was 56.7%, it had been assumed during the experiment that the harvest population would be 80% of number stocked. This overestimation of shrimp survival could have contributed to overfeeding. Another source of uncertainty in feed provision arose from shrimp being weighed weekly. To estimate appropriate increases in feed provision each day between weighings, the subsequent week's shrimp biomass was projected based on experience with prior batches. This method did not always produce accurate projections, and overestimating future biomass could lead to overfeeding. Since the bioenergetics model can simulate shrimp growth that closely matches experimental growth curves (Figure 31), it can be leveraged to enhance feed efficiency during future RAS operation by providing more accurate daily estimates of shrimp biomass.

Simulations can help inform biofilter design and operation

Peak TAN production rate occurred at every harvest, when the shrimp in the large tanks reached their maximum reared size (Figure 38). Accordingly, maximum daily TAN

loading on the biofilter also occurred concurrently, and this maximum value was set as design TAN removal capacity. Comparing simulation results from a biofilter operating at full design capacity against one operating at 75% of capacity demonstrates that sufficient and reliable TAN removal is essential to avoiding accumulation of ammonia to toxic levels (Figure 40, Figure 41). Peak TAN production is dependent on the quantity and size of shrimp across all rearing tanks, which in turn are affected by many other factors, including number stocked, mortality rates, and growth rates. Therefore, if model parameters are changed to simulate different RAS scenarios, peak TAN production would most likely be different from its value in the base model. Keeping this in mind, the model can be used either to assess what production can be pursued as constrained by a set biofilter capacity or to aid in designing a biofilter with sufficient capacity for a desired production level.

In addition to assisting biofilter design, the model can also inform biofilter operation. TAN removal is carried out by microbial communities present in the biofilter, either autotrophically through nitrification and cell synthesis or heterotrophically through cell synthesis alone (Ebeling et al. 2006). A potential benefit of the rotational stocking schedule is reduced variability in system water quality; when three batches are always reared concurrently, combined daily biofilter TAN remains within a relatively stable range, dropping only to a minimum of 22 g N at the harvest of the biggest batch (Figure 39B). Metabolic rates are dependent upon substrate concentrations (Chen et al. 2006), so maintaining daily TAN loading within 22–33 g N may enable more stable microbiological conditions within the biofilter, including TAN removal kinetics and community composition. Though my model does not directly account for the details of microbial metabolisms, it provides coarse estimates of required oxygen and alkalinity by applying stoichiometric factors derived by Ebeling et al. for both autotrophic and heterotrophic TAN removal. Comparing the two mechanisms, oxygen required per unit of TAN removed autotrophically is around 90% of oxygen required for heterotrophic removal, whereas alkalinity required per unit of TAN removed autotrophically is double that required for heterotrophic removal (Table 9, Figure 42). Evidently, microbial composition within the biofilter would influence the quantity of chemical inputs required to support sufficient TAN removal and prevent toxic ammonia accumulation. An important distinction is that the estimated oxygen required to support microbial metabolism does not equate to total aeration required, as dissolved oxygen

in the bulk water must be maintained at high enough levels to drive sufficient oxygen diffusion into biofilms.

Although the model can provide useful insights into TAN loading and biofiltration requirements, one unexpected characteristic can be noted in the simulation results. All the simulation outputs related to biofiltration dynamics display oscillatory behavior, alternating between zero and a non-zero value (Figure 39–41). This pattern does not reflect actual RAS conditions; though TAN production in the rearing tanks remains steady without falling to zero every other day (Figure 38), TAN flowing into the biofilter from the rearing tanks oscillates (Figure 39A). One could expect that in reality, each point simulated to be at zero would instead fall between its adjacent non-zero points. Depending on what future goals this model would be used to inform, it may be necessary to consider this when interpreting simulation results.

Energy efficiency depends on shrimp production and facility design

Critical for RAS operation are the devices employed to achieve rearing conditions required for shrimp production. To maintain desired TAN, DO, temperature, and light-dark conditions, the electrical components listed in Table 10 provide recirculation, aeration, heating, and lighting. The combined electricity requirement of 30 kWh/d does not account for non-electric energy expenditures such as central heating of the RAS facility. Energy consumption index of the modeled RAS was 232 kWh/kg, substantially higher than a reported range of 2.9–81.48 kWh/kg compiled from 15 studies of RAS producing a variety of fish species (Badiola et al. 2018). This discrepancy suggests that energy efficiency of the modeled RAS could be further improved such that shrimp production would be possible with lower operating costs and reduced carbon emissions. System management interventions that improve net production of shrimp, for example increasing survival rate beyond 56.7%, would improve energy efficiency, as the same energy expenditure becomes distributed across larger harvests. All the same components need to be operated even when rearing density is much lower than what the system was designed to accommodate, so failure to use the RAS to its design capacity results in less efficient energy use.

Beyond improving shrimp production, RAS energy efficiency can also be improved by implementing alternatives to electrical components, selecting higher-efficiency

components, or designing the system to minimize energy use. For the electricity use currently modeled, the largest portion went toward temperature control of system water: 73% of total daily demand was needed to operate the six aquarium heaters used in the pilot RAS to maintain mean rearing tank temperature of 28 ºC for Batch 4 (Figure 43). This breakdown is consistent with findings from an energy audit of a pilot-scale codfish RAS, wherein temperature maintenance carried out by a heat pump consumed 71.8% of energy used over the experimental period (Badiola et al. 2017). Given the large expenditures associated with water heating, solar heating has been evaluated as an alternative to electrical heating devices (Fuller 2007). As influenced by site-dependent climate, greenhouse and solar collector design, and ventilation conditions, large reductions in conventional energy use can be enabled by solar heating of RAS (Fuller 2007). Another strategy to reduce electricity requirement is to select devices with higher energy efficiency when outfitting the system with electrical components. For example, LED lights could be chosen to implement a light-dark cycle rather than fluorescent lights, as their higher energy efficiency would reduce electricity use. Minimizing the energy required for RAS operation is only possible through a system design approach that actively and comprehensively targets energy efficiency alongside the goals of shrimp production and effective biofiltration.

Model assumptions set limitations on applicability

Which types of analyses a model can support depends on its underlying assumptions. One limitation of my model is that shrimp survival and bioenergetics fractions are not dependent on water quality or system operation inputs, but rather set as constant values (Table 8). Therefore, the model cannot be used to assess potential effects of temperature, salinity, feed protein, etc. on RAS production. Different stocking densities can be simulated to estimate effects on harvest and biofiltration requirements, but assumptions would need to be made regarding how shrimp density relates to growth and survival. Effects of shrimp size on growth and survival are also not directly accounted for. Because all bioenergetic processes are modeled as constant portions of consumed energy, size-dependency of growth and other bioenergetic processes rely solely on variable feed rate recommendations from the feed manufacturer (Figure 27). While model outputs of metabolic rate and specific metabolic rate show expected size-dependent trends (Figure 35), these are both determined by how Rangen

feed rate data defines feed ingestion rate. So, the bioenergetics model would not be suitable for shrimp reared with different feed protein content. Modeled shrimp survival reflects Batch 4 data at only stocking, transfer, and harvest while assuming a constant mortality fraction in between (Figure 29), so survivorship patterns may not be accurate. In utilizing this model to simulate experiments and help inform RAS management, it is important to be conscious of the assumptions used and to adjust parameters or expand the model to enhance accuracy as needed for the specific application.

Model can be integrated with other tools to enhance further inform RAS sustainability

The current model generates estimates for the quantity of shrimp post-larvae, feed, oxygen, biofiltration capacity, alkalinity, water, and electricity required to produce a harvest of 20-g shrimp after a set operation duration. However, it does not account for the material and energy inputs and outputs associated with upstream or downstream processes outside of the system boundary considered (Figure 25). Because the production of inputs and the disposal of waste outputs exert environmental impacts and incur monetary costs, modeling the bioenergetics and operation of the system can provide insight on sustainability and viability for these complex systems. Specifically, the RAS model can be integrated with LCA and economic analysis methods to evaluate sustainability. LCA has been identified as an important tool to evaluate and compare impacts associated with aquaculture, and this approach can inform efforts to improve system performance with respect to environmental sustainability (Cao et al. 2013). A bioeconomic model combining shrimp production metrics and price data was effective in generating insights for revenue-maximizing harvesting and payback periods (Zhou and Hanson 2017). Incorporating model insights into the design and operation of shrimp production systems and using production data in turn to improve model accuracy and capability can be an effective part of an adaptive management approach to aquaculture. Using the current model to simulate different operating scenarios, in conjunction with iterative verification using the pilot-scale system, could guide more efficient and sustainable RAS operation strategies.

Systems modeling is a powerful tool for sustainable RAS development

Success of an aquaculture system is governed by complex interactions between cultured shrimp, microbial community, and water quality. Complex as they are, these dynamics are only one aspect of the overall sustainable shrimp production landscape. Sustainability of aquaculture is linked to a suite of context-dependent factors spanning across a wide range of scales (Bush et al. 2010). The dynamics within an aquaculture operation determine the upstream impacts from inputs and the downstream impacts from outputs, which affect ecological health local to the aquaculture site as well as distributed across wider areas. Therefore, well-informed policy development is essential to ensuring that aquaculture operations are simultaneously free to develop and beholden to environmental responsibility. Systems modeling can be used to evaluate potential policy interventions based on how they affect simulated aquaculture sustainability, thereby helping to identify effective policies and avoid unintended consequences. From the perspective of financial viability, the success of commercial aquaculture operations depends on local and global markets of not only shrimp but also feed and other required inputs. Recognizing the importance of environmental and economic levers in determining the ability of RAS to compete with conventional means of production, models could be developed to investigate how exogenous factors such as climate change may create future benefits and risks for RAS versus conventional production.

Conclusion

In supplying whiteleg shrimp to fulfill increasing global demand for this high-value seafood, environmental sustainability must not be neglected at the expense of sensitive coastal ecosystems, local water quality, and natural resource conservation. RAS provide the ability to isolate shrimp production from impacting local environment, thereby presenting an opportunity for more sustainable aquaculture. Accurately characterizing complex interactions governing RAS is a key aspect of informing effective management. The pilot study presented here demonstrated that shrimp can be grown to marketable sizes in low-salinity indoor RAS, and that good system design and management are essential for stable long-term operation. A modeling approach integrating operational parameters, shrimp bioenergetics, and biofilter function generated estimates for inputs and outputs associated with a given level of shrimp production. Because inputs and outputs define both environmental impacts and monetary costs, the model can inform assessments of RAS sustainability and viability. Aquaculture is an important field with impacts ranging from local to global, and sustainable aquaculture requires balancing priorities at the food-energy-water nexus. Interdisciplinary collaboration is therefore essential for comprehensive understanding and successful implementation of sustainable aquaculture such that ecological, social, and economic factors are all accounted for comprehensively.

References

Æsøy, A., H. Ødegaard, and G. Bentzen. 1998. The effect of sulphide and organic matter on the nitrification activity in a biofilm process. *Water Science and Technology* 37:115–122.

American Public Health Association, American Water Works Association, and Water Environment Federation. 2005. *Standard Methods for the Examination of Water and Wastewater*.

Appelbaum, S., J. Garada, and J. K. Mishra. 2002. Growth and survival of the white leg shrimp (*Litopenaeus vannamei*) reared intensively in the brackish water of the Israeli Negev Desert. *The Israeli Journal of Aquaculture - Bamidgeh* 54:41–48.

Araneda, M., E. P. Pérez, and E. Gasca-Leyva. 2008. White shrimp *Penaeus vannamei* culture in freshwater at three densities: Condition state based on length and weight. *Aquaculture* 283:13–18.

Avnimelech, Y., and G. Ritvo. 2003. Shrimp and fish pond soils: Processes and management. *Aquaculture* 220:549–567.

Ayer, N. W., and P. H. Tyedmers. 2009. Assessing alternative aquaculture technologies: life cycle assessment of salmonid culture systems in Canada. *Journal of Cleaner Production* 17:362–373.

Badiola, M., O. C. Basurko, G. Gabiña, and D. Mendiola. 2017. Integration of energy audits in the life cycle assessment methodology to improve the environmental performance assessment of recirculating aquaculture systems. *Journal of Cleaner Production* 157:155–166.

Badiola, M., O. C. Basurko, R. Piedrahita, P. Hundley, and D. Mendiola. 2018. Energy use in Recirculating Aquaculture Systems (RAS): A review. *Aquacultural Engineering* 81:57–70.

Biesterfeld, S., G. Farmer, P. Russell, and L. Figueroa. 2003. Effect of alkalinity type and concentration on nitrifying biofilm activity. *Water Environment Research* 75:196–204.

Bray, W. A., A. L. Lawrence, and J. R. Leung-Trujillo. 1994. The effect of salinity on growth and survival of *Penaeus vannamei*, with observations on the interaction of IHHN virus and salinity. *Aquaculture* 122:133–146.

Browdy, C. L., and S. M. Moss. 2005. Shrimp culture in urban, super-intensive closed systems. Pages 173–185 *Urban Aquaculture, CAB International, eds Costa-Pierce, B., A. Desbonnet, P. Edwards, and D. Baker*.

Bureau, D. P., P. A. Azevedo, M. Tapia-Salazar, and G. Cuzon. 2000. Pattern and cost of growth and nutrient deposition in fish and shrimp: Potential implications and applications. Pages 111–140 *Avances en Nutrición Acuícola V. Memorias del V Simposium Internacional de Nutrición Acuícola. 19-22 Noviembre, 2000. Mérida, Yucatán, Mexico*.

Bush, S. R., P. A. M. van Zwieten, L. Visser, H. van Dijk, R. Bosma, W. F. de Boer, and M. Verdegem. 2010. Scenarios for resilient shrimp aquaculture in tropical coastal areas. *Ecology and Society* 15:26.

Cao, L., J. S. Diana, and G. a Keoleian. 2013. Role of life cycle assessment in sustainable aquaculture. *Reviews in Aquaculture* 5:61–71.

Cao, L., J. S. Diana, G. a Keoleian, and Q. Lai. 2011. Life cycle assessment of Chinese shrimp farming systems targeted for export and domestic sales. *Environmental Science and Technology* 45:6531–6538.

Chen, S., J. Ling, and J.-P. Blancheton. 2006. Nitrification kinetics of biofilm as affected by water quality factors. *Aquacultural Engineering* 34:179–197.

Chockley, B. R., and C. M. St. Mary. 2003. Effects of body size on growth, survivorship, and reproduction in the banded coral shrimp, Stenopus hispidus. *Journal of Crustacean Biology* 23:836–848.

Cuvin-Aralar, M. L. A., A. G. Lazartigue, and E. V. Aralar. 2009. Cage culture of the Pacific white shrimp *Litopenaeus vannamei* (Boone, 1931) at different stocking densities in a shallow eutrophic lake. *Aquaculture Research* 40:181–187.

Diana, J. S. 2009. Aquaculture production and biodiversity conservation. *BioScience* 59:27–38.

Diana, J. S. 2012. Is lower intensity aquaculture a valuable means of producing food? An evaluation of its effects on near-shore and inland waters. *Reviews in Aquaculture* 4:234–245.

Diana, J. S., H. S. Egna, T. Chopin, M. S. Peterson, L. Cao, R. Pomeroy, M. Verdegem, W. T. Slack, M. G. Bondad-Reantaso, and F. Cabello. 2013. Responsible aquaculture in 2050: Valuing local conditions and human innovations will be key to success. *BioScience* 63:255–262.

Ebeling, J. M., M. B. Timmons, and J. J. Bisogni. 2006. Engineering analysis of the stoichiometry of photoautotrophic, autotrophic, and heterotrophic removal of ammonia-nitrogen in aquaculture systems. *Aquaculture* 257:346–358.

Elliott, J. M., and W. Davison. 1975. Energy equivalents of oxygen consumption in animal energetics. *Oecologia* 19:195–201.

Emerson, K., R. C. Russo, R. E. Lund, and R. V Thurston. 1975. Aqueous ammonia equilibrium calculations: Effect of pH and temperature. *Journal of the Fisheries Research Board of Canada* 32:2379–2383.

Esparza-Leal, H. M., J. T. Ponce-Palafox, E. A. Aragón-Noriega, J. L. Arredondo-Figueroa, M. García-Ulloa Gómez, and W. Valenzuela-Quiñonez. 2010a. Growth and performance of the whiteleg shrimp *Penaeus vannamei* (Boone) cultured in low-salinity water with different stocking densities and acclimation times. *Aquaculture Research* 41:878–883.

Esparza-Leal, H. M., J. T. Ponce-Palafox, W. Valenzuela-Quiñónez, J. L. Arredondo-Figueroa, and M. García-Ulloa Gómez. 2010b. Effects of density on growth and survival of juvenile Pacific white shrimp, *Penaeus vannamei*, reared in low-salinity well water. *Journal of the World Aquaculture Society* 41:648–654.

Esparza-Leal, H. M., J. T. Ponce-Palafox, W. Valenzuela-Quiñonez, H. C. Beltrán, and J. L. Arredondo-Figueroa. 2009. The effect of low salinity water with different ionic composition on the growth and survival of *Litopenaeus vannamei* (Boone, 1931) in intensive culture. *Journal of Applied Aquaculture* 21:215–227.

FAO. 2017. *Fishery and Aquaculture Statistics 2015*.

Feng, C., X. Tian, S. Dong, Y. Su, F. Wang, and S. Ma. 2008. Effects of frequency and amplitude of salinity fluctuation on the growth and energy budget of juvenile *Litopenaeus vannamei* (Boone). *Aquaculture Research* 39:1639–1646.

Fóes, G., D. Krummenauer, G. Lara, L. Poersch, and W. Wasielesky Jr. 2016. Long term storage and the compensatory growth of white shrimp *Litopenaeus vannamei* in aquaculture ponds. *Latin American Journal of Aquatic Research* 44:588–594.

Fuller, R. J. 2007. Solar heating systems for recirculation aquaculture. *Aquacultural Engineering* 36:250–260.

Godfray, H. C. J., J. R. Beddington, I. R. Crute, L. Haddad, D. Lawrence, J. F. Muir, J. Pretty, S. Robinson, S. M. Thomas, and C. Toulmin. 2010. Food security: The challenge of feeding 9 billion people. *Science* 327:812–818.

Gutierrez-Wing, M. T., and R. F. Malone. 2006. Biological filters in aquaculture: Trends and research directions for freshwater and marine applications. *Aquacultural Engineering* 34:163–171.

Hu, Y., B. Tan, K. Mai, Q. Ai, S. Zheng, and K. Cheng. 2008. Growth and body composition of juvenile white shrimp, *Litopenaeus vannamei*, fed different ratios of dietary protein to energy. *Aquaculture Nutrition* 14:499–506.

Iwama, G. K., and A. F. Tautz. 1981. A simple growth model for salmonids in hatcheries. *Canadian Journal of Fisheries and Aquatic Sciences* 38:649–656.

Jiménez-Yan, L., A. Brito, G. Cuzon, G. Gaxiola, T. García, G. Taboada, L. A. Soto, and R. Brito. 2006. Energy balance of *Litopenaeus vannamei* postlarvae fed on animal or vegetable protein based compounded feeds. *Aquaculture* 260:337–345.

Jones, D. B. 1941. Factors for converting percentages of nitrogen in foods and feeds into percentages of proteins. *United States Department of Agriculture, Washington, D.C.*

Kamstra, A., E. Blom, and B. F. Terjesen. 2017. Mixing and scale affect moving bed biofilm reactor (MBBR) performance. *Aquacultural Engineering* 78:9–17.

Khoo, K. H., C. H. Culberson, and R. G. Bates. 1977. Thermodynamics of the dissociation of ammonium ion in seawater from 5 to 40 °C. *Journal of Solution Chemistry* 6:281–290.

Kuhn, D. D., G. D. Boardman, A. L. Lawrence, L. Marsh, and G. J. Flick Jr. 2009. Microbial floc meal as a replacement ingredient for fish meal and soybean protein in shrimp feed. *Aquaculture* 296:51–57.

Kuhn, D. D., S. A. Smith, G. D. Boardman, M. W. Angier, L. Marsh, and G. J. Flick Jr. 2010. Chronic toxicity of nitrate to Pacific white shrimp, *Litopenaeus vannamei*: Impacts on survival, growth, antennae length, and pathology. *Aquaculture* 309:109–114.

Li, E., L. Chen, C. Zeng, X. Chen, N. Yu, Q. Lai, and J. G. Qin. 2007. Growth, body composition, respiration and ambient ammonia nitrogen tolerance of the juvenile white shrimp, *Litopenaeus vannamei*, at different salinities. *Aquaculture* 265:385–390.

Li, T., E. Li, Y. Suo, Z. Xu, Y. Jia, J. G. Qin, L. Chen, and Z. Gu. 2017. Energy metabolism and metabolomics response of Pacific white shrimp *Litopenaeus vannamei* to sulfide toxicity. *Aquatic Toxicology* 183:28–37.

Lin, Y.-C., and J.-C. Chen. 2001. Acute toxicity of ammonia on *Litopenaeus vannamei* Boone juveniles at different salinity levels. *Journal of Experimental Marine Biology and Ecology* 259:109–119.

Lin, Y.-C., and J.-C. Chen. 2003. Acute toxicity of nitrite on *Litopenaeus vannamei* (Boone) juveniles at different salinity levels. *Aquaculture* 224:193–201.

Lorenzen, K. 1996. The relationship between body weight and natural mortality in juvenile and adult fish: A comparison of natural ecosystems and aquaculture. *Journal of Fish Biology* 49:627–647.

Lotz, J. M. 1997. Special topic review: Viruses, biosecurity and specific pathogen-free stocks in shrimp aquaculture. *World Journal of Microbiology and Biotechnology* 13:405–413.

Malone, R. F., and T. J. Pfeiffer. 2006. Rating fixed film nitrifying biofilters used in recirculating aquaculture systems. *Aquacultural Engineering* 34:389–402.

Martins, C. I. M., E. H. Eding, M. C. J. Verdegem, L. T. N. Heinsbroek, O. Schneider, J. P. Blancheton, E. R. D'Orbcastel, and J. A. J. Verreth. 2010. New developments in recirculating aquaculture systems in Europe: A perspective on environmental sustainability. *Aquacultural Engineering* 43:83–93.

McGraw, W. J., and J. Scarpa. 2004. Mortality of freshwater-acclimated *Litopenaeus vannamei* associated with acclimation rate, habituation period, and ionic challenge. *Aquaculture* 236:285–296.

McQuarrie, J. P., and J. P. Boltz. 2011. Moving bed biofilm reactor technology: Process applications, design, and performance. *Water Environment Research* 83:560–575.

Mena-Herrera, A., C. Gutierrez-Corona, M. Linan-Cabello, and H. Sumano-Lopez. 2006. Effects of stocking densities on growth of the Pacific white shrimp (*Litopenaeus vannamei*) in earthen ponds. *The Israeli Journal of Aquaculture - Bamidgeh* 58:205–213.

Mirzoyan, N., S. Parnes, A. Singer, Y. Tal, K. Sowers, and A. Gross. 2008. Quality of brackish aquaculture sludge and its suitability for anaerobic digestion and methane production in an upflow anaerobic sludge blanket (UASB) reactor. *Aquaculture* 279:35–41.

Mirzoyan, N., Y. Tal, and A. Gross. 2010. Anaerobic digestion of sludge from intensive recirculating aquaculture systems: Review. *Aquaculture* 306:1–6.

Moss, S. M., G. D. Pruder, K. M. Leber, and J. A. Wyban. 1992. The relative enhancement of *Penaeus vannamei* growth by selected fractions of shrimp pond water. *Aquaculture* 101:229–239.

Naylor, R. L., R. J. Goldburg, J. H. Primavera, N. Kautsky, M. C. M. Beveridge, J. Clay, C. Folke, J. Lubchenco, H. Mooney, and M. Troell. 2000. Effect of aquaculture on world fish supplies. *Nature* 405:1017–1024.

Ødegaard, H., B. Rusten, and T. Westrum. 1994. A new moving bed biofilm reactor - applications and resultsWater Science and Technology.

Otoshi, C. A., A. D. Montgomery, E. M. Matsuda, and S. M. Moss. 2006. Effects of artificial substrate and water source on growth of juvenile Pacific white shrimp, *Litopenaeus vannamei*. *Journal Of The World Aquaculture Society* 37:210–213.

Páez-Osuna, F. 2001. The environmental impact of shrimp aquaculture: Causes, effects, and mitigating alternatives. *Environmental Management* 28:131–140.

Pascual, C., E. Zenteno, G. Cuzon, A. Sánchez, G. Gaxiola, G. Taboada, J. Suárez, T. Maldonado, and C. Rosas. 2004. *Litopenaeus vannamei* juveniles energetic balance and immunological response to dietary protein. *Aquaculture* 236:431–450.

Patnaik, S., and T. M. Samocha. 2009. Improved feed management strategy for *Litopenaeus vannamei* in limited exchange culture systems. *World Aquaculture* 40:57–59.

Ponce-Palafox, J., C. A. Martinez-Palacios, and L. G. Ross. 1997. The effects of salinity and temperature on the growth and survival rates of juvenile white shrimp, *Penaeus vannamei*, Boone, 1931. *Aquaculture* 157:107–115.

Ray, A. J., T. H. Drury, and A. Cecil. 2017. Comparing clear-water RAS and biofloc systems: Shrimp (*Litopenaeus vannamei*) production, water quality, and biofloc nutritional contributions estimated using stable isotopes. *Aquacultural Engineering* 77:9–14.

Ray, A. J., and J. M. Lotz. 2017. Shrimp (*Litopenaeus vannamei*) production and stable isotope dynamics in clear-water recirculating aquaculture systems versus biofloc systems. *Aquaculture Research* 48:4390–4398.

Rinaudo, M. 2006. Chitin and chitosan: Properties and applications. *Progress in Polymer Science* 31:603–632.

Roy, L. A., D. A. Davis, I. P. Saoud, C. A. Boyd, H. J. Pine, and C. E. Boyd. 2010. Shrimp culture in inland low salinity waters. *Reviews in Aquaculture* 2:191–208.

Samocha, T. M., A. L. Lawrence, C. A. Collins, F. L. Castille, W. A. Bray, C. J. Davies, P. G. Lee, and G. F. Wood. 2004. Production of the Pacific white shrimp, *Litopenaeus vannamei*, in high-density greenhouse-enclosed raceways using low salinity groundwater. *Journal of Applied Aquaculture* 15:1–18.

Saoud, I. P., D. A. Davis, and D. B. Rouse. 2003. Suitability studies of inland well waters for *Litopenaeus vannamei* culture. *Aquaculture* 217:373–383.

Sarac, H. Z., N. P. McMeniman, H. Thaggard, M. Gravel, S. Tabrett, and J. Saunders. 1994. Relationships between the weight and chemical composition of exuvia and whole body of the black tiger prawn, *Penaeus monodon*. *Aquaculture* 119:249–258.

Sowers, A. D., J. R. Tomasso Jr., C. L. Browdy, and H. L. Atwood. 2006. Production characteristics of *Litopenaeus vannamei* in low-salinity water augmented with mixed salts. *Journal of the World Aquaculture Society* 37:214–217.

Su, Y., S. Ma, and C. Feng. 2010. Effects of salinity fluctuation on the growth and energy budget of juvenile *Litopenaeus vannamei* at different temperatures. *Journal of Crustaean Biology* 30:430–434.

van Rijn, J. 2013. Waste treatment in recirculating aquaculture systems. *Aquacultural Engineering* 53:49–56.

van Rijn, J., Y. Tal, and H. J. Schreier. 2006. Denitrification in recirculating systems: Theory and applications. *Aquacultural Engineering* 34:364–376.

Venero, J. A., D. A. Davis, and D. B. Rouse. 2007. Variable feed allowance with constant protein input for the Pacific white shrimp *Litopenaeus vannamei* reared under semi-intensive conditions in tanks and ponds. *Aquaculture* 269:490–503.

Wang, X., S. Ma, S. Dong, and M. Cao. 2004. Effects of salinity and dietary carbohydrate levels on growth and energy budget of juvenile *Litopenaeus vannamei*. *Journal of Shellfish Research* 23:231–236.

Whitfield, M. 1974. The hydrolysis of ammonium in sea water - A theoretical study. *Journal of the Marine Biological Association of the United Kingdom* 54:565–580.

Williams, A. S., D. A. Davis, and C. R. Arnold. 1996. Density-dependent growth and survival of *Penaeus setiferus* and *Penaeus vannamei* in a semi-closed recirculating system. *Journal of the World Aquaculture Society* 27:107–112.

Wyban, J., W. A. Walsh, and D. M. Godin. 1995. Temperature effects on growth, feeding rate and feed conversion of the Pacific white shrimp (*Penaeus vannamei*). *Aquaculture* 138:267–279.

Xu, W.-J., and L.-Q. Pan. 2012. Effects of bioflocs on growth performance, digestive enzyme activity and body composition of juvenile *Litopenaeus vannamei* in zero-water exchange tanks manipulating C/N ratio in feed. *Aquaculture* 356–357:147–152.

Xu, W.-J., L.-Q. Pan, D.-H. Zhao, and J. Huang. 2012. Preliminary investigation into the contribution of bioflocs on protein nutrition of *Litopenaeus vannamei* fed with different dietary protein levels in zero-water exchange culture tanks. *Aquaculture* 350–353:147–153.

Yan, B., X. Wang, and M. Cao. 2007. Effects of salinity and temperature on survival, growth, and energy budget of juvenile *Litopenaeus vannamei*. *Journal of Shellfish Research* 26:141–146.

Zhou, X., and T. Hanson. 2017. Economic optimization of super-intensive biosecure recirculating shrimp production systems. *Aquaculture International* 25:1469–1483.

Zhu, C., S. Dong, F. Wang, and G. Huang. 2004. Effects of Na/K ratio in seawater on growth and energy budget of juvenile *Litopenaeus vannamei*. *Aquaculture* 234:485–496.